BIOGEOGRAPHICAL INSIGHTS INTO THE AQUATIC METAL AND ANTIBIOTIC RESISTOME

By

Cory Joyner

July 2024

Director of Thesis. Erin K. Field

Major Department: Biology

Abstract

Antibiotic resistance in environmental microbiota is a naturally occurring, yet looming threat to global society and is estimated to contribute to over 10 million deaths annually by 2050. While human-derived contamination from industrial activity and wastewater worsens this, other environmental stressors like heavy metals and the genes conferring their resistance (MRGs) within microbes may enhance antibiotic resistance genes (ARGs). Ultimately, this leads to their persistence due to shared export mechanisms and coupled transcriptional regulation. However, the occurrence and relative abundance of MRGs and ARGs remains poorly understood across aquatic ecosystems and geographies. Here, we hypothesized that estuary ecosystems and highly industrialized countries would harbor the most abundant and diverse repertoire of ARGs and MRGs within its waters, showing ecosystem and geographic differences in resistome composition that could reflect the extent of human contamination within. 57 aquatic shotgun sequencing projects were downloaded from MG-RAST and the SRA spanning global waters and their nucleotide sequences annotated using the two-step ARGs-oap pipeline built from the Structured Antibiotic Resistance Gene Database (SARG), the Bacterial Metals and Biocides Database (BacMet), and a custom mobile genetic element (MGE) database curated to include plasmid, transposase, and integrase sequences. To determine the most abundant and frequently co-occurring ARG and MRG types, the relative abundances were stratified and plotted by ecosystem, country, continent, and hemisphere, while pairwise spearman correlation matrices were constructed to assess co-occurrence patterns and the results visualized with network analysis. Lastly, co-resistance was studied further within the environmental isolate *Arthrobacter aurescens* TC1 using chromium-enriched and marine salt

antibiotic Kirby-Bauer disk diffusion assays. It was found that estuaries were more likely to have higher abundances of resistance genes for tetracycline resistance compared to marine environments, but held elevated concentrations of zinc, chromium, iron, arsenic and lead compared to freshwater and marine environments. Kenya carried an elevated abundance of tetracycline and sulfonamide resistance genes compared to both the industrialized nations of the USA and China, but no differences in MRG abundance were observed. Network analysis revealed that some multidrug efflux genes were highly correlated to MRGs for copper resistance, but genes conferring resistance to biocides and multi-metals may play an undermined role within aquatic ecosystems due to their prominence. Laboratory studies revealed that low concentrations of Cr(VI) under estuarine salinity conditions improved the resistance of known metal-resistant *A. aurescens* TC1 to many antibiotics, including bacitracin. These results suggest that estuaries and freshwater environments are more at-risk environments for ARG/MRG co-occurrence compared to marine systems, and Lake Victoria in Kenya is at a risk for ARG/MRG co-occurrence and possibly co-resistance, highlighting it as a promising location for future studies.

BIOGEOGRAPHICAL INSIGHTS INTO THE AQUATIC METAL AND ANTIBIOTIC RESISTOME

A Thesis

Presented to the Faculty of the Department of Biology

East Carolina University

In Partial Fulfillment of the Requirements for the Degree

Master of Science in Biology

By

Cory Joyner

July 2024

Director of Thesis: Erin Field, Ph.D.

Thesis Committee Members:

Michael Brewer, Ph.D.

Jinling Huang, Ph.D.

Acknowledgements

I'd like to personally thank all the people who have helped me in my academic career thus far and especially those who assisted with this project and its development. Thank you to committee member Dr. Michael Brewer for the bioinformatics support provided in and outside of the classroom, as well as granting access to ECU's HPC to carry out the initial steps of this work. It means so much to me to have had your input and expertise on all the computational analyses that were incredibly daunting at first. Additional thanks to committee member Dr. Jinling Huang for his expertise on horizontal gene transfer as well as bioinformatics. Your bioinformatics course provided me with so many valuable resources used throughout this work. Thank you most of all to Dr. Erin Field for the continued support, advice, and expertise in microbiology on this project. Your dedication to student success, guidance and mentorship has been amazing these last two years and I can't thank you enough for taking me on as a graduate student so I could learn how cool aquatic microbes and microbial genomics are!

I'd also like to give a shout-out to two professors from my alma mater, Barton College, for their influence in my decision to pursue a graduate degree. Thank you to Dr. Scott Salger for being the person to introduce me almost 4 years ago to the world of microbiology and microbial ecology. It's crazy to think if you hadn't randomly offered me that microbiology lab worker position that I'd be in a completely different place now. When you added bioinformatics to our classes, it did so much to introduce me to the field and really propelled me forward in learning more about it. Additional thanks to Dr. Chelsie Batten, who served as my calculus professor but also became a mentor to me during my three years as a math tutor. You inspired me to become a better educator and learn how to approach difficult problems with an open mind, and I still value today the many conversations about math and life in general that you've had with me!

Thank you to my family and my parents, Susan, and George, for supporting me in my decision to become the first person in the family to pursue and graduate with a college degree, let alone a graduate degree. Lastly, thank you to my friends Sadie and Israel, Mia, and Olivia, for putting up with me these

last 16 years. Our conversations and time together really keep me sane, and I've done nothing but value that friendship even more as I've completed this degree.

Table of Contents

List of Tables

List of Figures

Introduction & Review of Literature

Antibiotic resistance is a global health concern - even outranking major diseases such as Malaria in its death toll in some countries (Murray et al. 2022). This contributes to what is known as the global "resistome", or the entire collection of resistance genes found in an environment. The resistome is expanded often by wastewater from industrial, hospital, or agricultural sources (Baquero et al. 2008), where runoff into watersheds causes their accumulation in sediments and their degradation prolonged. Environmental evidence of antibiotic resistance is necessary to answer larger questions about antibiotic resistance gene (ARG) abundance, diversity, spread, and the factors that may drive their persistence, especially in aquatic environments which serve as a primary vehicle for contaminant mobility (Bashir et al. 2020; Bombaywala et al. 2021).

Input from anthropogenic activity imparts selective pressure for ARGs, but it isn't necessarily the source of it; the genetic machinery responsible is highly conserved and found naturally in aquatic microbiota. Bacitracin, which is a common antibiotic included in over-the-counter triple antibiotic ointment, originates from the genus *Bacillus.* Further, the bulk of antibiotics used in medicine have been isolated from members of *Streptomyces* (Denyer et al. 2007). They exist in distinct classes: The beta-lactam antibiotics which include penicillin and cephalosporins, the tetracyclines and their derivatives, aminoglycoside-aminocyclitols, macrolides, streptogramins, glycopeptide antibiotics like vancomycin, and a few synthetic members such as the sulfonamides, quinolones, and nitrofurans. Hence, it is quite a challenge to discern if an aquatic resistome carries resistance naturally, or due to other factors using presence/absence as the sole indicator - heavily implying a need for context to make larger conclusions of the extent of contamination.

In the early 2010s, healthcare providers prescribed over 262.5 million antibiotics to patients in the USA (Hicks et al. 2015). Penicillins and macrolides were the most common classes utilized. Interestingly, the prescription rate in southern areas (Texas, Oklahoma, Louisiana, Missouri, Alabama, Tennessee,

Kentucky, North and South Carolina, Virginia and West Virginia and Florida) was much higher than other regions suggesting there may be a geographical impact on the global resistome. For example, geospatial analyses of ARGs sampled from 1.2 million kilometers of river and streams across the United States found higher abundances of class I integron-integrase, concentrations of sulfonamide resistance genes, and tetracycline resistance genes in Southeastern regions, which are proposed indicator genes for wastewater contamination (Keely et al. 2022). From this study alone, there isn't a clear answer that the most prescribed antibiotics would have the most resistance genes sampled from proximate waters; however, this could reflect regionally based differences and the influence of other environmental factors that may control the fate and exposure of these compounds to microbes. It is also plausible that those antibiotics are present, but not in concentrations that would cause persistence. One hypothesis is that natural waters without a steady inflow of antibiotics are less likely to harbor resistance genes, and their low concentrations are unlikely to pose major selection events. With the advent and development of next-generation sequencing (NGS) technologies, it is possible now more than ever to combine shotgun sequencing data across multiple sites to gain further insight into this.

It is known that antibiotic resistance genes and metal resistance genes often co-occur together and can indirectly drive both their maintenance and proliferation across bacterial species (Perron et al. 2004; Seiler and Berendonk 2012; Di Cesare et al. 2016; Bombaywala et al. 2021). One mechanism that confers cross-resistance is the drug efflux pump. The pump may be specific, or it can be problematically broad-spectrum, leading to the export of several contaminant classes. Multi-drug transporters in the ABC family

Table 1*: Shared metal and antibiotic resistance mechanisms. Metal ions often cited to be problematic for bacteria have evidence of decreasing susceptibility of the bacterium to an antibiotic. [Adapted from Baker-Austin 2006]*

Resistance mechanism	Metal ions	Antibiotics	Refs
Reduction in permeability[b]	As, Cu, Zn, Mn, Co, Ag	Cip, Tet, Chlor, ß-lactams	[68,69]
Drug and metal alteration[c]	As, Hg	ß-lactams, Chlor	[70,71]
Drug and metal efflux[d]	Cu, Co, Zn, Cd, Ni, As	Tet, Chlor, ß-lactams	[72,73]
Alteration of cellular target(s)[e]	Hg, Zn, Cu	Cip, ß-lactams, Trim, Rif	[74,75]
Drug and metal sequestration[f]	Zn, Cd, Cu	CouA	[76,77]

[a]Abbreviations: Chlor, chloramphenicol; Cip, ciprofloxacin; CouA, coumermycin A; Rif, rifampicin; Tet, tetracycline; Trim, trimethoprim.
[b]Includes reduction of membrane permeability to metals and antibiotics.
[c]Includes drug and metal inactivation and modification.
[d]Includes rapid efflux of the metal and antibiotic.
[e]Includes alteration of a cellular component to lower its sensitivity to the toxic metal and antibiotic.
[f]Includes drug and metal sequestration.

require ATP as an energy source, while other sub-classes require an electrochemical gradient established within the bacterial membrane (Du et al. 2018). The genes encoding them are highly conserved hinting that they may be widespread outside of pathogenic bacteria. Some pumps are even studied for their ability to transport lipids and some metals (Blanco et. al 2016), indicating a role in normal physiology outside of being a response to antibiotic or metal stress. Additionally, resistance genes closer together on either a chromosome or plasmid may infer a similar resistance phenotype (Baker-Austin et al. 2006). Aside from shared efflux, MRGs and ARGs may be co-regulated through the expression of certain transcriptional and translational factors in response to either stressor. One laboratory study found that excess zinc stress in a metal tolerant strain of *P. aeruginosa* also decreased the expression of the *oprD* porin, leading to resistance against a carbapenem antibiotic (Perron et al. 2004). Multiple metal resistance mechanisms such as those for copper and zinc reduce the permeability of antibiotics, rendering them less effective (Table 1). As a result, metals are under increasing attention for their ability to indirectly drive antibiotic resistance.

Metal stress in microbial communities primarily stems from anthropogenic activity, where excessive mining, deforestation, and terrestrial erosion all contribute to increasing amounts entering the water supply (Zaynab et al. 2022). Certain heavy metals, such as mercury, chromium, copper, and arsenic are relatively toxic to microbial communities, suggesting that genes conferring their resistance should be abundant in most environments (Singh et al. 2023). However, other metals such as iron and manganese are biologically essential, meaning their uptake is vital to normal physiology. In a mangrove estuary, it was found that elevated amounts of reduced iron and manganese could've resulted from a rise in sea level – a clear implication of climate change (Sanders et al. 2012). It is understood that the oxidation of reduced iron in aquatic environments results in the formation of reactive oxygen species (ROS) which are especially damaging to bacterial DNA. An interesting connection formed here is uncovered through mutagenesis induced by oxidative stress which could provide similar selective pressure to some antibiotics like ciprofloxacin, which has been shown to induce cell death through secondary ROS

production, potentially linking "biologically essential" metals as potential drivers of the antibiotic resistome through indirect selective pressures (Bombaywala et al. 2021). In this context, all metals, regardless of toxicity, should be considered.

Salinity is likely one variable affecting the composition of ARGs and MRGs, which is used to characterize most aquatic environments. Freshwater rivers, lakes, ponds, streams, and wetlands all interconnect to exchange dissolved organic and inorganic material with estuarine and oceanic waters (Fergus et al. 2017). The mobility of certain metal compounds in freshwater and sediments has historically been used to gain insight into differences in contamination over time. Lowered concentrations of both lead and mercury in deeper sediments of Lake Geneva have been described, but surface-level sediment samples presented a higher concentration attributed to natural weathering versus an increase in human activity later on (Thevenon et al. 2011). It is plausible that freshwater connections to terrestrial land serve as entry points to urban and rural water supplies, thus making geography and location an important factor to consider.

Along the ocean floor, crusts are composed largely of basalt which is a significant source of reduced iron. Reduced iron (Fe^{2+}) can abiotically oxidize into ferrous iron (Fe^{3+}) in the presence of oxygen, but new studies are highlighting the role of biotic iron-oxidation in global iron cycling. Areas such as hydrothermal vents, volcanic mounts, and seafloor crusts have come under recent attention for their ability to harbor iron-oxidizing bacteria (FeOB) capable of transforming this reduced iron into insoluble ferrous iron (Kappler et al. 2021). The *Zetaproteobacteria* contribute to this and make up some of the known microaerophilic, neutrophilic marine FeOB and include *Mariprofundus spp*. and *Ghiorsea spp.* (Emerson et al. 2010; Mori et al. 2017). Studies have investigated the genetic mechanisms of iron-oxidation for these species and have found that a cytochrome-porin encoded by the Cyc2 gene was abundantly expressed in a meta-transcriptomics study of FeOB at a marine hydrothermal vent (McAllister et al. 2020). Conversely, copper (which exhibits antimicrobial activity itself) is the most abundant in oxygen-limiting zones at low depths of the ocean where it is commonly bound to organic material

(Richon and Tagliabue 2019). Most literature highlights its importance to phytoplankton, but copper also indirectly supports the cycling of other abundant elements like iron and carbon (Merchant and Helmann 2012). A novel copper-dependent iron transport system in a marine *Vibrio sp.* strain has demonstrated this type of interconnection (Dubbels et al. 2004). Additional studies have reported the necessity of copper for iron-cycling in other marine microorganisms, like a plasma-bound copper-containing oxidase in diatoms (Maldonaldo 2006) and various microalgaes (Kong 2022). In bacteria, copper regulation could be governed by several genes including *copA, cueO,* and *cusCFBA*, which encode a P-type ATPase, a Multicopper Oxidase, and a Copper Efflux Pump, respectively (Rensing and Grass 2003). Depth dynamics play a crucial role in metal availability in marine environments, and although not a variable in this study, does suggest that metals are not expected to be stressful in surface samples and therefore, their resistance genes may be less abundant.

Estuaries model an environmental mixing zone where freshwater inflow meets seawater, and this often causes metals to accumulate due to differences in redox potential, solubility and pH (Muller and Forstner 1975). Estuarine metal accumulation is affected greatly by the source of pollution, which is often anthropogenic (De Souza Machado et al. 2016) Wastewater from neighboring industrial and agricultural operations does appear to impact the metal content in nearby estuaries to some extent, even if the source is found much further upstream (Hossain et al. 2019). Estuaries neighboring major cities with a high population density were found to be more contaminated by metals than coasts without major cities (Chakraborty et al. 2014). This may reflect the role industrialization plays in contaminant exposure. In China, it is reported that heavy industrialization has increased the metal content in industrial and domestic wastewater which is causing a similar accumulation in nearby estuaries (Pan and Wang 2012). Further, elevated concentrations of zinc and chromium in the Yangtze River estuary significantly influenced the microbial community composition at the phylum level, while only zinc appeared to be significant for lower taxonomic levels (Yi et al. 2021). While sulfur-cycling community members such as those in the order *Desulfobacteriales* were focused on, it is likely they can tolerate higher amounts of zinc compared

to other community members, which could explain their dominance here. As taxa may change, the necessary function to resist zinc stress was still present and widely abundant. Estuaries due to their chemistry and proximity to people could provide valuable insights into the environmental co-selection of MRGs and ARGs.

Characterization of the global resistome has been conducted largely in soils. In global soils, it was found through a random forest algorithm that various anthropogenic sources, primarily population density, land use, and agriculture explained the profiles of annotated microbial sequences from nearly 1088 samples. The most frequently observed resistance genes were for multidrug systems (Zheng et al. 2022), but their database did not include MRGs. Subsequently, the aquatic resistome was characterized in freshwater and marine environments and it was found that bacitracin resistance genes, followed by multidrug were more abundant in marine samples compared to freshwater (Yang et al. 2019). In some estuary environments, salinity negatively correlated with MRGs and ARGs (Lu and Liu 2021), but in other studies involving sediments, salinity was one of the main factors driving the reported ARG profiles (Zhang et al. 2019). More data is needed to explore this in aquatic environments, and if differences are site-specific or a phenomenon with salinity, where it could further contribute to MRG and ARG co-selection.

This thesis explores the aquatic resistome to gain a further understanding of the abundance and diversity of MRGs and ARGs within and between aquatic environments considering geography as a variable. Here, it is expected that aquatic ecosystems will reflect the surrounding environmental conditions and areas with high abundances of ARGs and MRGs may be experiencing higher stress from anthropogenic activity and wastewater input and thus, a higher potential for co-selection and spread of antibiotic resistance. Further, co-occurrence patterns between ARGs and MRGs are revealed via network analysis to uncover new relationships between MRGs and ARGs that exist here. Lastly, the interactions between the heavy metal chromium Cr(VI), marine salts, and antibiotic resistance are assessed within the environmental isolate *Arthrobacter aurescens* TC1

CHAPTER 1: BIOGEOGRAPHICAL ASSESSMENT OF AQUATIC ARG, MRG, AND MGE ABUNDANCE AND DIVERSITY

1.1 Introduction

Cross-resistance between ARGs and MRGs may be implemented by dual-action efflux pumps and coupled transcriptional regulation. It is well-understood in clinical pathogens (Mata et. al 2000), and only within the last 20 years or so has this begun to be studied in environmental isolates (Perron et al. 2004; Di Cesare et al. 2016). Fluctuations in water chemistry can affect the concentrations of metals and antibiotics; therefore, impacting their accumulation and mobility in the surrounding environment (Emerson and Weiss 2004; Sanders et al. 2012). Little insight is given into the genomic content, where there traditionally has not been a quantitative metric outside of qPCR to define ARGs and MRGs due to limitations in resource allocation, time, and available personnel, making large geographic characterization difficult. The advent and improvement of next-generation sequencing technologies has resulted in the generation of billions of metagenomic sequences that get published to databases like the SRA and MG-RAST, and this provides new means to analyze trends without sample collection. The Antibiotic Resistance Genes Online Analysis Platform (ARGS-oap) implements a command-line shotgun sequencing annotation software based on customized database mappings to report the abundance of genes mapping to ARGs and MRGs normalized against the abundance of 16s rRNA gene copies. This method scales the abundances to the estimated number of bacterial cells, which is comparable to qPCR-based methods (Yang et al. 2016).

ARG and MRG abundance and diversity across environments is complex, yet many studies suggest that anthropogenic variables like industrial activity and various waste-management strategies contribute to local and geographic differences in the core resistome (Pei et al. 2006; Wright et al. 2008;

Chakraborty et al. 2014; Berglund 2015; Keely et al. 2022; Zheng et al. 2022). Here, trends in ARG and MRG relative abundance across geographies as well as three aquatic ecosystem subtypes (marine, estuary, and freshwater) are analyzed to see if certain water bodies are more likely to harbor ARGs, MRGs, and their potential carrier MGEs.

1.2 Research Question

Do MRG and ARG abundances and diversity vary in aquatic environments and by geographic stratifications such as country, continent, and hemisphere?

1.3 Hypotheses

(1) Estuarine environments will have the most diverse and abundant repertoire of metal and antibiotic resistance genes since their chemistry and location as a "middle-man" receives freshwater inflow that dilutes downstream marine waters, causing a build-up of metal and antibiotic waste.

(2) I hypothesize that ARG and MRG abundance also vary geographically based on hemisphere sampled (north, east, south, and west) and the highest gene abundance would be from the Northern and Eastern Hemispheres, since waters from Asia may be more likely to reflect the highly populated, highly industrialized, and highly polluted atmospheres.

1.4 Methods

Database preparation

The Bacterial Metals and Biocides Experimentally confirmed (2.0) and Structured Antibiotic Resistance Genes (2.0) databases were downloaded via the command-line in fasta format. The two databases were combined using the "cat" command and re-directed into a new text file for analysis. To avoid redundancy, seqkit v.2.8.0 (Shen et al. 2016) was used to remove redundant nucleotide entries that were 100% similar, only keeping one respective entry of the gene. For each gene, a customized mapping file was generated based on the database annotation. This file mapped each gene back to the compound it

confers resistance to, allowing for broader comparisons to be made if more than one gene conferred resistance to a compound.

A third, manually curated database of mobile genetic elements (MGEs), including integrase, transposons and plasmid entries was downloaded separately but not combined with the SARG and BacMet databases. In the combined database for BacMet and SARG, a customized list of integrase genes was initially included but did not appear at all in the final output due to issues with older file formatting that were not realized until after; therefore, the data was analyzed again using the custom MGE database and mapping file to include missing MGEs (Pärnänen et al. 2018; Delgado-Baquerizo et al. 2022).

Acquisition of shotgun-sequencing metagenomes & quality control

Shotgun metagenomes were first searched for using the MG-RAST server by performing key-term searches including environments with "seawater", "marine", "ocean", freshwater", "estuarine", "brackish", "pond", or "river" in the name. This generated a comprehensive metadata file of sequencing sets including their descriptions, geographic coordinates, and the date the sample was taken. The projects were further filtered to only include paired and single end reads from Illumina sequencing platforms, projects that were not metatranscriptomes, and did not come directly from a wastewater treatment site to limit biases or strong outlier samples in the results. A custom command line script was used to automate the download of the metagenomes using the python helper scripts included in MG-RAST-Tools v.0.1.1 (Paczian et al. 2019). Similarly, additional SRA studies were also included which met the same criteria as above, but data were downloaded using an automated script incorporating the SRA-Toolkit v.3.1.1(https://github.com/ncbi/sra-tools). SRA data were downloaded and analyzed February 20th, 2024, and MG-RAST data October 18th, 2023.

One hurdle faced here is that it is often not possible to pull raw, user-submitted fastq files from the MG-RAST server. Data was pulled from the middle of the pipeline after it had been trimmed using SolexaQA as part of the MG-RAST analysis pipeline, and entries were also filtered for contamination using bowtie against user-specified genomes (such as *E. coli* or most commonly the human genome),

meaning they downloaded with quality control parameters in place. For SRA data, raw fastq files were downloaded and the paired-end reads were trimmed using default fastp v.0.23.4 (Chen et al. 2018) parameters with a Phred score quality threshold ≥ 20. For MG-RAST data, the number of sequences remaining after filtering with SolexaQA was reported. All relative abundances are reported as the average copy of a resistance gene per copy of the 16s rRNA gene, which is also normalized further for sequencing depth by dividing each relative abundance by the size of the sequencing library for each project.

Before analysis, each metagenome was also renamed to keep track of which project the metagenome came from, making it easier to batch large numbers of metagenomes from multiple projects to run at the same time. This was accomplished using a custom bash script that appended the project identifier to each of the metagenomes located in its directory. From here, all the metagenomes were moved to one singular directory for subsequent analysis. The final dataset (Figures 1 and 2) included data from over 18 unique countries and 7 continents including Antarctica and Oceania, spanning aquatic

environments comprising freshwater, marine and estuary samples.

Figure 1: *Global map of MG-RAST and SRA projects included in this analysis. Yellow samples represent marine ecosystems, red samples represent freshwater ecosystems and purple estuarine ecosystems.*

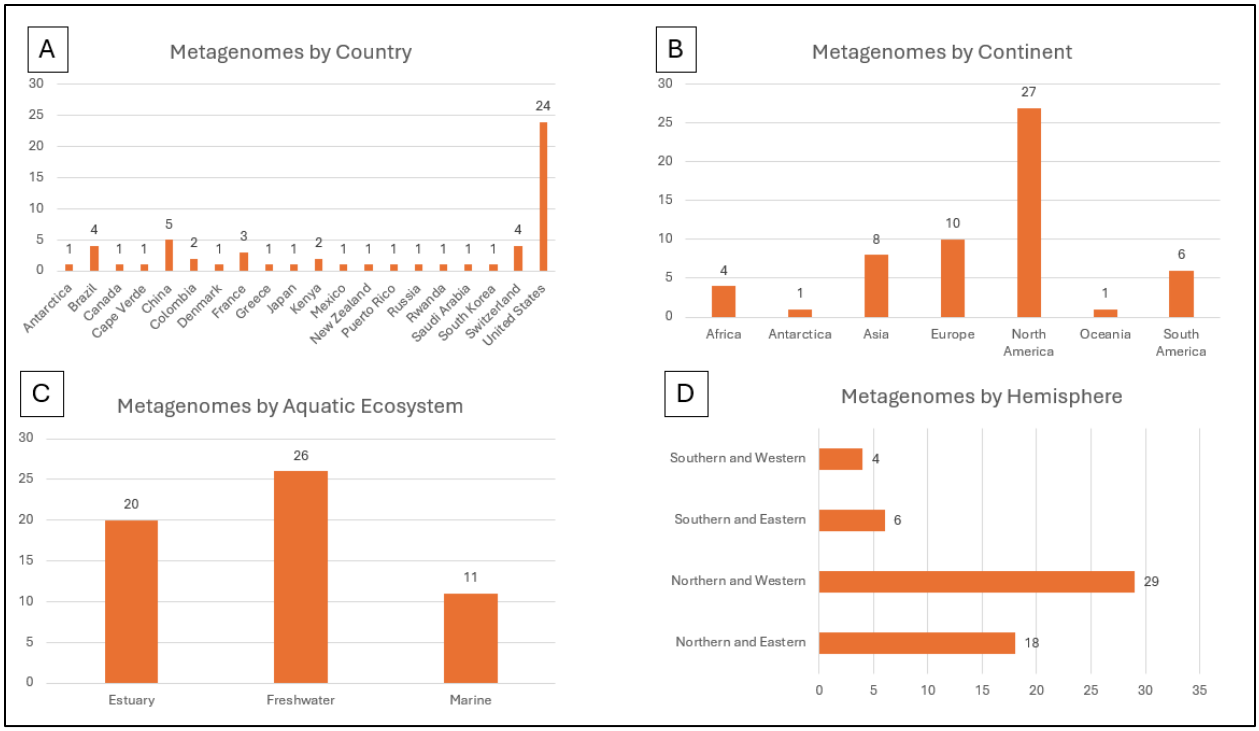

Figure 2: *Sample sizes of metagenomes when stratified by (A) country, (B) Continent), (C) Ecosystem, and (D) Hemisphere*

Annotation of shotgun metagenomes & post-processing

The aquatic shotgun sequences were analyzed with the ARGs-OAP 3.0 pipeline (Yang et al. 2016), ran via the command line on ECU's High Performance Computing Core. This program utilizes blastx searches to align the shotgun sequences to the database entries. The parameters for annotation were a minimum alignment length of 25 amino acids, 80% sequence similarity, and an E-value cut-off of 1 x 10^{-5} (Delgado-Baquerizo et al. 2022). MRG, ARG and MGE gene abundances were displayed in a variety of formats, but normalization against the number of 16s rRNA gene copies was used since it is the closest estimate to the number of bacterial cells per sample. The final output of ARGs-OAP also combines the gene information into larger "type" categories, as well as outputting the individual abundance of each gene in the database, which are labeled as "subtypes". These files were combined using the left_join parameter of R Studio's Dplyr package (Witham et. al 2023) to create two master files: one for the gene types and then one for the subtypes. From here, each metagenome of the same project was combined and then averaged together, where the average represented the sum of each individual type or subtype divided

by the total number of metagenomes that were annotated per project. This was done to avoid pseudo replicating metagenomes across the various geographic and ecosystem-level comparisons primarily because technical or biological replication was not easily discernible from the sequencing metadata.

Statistical analyses & visualizations

Assessing significance & boxplots

The final dataset was analyzed using R Studio (2023.12.01.402). Significant differences between relative gene abundance for select MRGs and ARGs were assessed using a non-parametric, 1-tail Wilcox test, and boxplots of the mean rank abundance per 16s rRNA gene copy were plotted using the ggpubr and ggplot2 packages. A comparison was considered significantly different if $p < 0.05$. While the boxplots represent the mean rank and distribution of the datapoints as a 5 number summary, the mean rank is also presented as a boxplot without error bars. This was included primarily due to extreme data points that fell outside of the boxplot range but were still included within the mean rank calculation.

Distances and diversity measures

Beta-diversity and alpha-diversity estimates were calculated using the vegan package v.2.6-6.1 to assess significant differences in the composition of ARGs/MRGs between samples and within samples, respectively. The beta-diversity was estimated via the Bray Curtis dissimilarity index, and the results plotted using NMDS ordination. To assess the impact of geographic stratification on the composition of the resistome, PERMANOVA was run with 999 permutations using country, continent, hemisphere, and ecosystem as groupings. The Shannon and Simpson diversity indexes were both represented, as the Shannon diversity estimate could be helpful in estimating diversity with respect to rare ARGs and MRGs present only at some sites, while the Simpson index could be more helpful in estimating diversity based on the total abundance of each gene at each site.

Selection of metavariables

Five metavariables were chosen to fit as environmental vectors onto the NMDS ordination plot via multiple regression analysis. They include the total abundance of class I integrase, the population density per square kilometer of land (World Bank), the amount of CO_2 emissions per year in kilotons (World Bank), the percentage of the population that has access to wastewater treatment (OECD), and an ecological footprint rank estimating ecological stewardship (Global Footprint Network). The metavariables were collected by the year the project was sampled, and at the country level of stratification.

1.5 Results

Abundance of ARGs and MRGs

To assess differences in ARG abundance between aquatic environments, the dataset was first subset by freshwater, estuary, and marine ecosystems (Figure 3). When compared to freshwater environments, estuaries carried a significantly higher number of resistance genes for bacitracin and polymyxin resistance ($p<0.05$) with average abundances at 1.24×10^{-8} and 2.61×10^{-8} per 16s rRNA gene, respectively, but were not significantly different in resistance gene abundance for genes related to multidrug, tetracycline, vancomycin, beta lactam, aminoglycoside, or sulfonamide resistance ($p>0.05$). However, when compared to marine environments, estuaries carried a significantly higher amount of bacitracin, polymyxin, and tetracycline resistance genes ($p<0.05$) with average abundances of 1.24×10^{-8}, 2.61×10^{-8}, and 1.75×10^{-10} 16s rRNA gene, respectively, but were not significantly different in the abundance of multidrug, vancomycin, beta lactam, or sulfonamide ($p>0.05$). Freshwater environments in comparison to marine environments had significantly higher abundances of bacitracin, tetracycline, aminoglycoside, and sulfonamide resistance genes at 2.57×10^{-9}, 1.12×10^{-9}, 9.94×10^{-10}, and 4.19×10^{-9} copies per 16s rRNA gene, respectively ($p<0.05$), but were not different in the abundance of multidrug, polymyxin, vancomycin, and beta lactam resistance ($p>0.05$). The most abundant ARG corresponded to

beta lactam resistance at 7.59 x 10^{-6} copies per 16s rRNA gene, while the least abundant ARG corresponded to vancomycin at 3.08 x 10^{-13} copies per 16s rRNA gene (Figure 4).

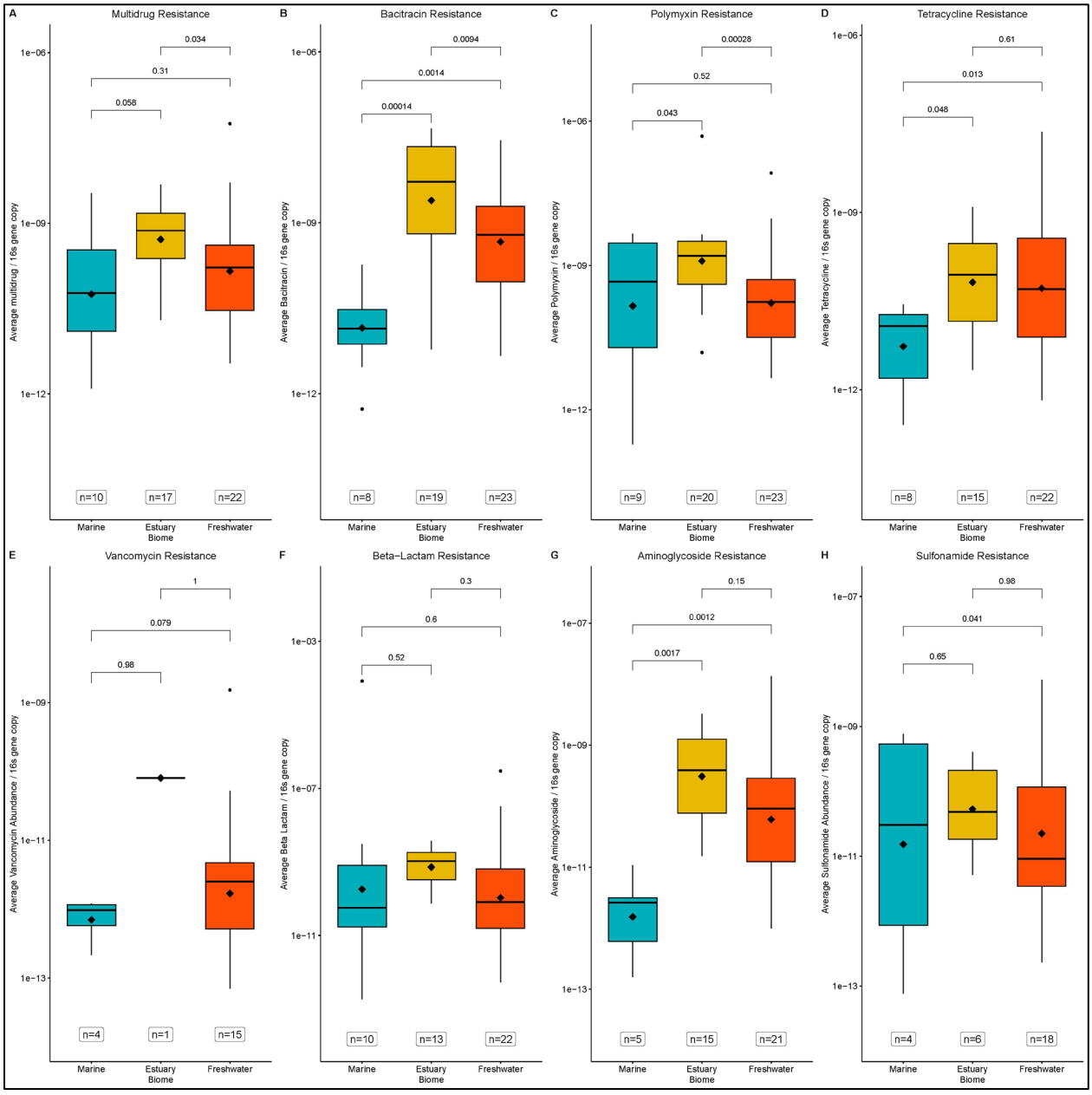

Figure 3*: Relative abundance of ARGs across aquatic ecosystems. (A) multidrug, (B) bacitracin, (C) polymyxin, (D) tetracycline, (E) vancomycin, (F) beta-lactam, (G) aminoglycoside, (H) sulfonamide. The abundances represent the average relative abundance of each ARG type per sequencing project, normalized by the total number of reads for that project reported by ARGs-oap (v.3.0). The mean of each category is represented as a black diamond.*

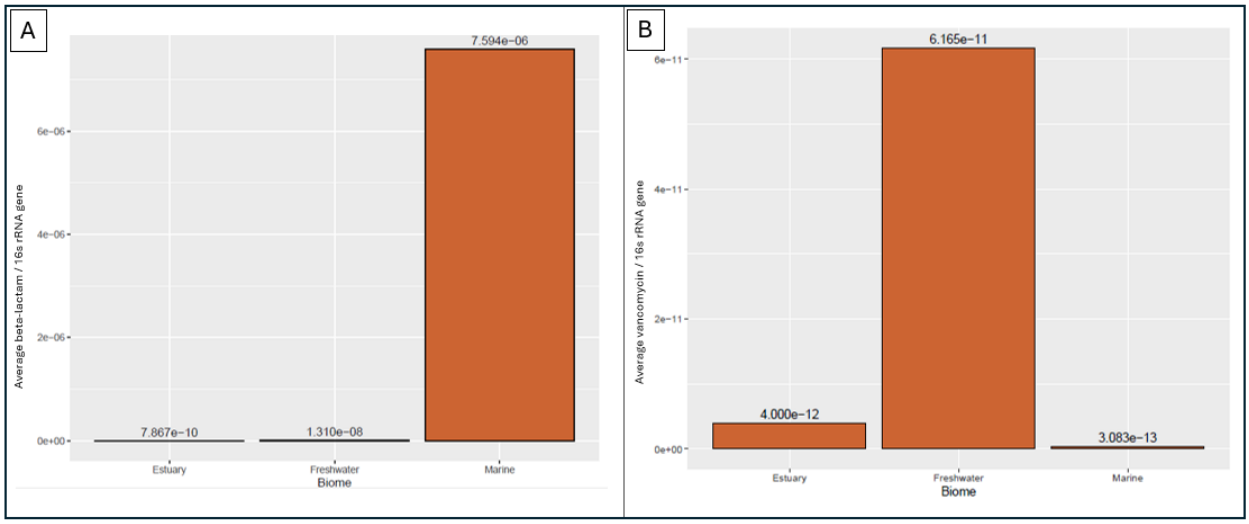

Figure 4: *(A) Mean of beta-lactam resistance genes and (B) mean of vancomycin resistance genes across aquatic ecosystems.*

For MRGs within aquatic ecosystems (Figure 5), zinc, chromium, iron, arsenic and lead resistance genes were all elevated in estuary samples in comparison to both freshwater and marine environments ($p<0.05$, Wilcox Test) with average abundances per 16s rRNA gene copy at 5.84×10^{-10}, 4.48×10^{-9}, 6.95×10^{-9}, 1.00×10^{-8}, and 8.16×10^{-10}, respectively. In freshwater samples, copper is elevated in comparison to both marine and estuary samples with an average abundance per 16s rRNA gene copy of 4.26×10^{-8} ($p<0.05$). Interestingly, cadmium resistance genes were not detected in any of the marine samples but were significantly elevated in freshwater samples compared to estuary samples with an average abundance of 4.68×10^{-12} copies per 16s rRNA gene ($p<0.05$, Wilcox Test). The abundance of mercury resistance genes was not significantly elevated in any aquatic ecosystem ($p>0.05$, Wilcox Test). The most abundant MRG corresponded to arsenic resistance at 1.00×10^{-8} copies per 16s rRNA gene, although copper resistance genes were close at 1.41×10^{-8} copies per 16s rRNA gene. The least abundant MRG corresponded to cadmium resistance at 6.5×10^{-13} copies per 16s rRNA gene (Figure 6).

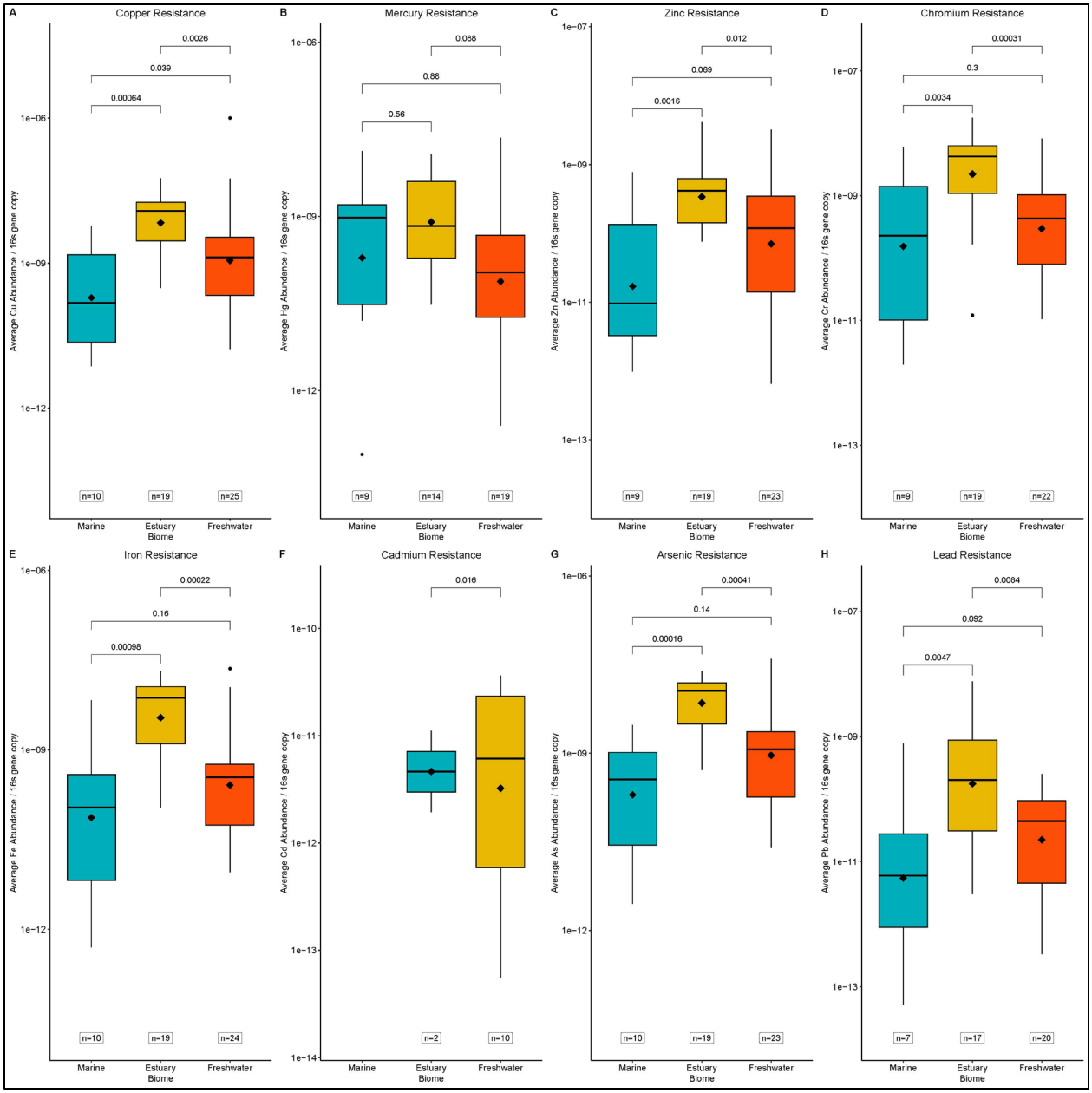

Figure 5: *Relative abundance of MRGs across marine, estuary and freshwater ecosystems (A) copper, (B) mercury, (C) zinc, (D) chromium, (E) iron, (F) cadmium, (G) arsenic) and (H) lead. The abundances represent the average relative abundance of each MRG type per sequencing project, normalized by the total number of reads for that project reported by ARGs-oap (v.3.0). A bracket represents a comparison of significance using a 1-tail Wilcox test. The mean of each category is represented as a black diamond.*

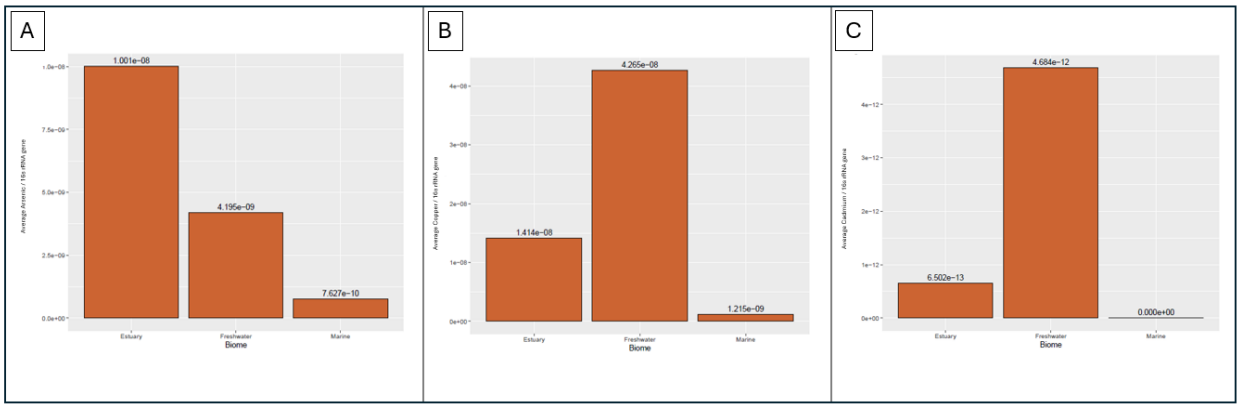

Figure 6: *(A) Mean of arsenic resistance genes, (B) mean of copper resistance genes, (C) mean of cadmium resistance genes by aquatic ecosystem.*

To display differences in ARG abundance and distribution, countries with enough data to construct the corresponding five number summary were chosen to display (Figure 7). In other words, samples that had a big enough sample size to compute a minimum value, first quartile, median value, third quartile and a maximum value. The countries included were the United States, Brazil, Switzerland, France, Kenya, and China. There were no reported differences in ARG abundance across these countries for multidrug, bacitracin, polymyxin, vancomycin, beta-lactam, and aminoglycoside resistance ($p>0.05$, Kruskal-Wallis Test). The two significantly different ARGs corresponded to tetracycline and sulfonamide resistance ($p<0.05$, Kruskal-Wallis Test). Within this, Kenya was significantly elevated in sulfonamide resistance with an average abundance of 3.28×10^{-9} copies per 16s rRNA gene compared to both China and the United States ($p<0.05$, Wilcox Test), but was not significantly different in sulfonamide resistance gene abundance compared to France ($p>0.05$, Wilcox Test). Kenya was also significantly elevated in average tetracycline abundance with 1.18×10^{-8} copies per 16s rRNA gene compared to China, The United States, and Switzerland ($p<0.05$, Wilcox Test) but not France ($p>0.05$, Wilcox Test). The most abundant ARG corresponded to polymyxin resistance in Colombia at 2.45×10^{-7} copies per 16s rRNA and the least abundant for vancomycin resistance in Canada at 1.69×10^{-14} copies per 16s rRNA gene (Figure 8). The MRGs (Figure 8) were not significantly different in the abundance of copper, zinc, chromium, iron, arsenic, mercury, lead nor cadmium resistance ($p>0.05$, Kruskal-Wallis Test). The most abundant MRG corresponded to copper resistance in Denmark at 1.00×10^{-6} copies per 16s rRNA gene

and the least abundant for cadmium resistance in Canada at 3.78 x 10^{-13} copies per 16s rRNA gene (Figure 10).

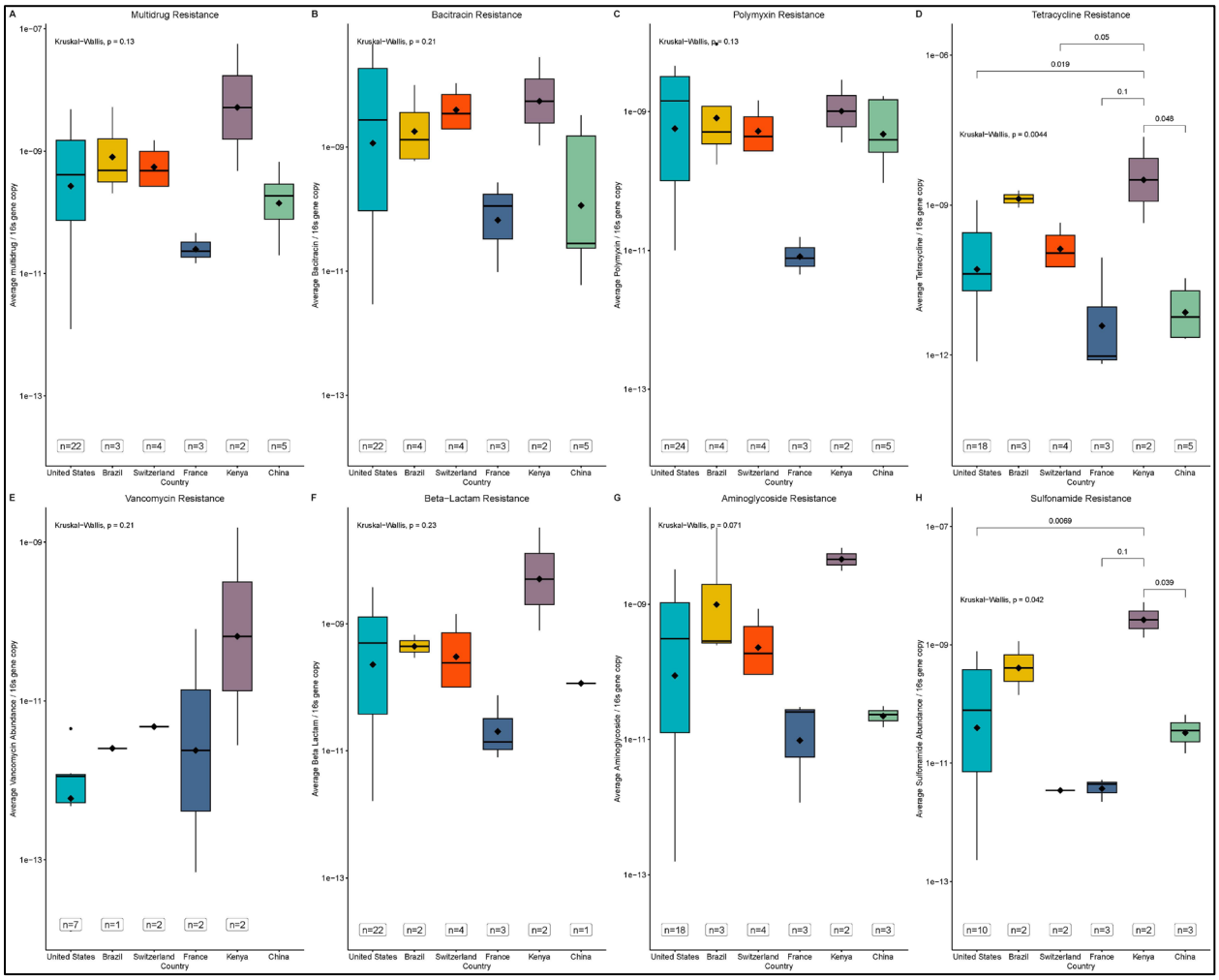

Figure 7*: Relative abundance of ARGs across countries with enough information to create a boxplot. (A) multidrug (B) bacitracin, (C) polymyxin, (D) tetracycline, (E) vancomycin, (F) beta-lactam, (G) aminoglycoside, (H) sulfonamide. The abundances represent the average relative abundance of each ARG type per sequencing project, normalized by the total number of reads for that project. A bracket represents a comparison of significance using a 1-tail Wilcox test (in this plot, only sulfonamide and tetracycline). The mean of each category is represented as a black diamond.*

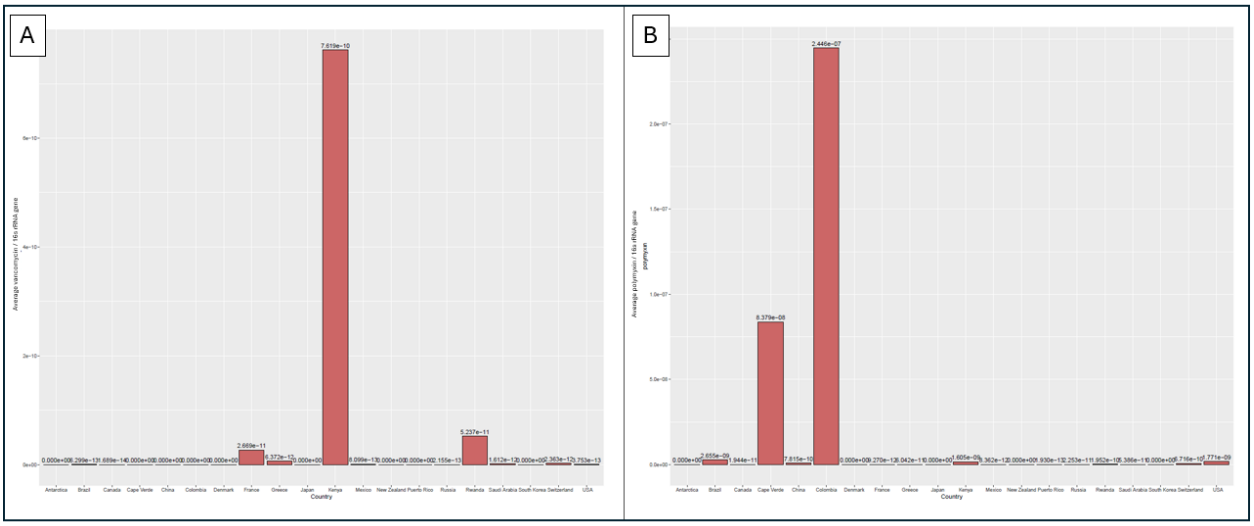

Figure 8: *(A) mean of vancomycin resistance genes and (B) mean polymyxin resistance genes across countries.*

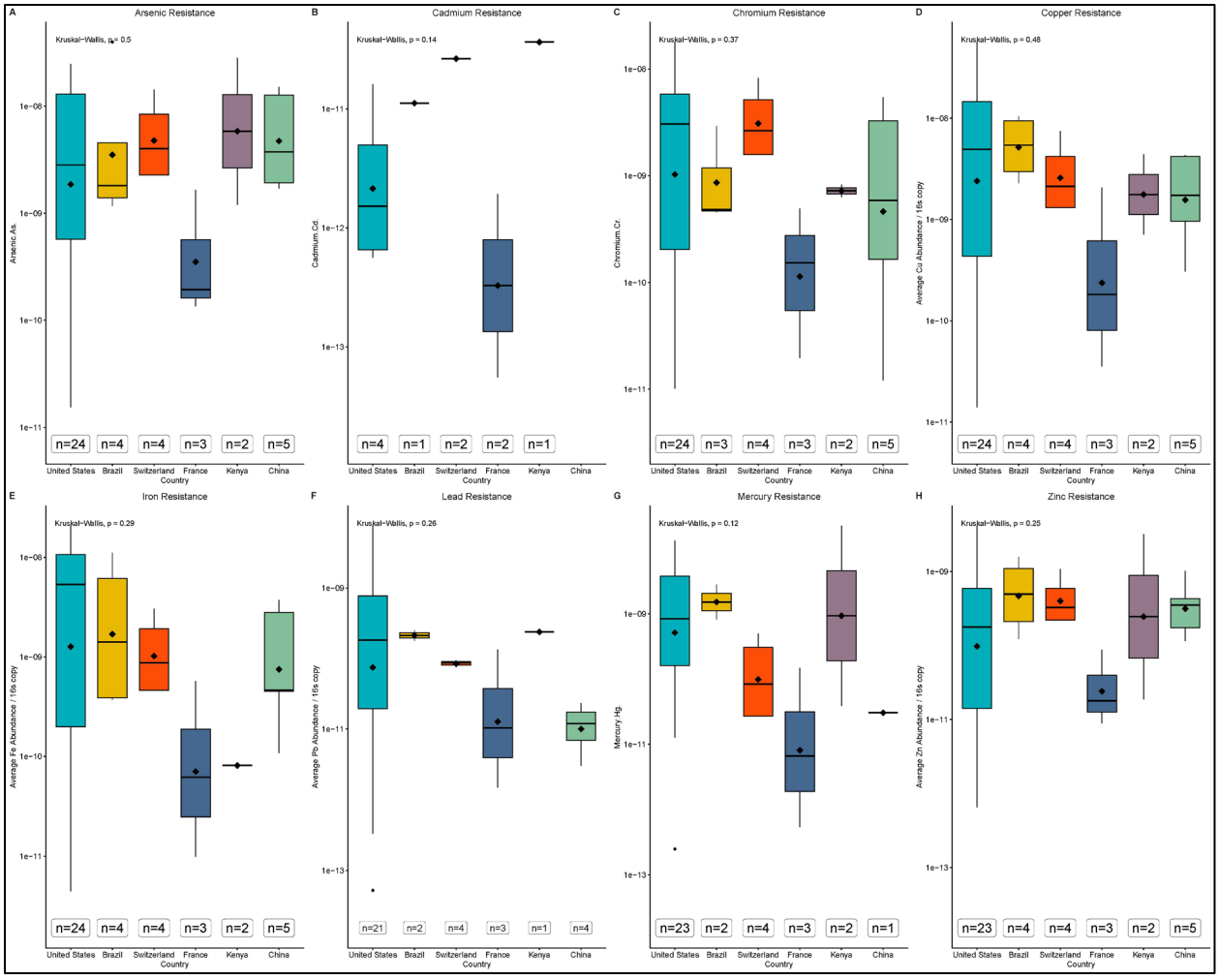

Figure 9: *Relative abundance of MRGs across countries with enough information to create a boxplot (A) arsenic, (B) cadmium, (C) chromium, (D) copper, (E) iron, (F) lead, (G) mercury, (H) zinc. The abundances represent the average relative abundance of each MRG type per sequencing project, normalized by the total number of reads for that project. The mean of each category is represented as a black diamond.*

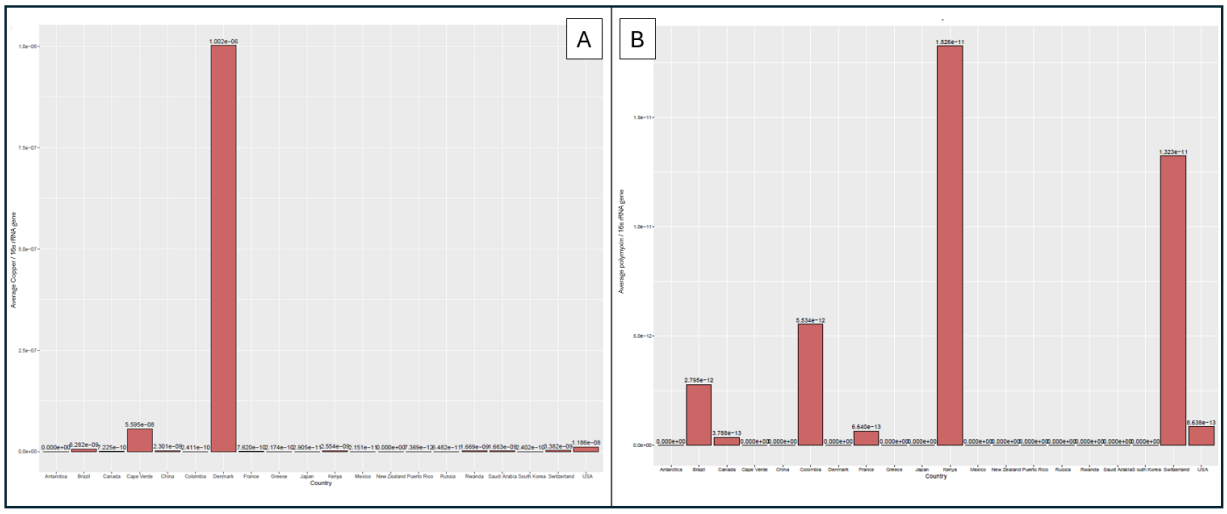

Figure 10: *(A) mean of copper resistance genes and (B) mean of cadmium resistance genes by country.*

The dataset was further stratified to the continent level to combine information from multiple countries. Still, differences in ARG abundance are evident again with tetracycline and sulfonamide resistance (Figure 11). The abundance of sulfonamide resistance genes was significantly elevated ($p<0.05$, Wilcox Test) in samples coming from Africa (now comprising Kenya, Rwanda, and Cabo Verde) compared to samples coming from North America (comprising New Mexico, the USA and Canada). Additionally, sulfonamide resistance genes were elevated ($p<0.05$, Wilcox Test) in Africa compared to Asia (comprising China and Saudi Arabia only). The abundance of tetracycline resistance genes was significantly different between continents ($p<0.05$, Kruskal-Wallis Test) but subsequent testing suggested that no statistical evidence supported that the genes were elevated between any two continents ($p>0.05$, Wilcox Test). This is likely because a one-tail hypothesis test has more statistical power to reject a false null hypothesis compared to a two-tail hypothesis test. Multidrug, bacitracin, polymyxin, vancomycin, beta lactam, and aminoglycoside resistance gene abundances were not significantly different between continents ($p>0.05$, Kruskal-Wallis Test). The continent of Antarctica did not have a single annotation for any of the ARGs (an abundance of 0), except for beta-lactam resistance, which was the highest of all sampled continents at an average abundance of 8.35×10^{-5} copies per 16s rRNA gene (Figure 12). Additionally, these samples did not have any MRGs annotated. The continent of Oceania did not have a single annotation for any ARG or MRG visualized here (but has annotations for some multi-

metal and biocidal resistance genes not presented in these figures), and further, the total abundance of MRGs across continents was not significantly different (Figure 12; $p>0.05$, Kruskal-Wallis Test). The least abundant ARG amongst the continents corresponded to vancomycin resistance in Asia at 2.02 x 10^{-12} copies per 16s rRNA gene (Figure 13). The most abundant MRG corresponded to copper resistance in Europe at 1.02 x 10^{-7} copies per 16s rRNA gene, while the least abundant corresponded to cadmium resistance at 7.82 x 10^{-12} copies per 16s rRNA gene (Figure 14).

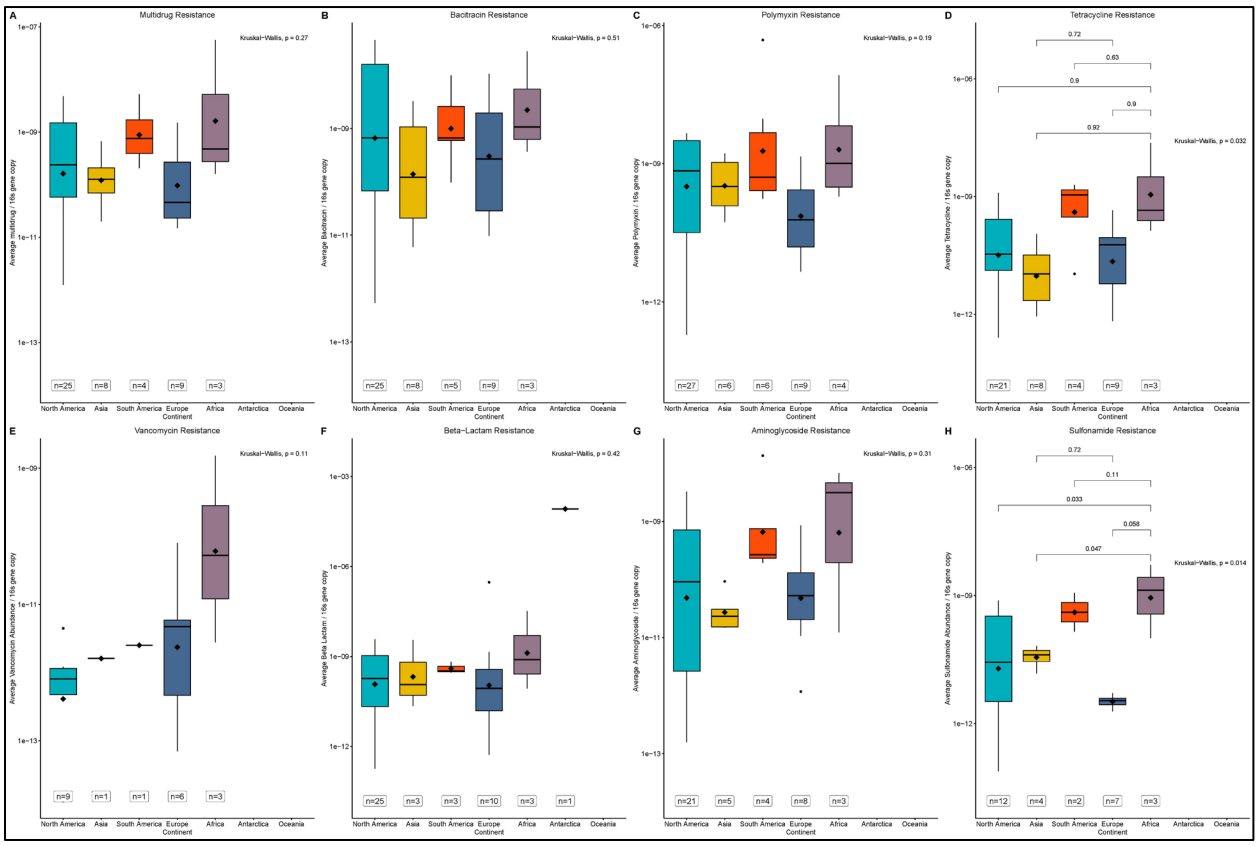

Figure 11: *Relative abundance of ARGs across continents. (A) multidrug, (B) bacitracin, (C) polymyxin, (D) tetracycline, (E) vancomycin, (F) beta-lactam, (G) aminoglycoside, (H) sulfonamide. The abundances represent the average relative abundance of each ARG type per sequencing project, normalized by the total number of reads for that project reported by ARGs-oap (v.3.0). A bracket represents a comparison of significance using a 1-tail Wilcox test (sulfonamide boxplot only). The global p-value for multiple pairwise comparisons is represented as a non-parametric Kruskal-Wallis test on each plot. The mean of each category is represented as a black diamond.*

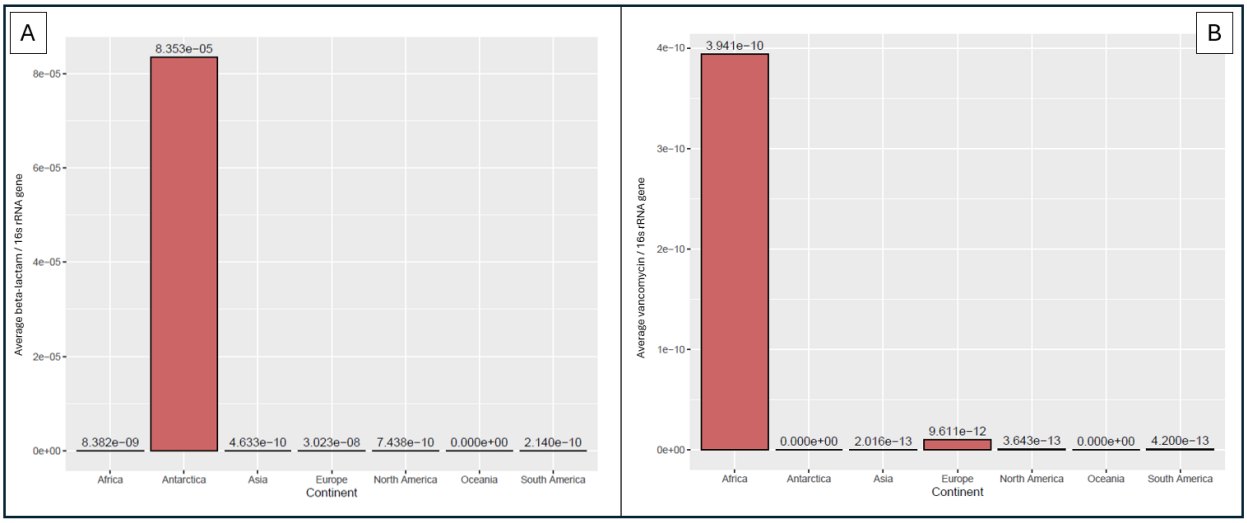

Figure 12: *(A) mean of beta-lactam resistance genes and (B) mean of vancomycin resistance genes across continents.*

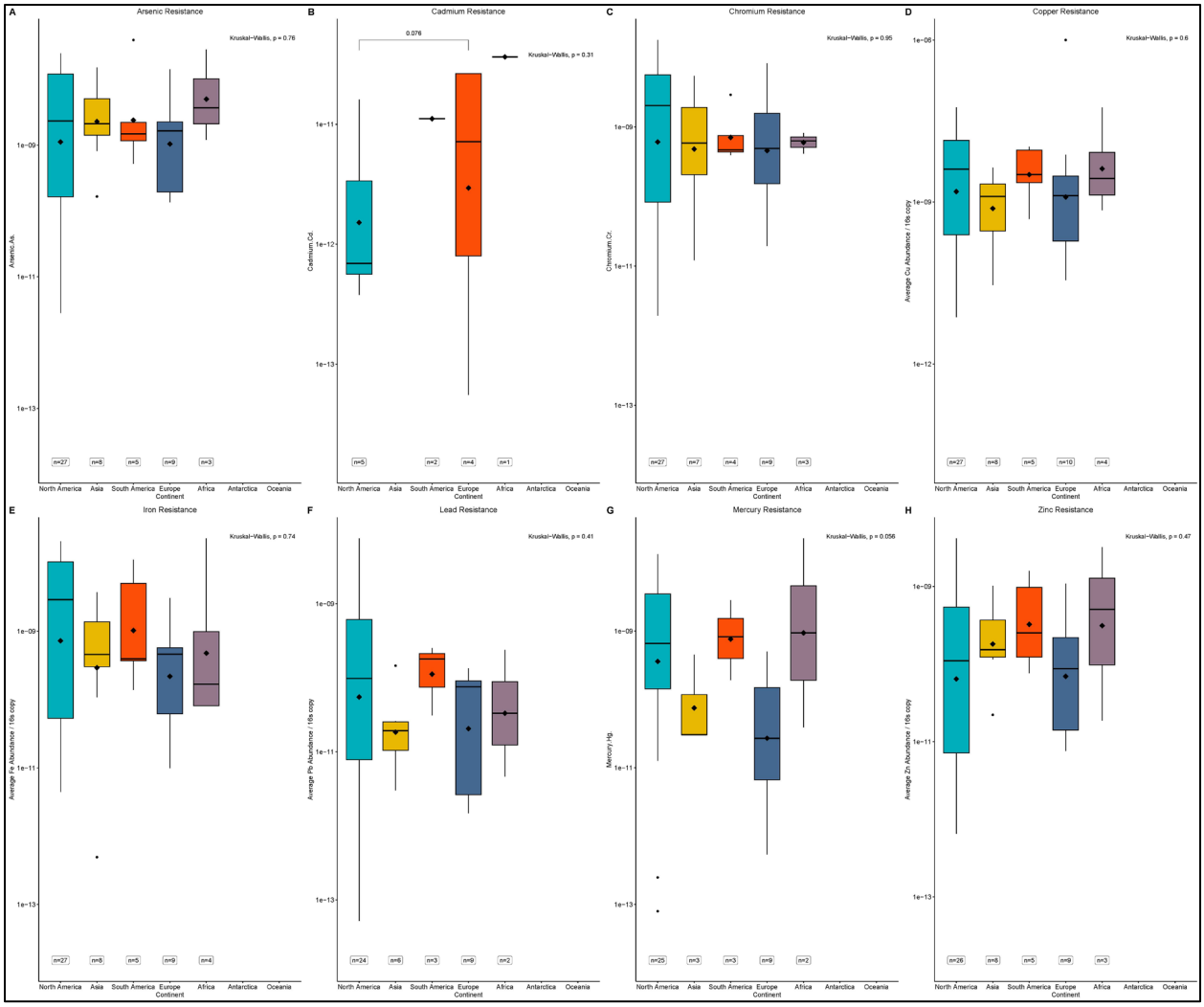

***Figure 13**: Relative abundance of MRGs across continents. (A) arsenic, (B) cadmium, (C) chromium, (D) copper, (E) iron, (F) lead, (G) mercury, (H) zinc. The abundances represent the average relative abundance of each ARG type per sequencing project, normalized by the total number of reads for that project reported by ARGs-oap (v.3.0). The global p-value for multiple pairwise comparisons is represented as a non-parametric Kruskal-Wallis test on each plot. The mean of each category is represented as a black diamond.*

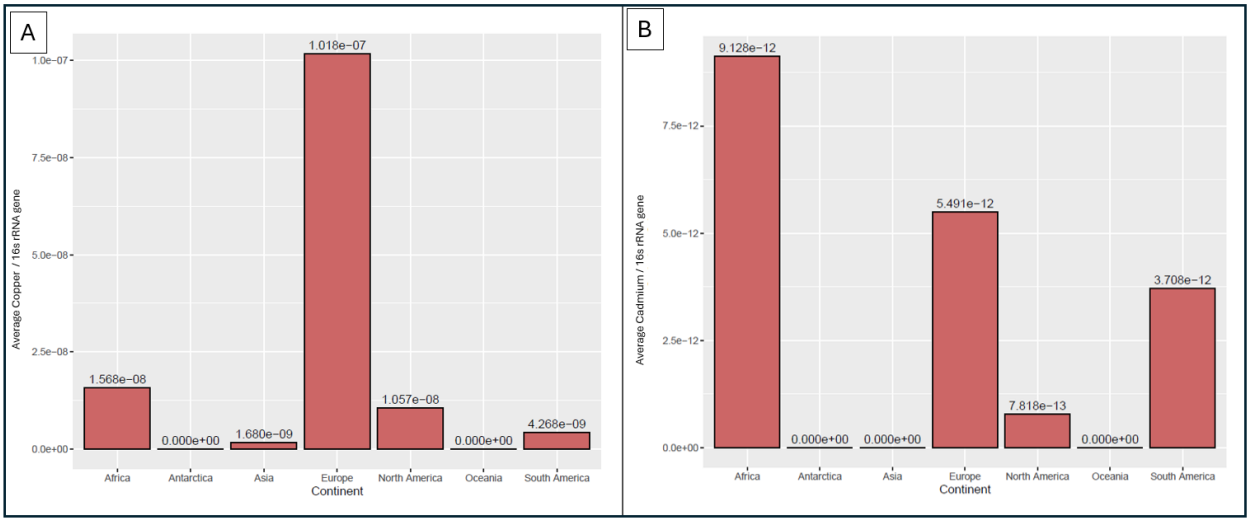

Figure 14: *(A) mean of copper resistance genes and (B) mean of cadmium resistance genes by continent.*

To visualize global differences in ARG and MRG abundance, the data was lastly stratified to the hemisphere level. Amongst this, the ARGs were not significantly more abundant for bacitracin, polymyxin, vancomycin, beta-lactam, and aminoglycoside resistance genes for any of the compared hemisphere groupings (Figure 15; $p>0.05$, Kruskal-Wallis Test). Tetracycline resistance genes were significantly elevated in the Southwestern hemisphere ($p<0.05$, Wilcox Test) with an average abundance of 4.75×10^{-9} copies per 16s rRNA gene compared to the Northwestern hemisphere, while there were no differences between the northwestern and southeastern, and the northeastern and southeastern hemispheres ($p>0.05$, Wilcox Test). For sulfonamide resistance, differences were detected ($p<0.05$, Kruskal-Wallis Test) but there were no differences between any hemispherical comparison ($p>0.05$, Wilcox Test). However, the southeastern hemisphere appears to be approaching significance ($p=0.07$) with a higher gene abundance compared to the northwestern hemisphere indicating more data may help resolve this. Additionally, vancomycin resistance gene abundance was approaching significance ($p=0.055$, Kruskal-Wallis Test), hinting that differences could exist but were not detected by a broad hypothesis test. Nonetheless, subsequent testing revealed that vancomycin resistance genes were elevated in the southeastern hemisphere with an average of 3.15×10^{-10} copies per 16s rRNA gene compared to the northwestern hemisphere ($p<0.05$, Wilcox-Test). The most abundant ARG at the hemisphere level was

for beta-lactam resistance, at 1.67 x 10^{-5} copies per 16s rRNA gene, while the least abundant was for vancomycin resistance at 3.27 x 10^{-13} copies per 16s rRNA gene (Figure 16).

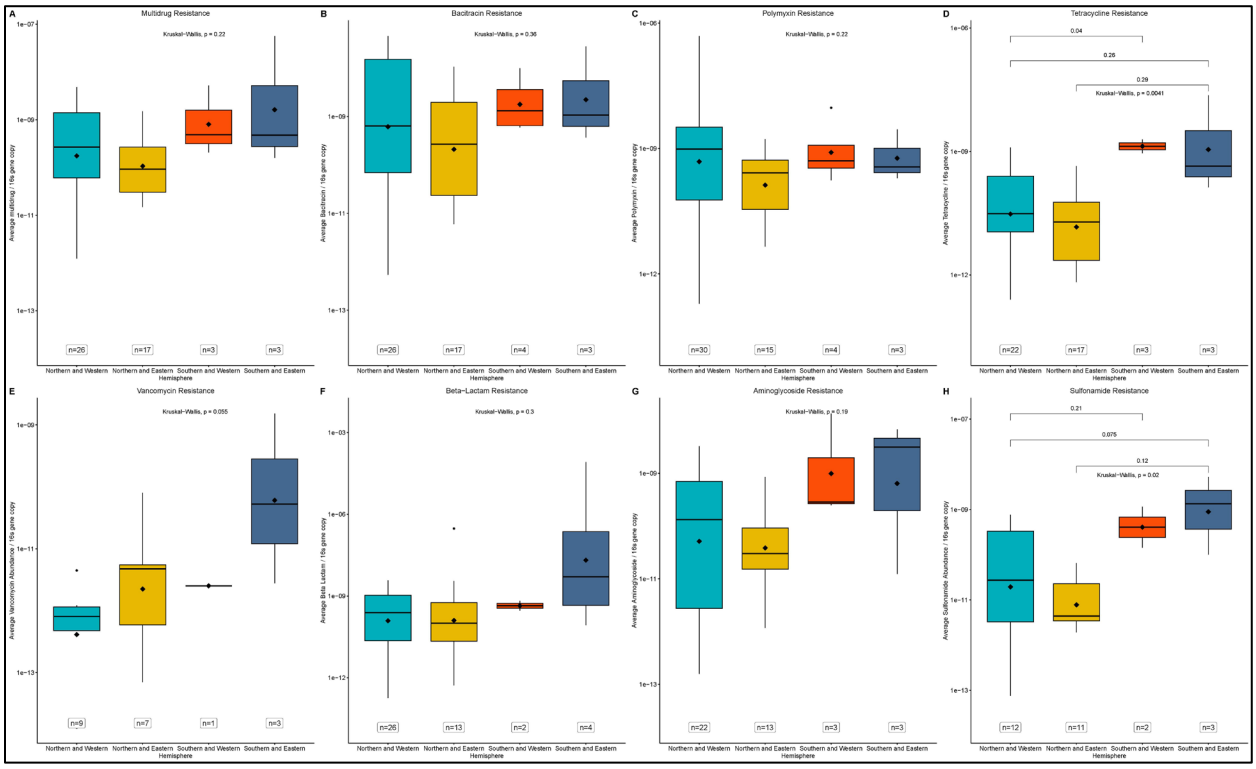

Figure 15*: Relative abundance of ARGs across hemispheres with enough information to create a boxplot. (A) multidrug, (B) bacitracin, (C) polymyxin, (D) tetracycline, (E) vancomycin, (F) beta-lactam, (G) aminoglycoside, (H) sulfonamide. The abundances represent the average relative abundance of each ARG type per sequencing project, normalized by the total number of reads for that project. A bracket represents a comparison of significance using a 1-tail Wilcox test. The global p-value is reported as a non-parametric Kruskal-Wallis test. The mean of each category is represented as a black diamond.*

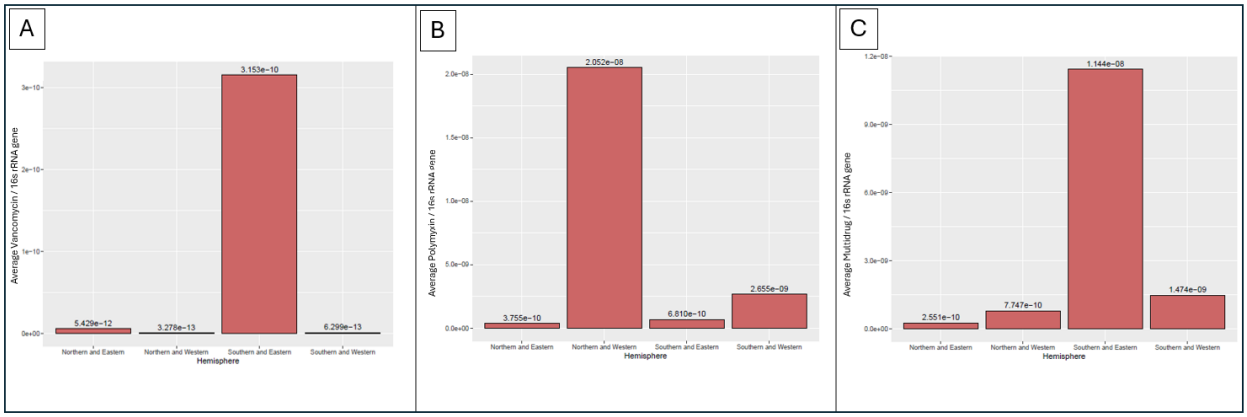

Figure 16: *(A) mean of vancomycin resistance, (B) mean of polymyxin resistance, and (C) mean of multidrug resistance across hemispheres.*

Within the MRGs, there were no differences in the abundance of iron, lead, zinc, arsenic, cadmium, chromium, or copper resistance genes by hemisphere (Figure 17; $p>0.05$, Kruskal-Wallis Test). However, mercury resistance genes were elevated in samples from the northwestern hemisphere with an average abundance of 2.12×10^{-9} copies per 16s rRNA gene compared to those from the northeastern hemisphere. The most abundant MRG corresponded to copper resistance with an average abundance of 5.73×10^{-8} copies per 16s rRNA gene, while the least abundant was for cadmium resistance at 1.07×10^{-12} copies per 16s rRNA gene (Figure 18).

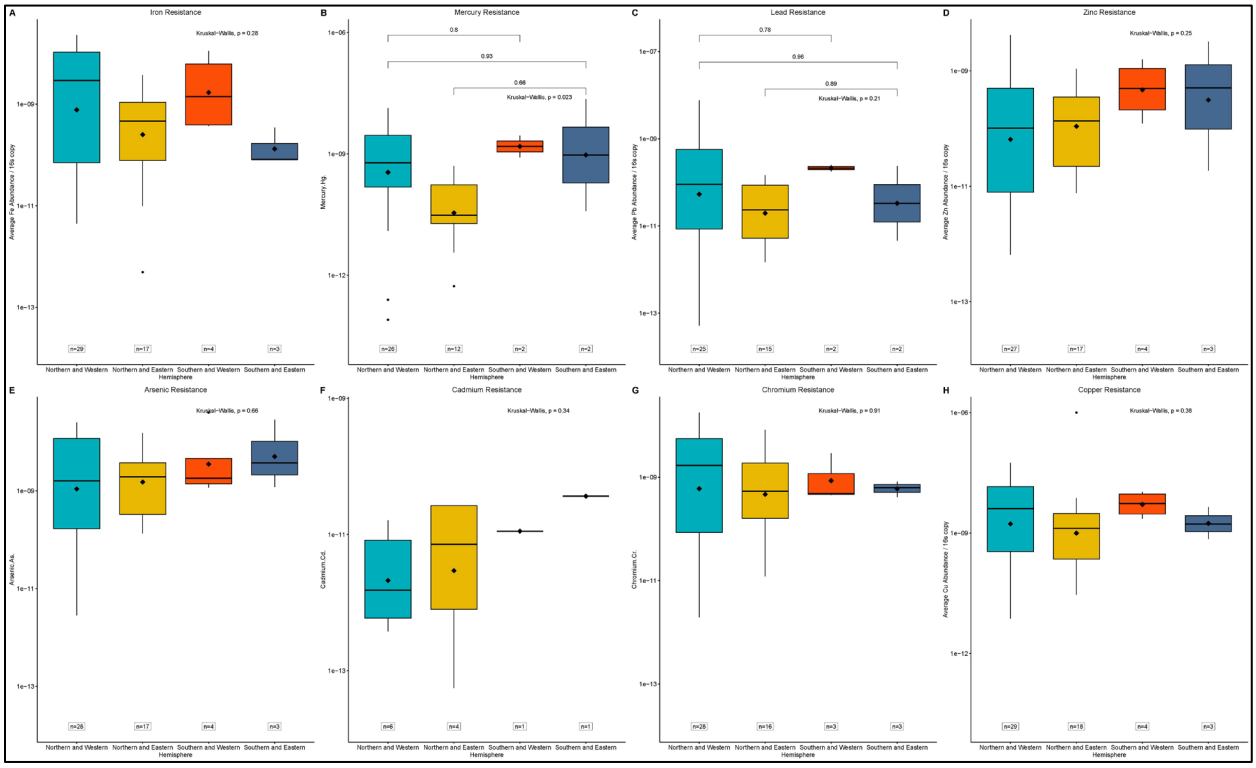

Figure 17: *Relative abundance of MRGs across hemispheres with enough information to create a boxplot. (A) iron, (B) mercury, (C) lead, (D) zinc, (E) arsenic, (F) cadmium, (G) chromium, (H) copper. The abundances represent the average relative abundance of each MRG type per sequencing project, normalized by the total number of reads for that project. A bracket represents a comparison of significance using a 1-tail Wilcox test. The global p-value is reported as a non-parametric Kruskal-Wallis test. The mean of each category is represented as a black diamond.*

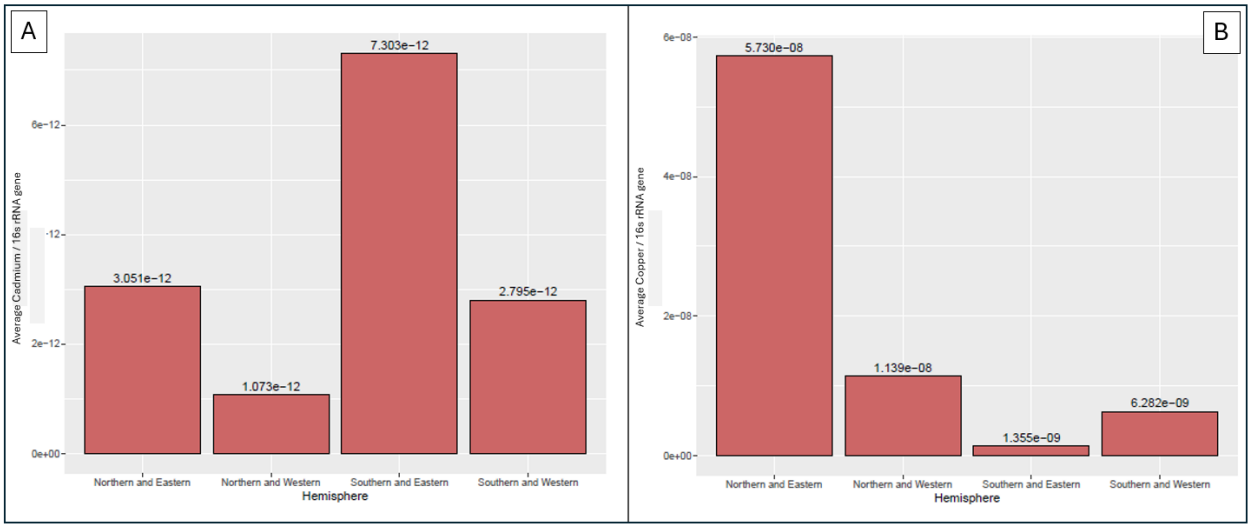

Figure 18: *(A) mean of cadmium resistance and (B) mean of copper resistance across hemispheres*

Abundance of MGEs

To determine if a particular type of mobile genetic element (MGE) was dominant at different geographic scales or the ecosystem level, the total abundance of integrase, transposon, and plasmids were annotated (Figure 19). The total abundance of plasmids was not significantly different across any stratification ($p>0.05$, Kruskal-Wallis Test), yet the highest average was within samples from freshwater ecosystems (Figure 20) at 2.95×10^{-10} copies per 16s rRNA gene. One trend that did not have statistical support but is still worth considering further is that marine samples associated with higher transposase abundance, and most of the gene annotations correspond to marine-associated metagenomes. Estuaries conversely were associated with higher integrase and freshwater samples with plasmids. More data is needed to assess if this could be biologically or statistically relevant (Figure 20).

Next, integrase abundances were significantly different between aquatic ecosystems, between continents and then between hemispheres (Figure 21; $p<0.05$, Kruskal-Wallis Test), but not between countries ($p>0.05$, Kruskal-Wallis Test). However, subsequent statistical testing suggests that the mean rank abundance of integrase between each aquatic ecosystem is not significantly higher in estuaries compared to freshwater or marine sources ($p>0.05$, Wilcox-Test), despite it having the highest average per 16s gene copy at 1.59×10^{-9} (Figure 20). The abundance of integrase was significantly higher in

samples from Asia compared to Europe ($p<0.05$, Wilcox-Test), with an average of 1.25×10^{-11} copies per 16s rRNA gene (Figure 21), but Africa did not contain a significantly higher abundance of integrase compared to the United States nor China ($p>0.05$, Wilcox-Test).

Transposases were also considered to assess a potential viral role in some environments or geographies. Transposase was not significantly different at the ecosystem level ($p>0.05$, Kruskal-Wallis Test), but was significantly different at the country, continent, and hemisphere level of stratification ($p<0.05$, Kruskal-Wallis Test). However, it is likely that this is primarily driven by one interesting sample from Antarctica (Figure 22), which has a relatively high abundance of transposase and is influencing the significance of the test at higher stratifications (especially hemisphere) but was not significantly more abundant likely due to low sample size. However, Antarctica still had a significantly higher abundance of transposase compared to the United States ($p<0.05$, Wilcox Test).

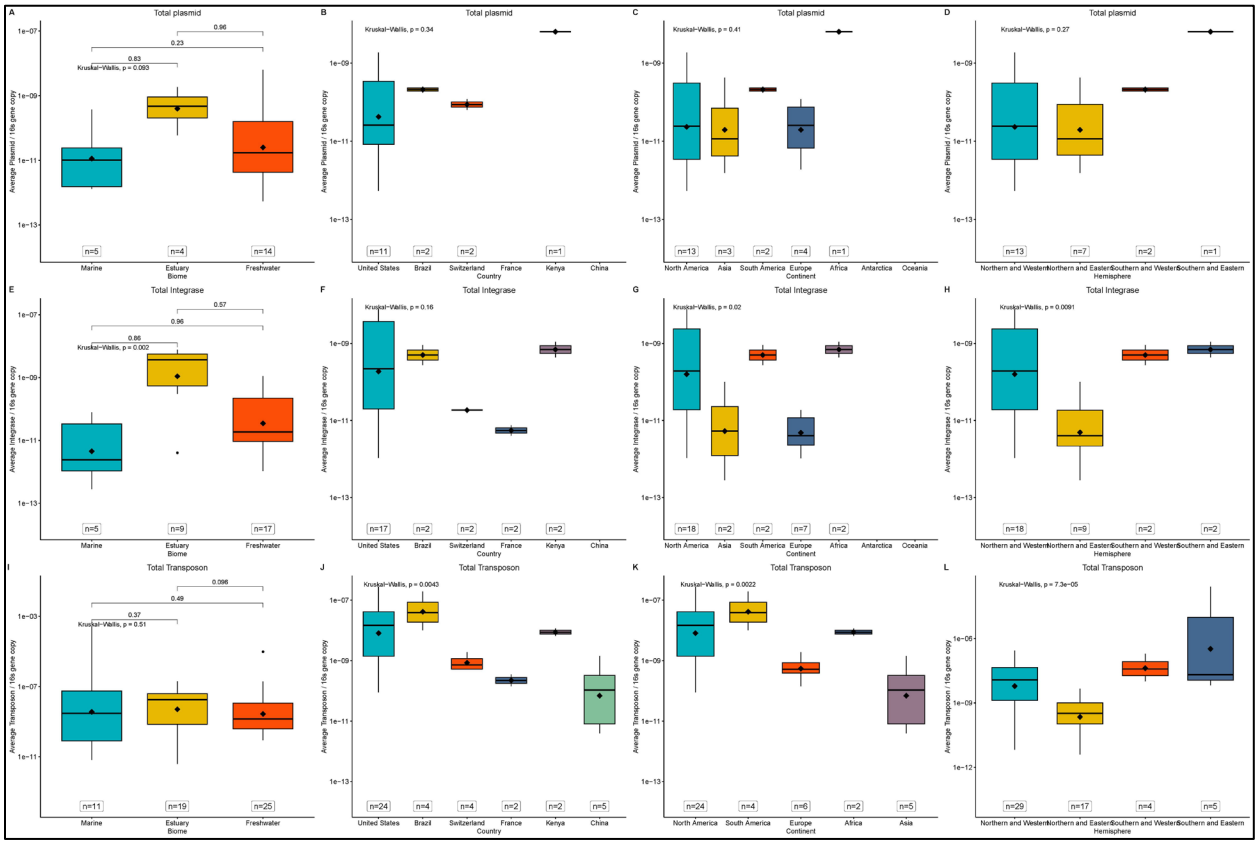

Figure 19: *Relative abundance of mobile genetic elements (MGEs) across ecosystem, country, continent, and hemisphere stratification. (A-D) plasmids, (E-H) integrases, (I-L) transposons. The abundances represent the average relative abundance of*

each ARG type per sequencing project, normalized by the total number of reads for that project. The global p-value is reported as a non-parametric Kruskal-Wallis test. The mean of each category is represented as a black diamond.

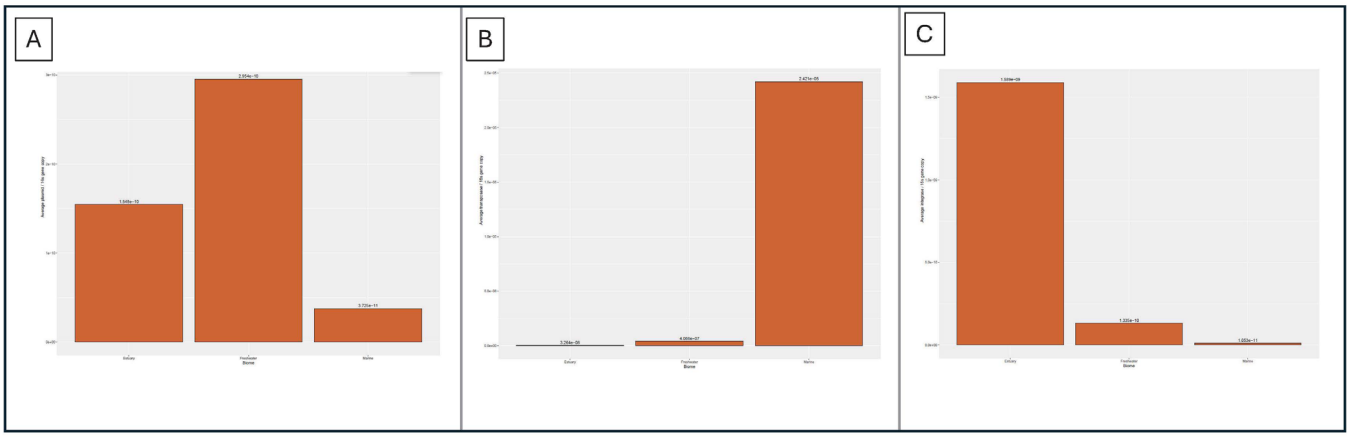

Figure 20: *(A) mean of total plasmid abundance, (B) mean of transposase abundance, and (C) integrase abundance*

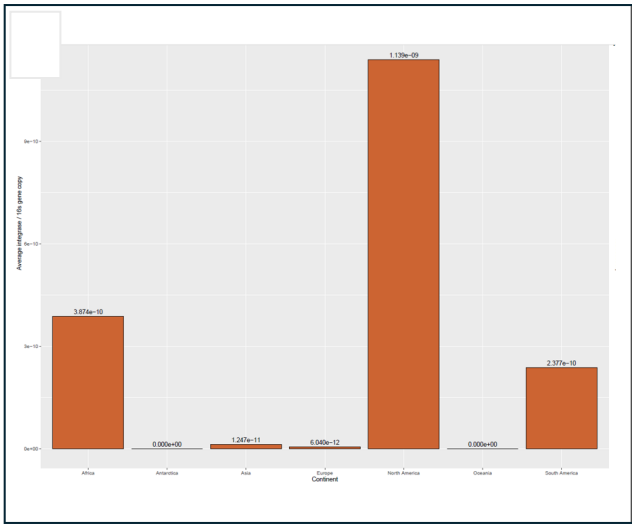

Figure 21: *The abundance of integrase by continent.*

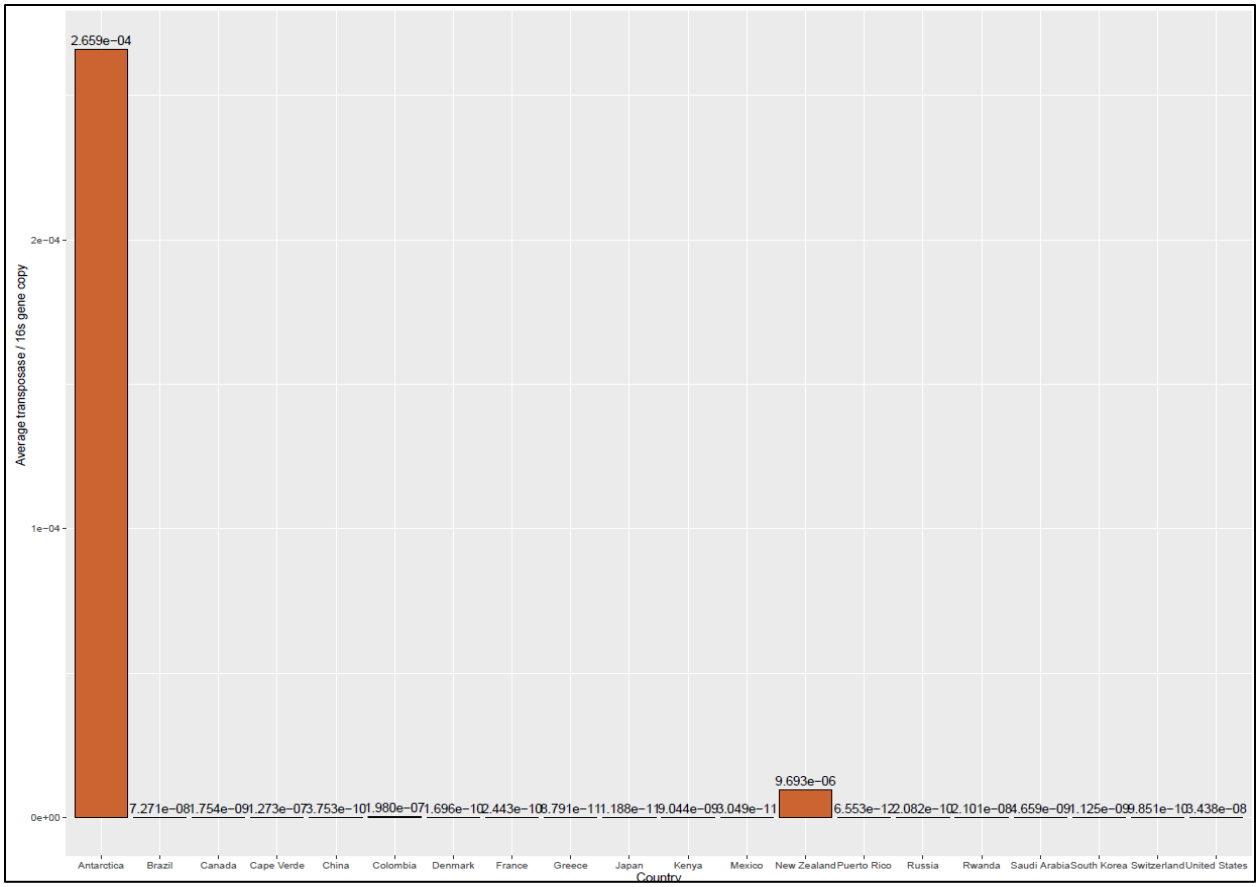

Figure 22. *Mean abundance of transposase by country.*

Composition and diversity of ARGs and MRGs

To understand the diversity of the resistome within samples, the Shannon-Wiener and Simpson diversity indices were measured (Figure 23). An initial assessment supported that most significant variation was seen at the smallest stratification (i.e the ecosystem and country level) ($p<0.05$, Kruskal-Wallis Test) while no statistical support existed for higher stratifications ($p>0.05$, Kruskal-Wallis Test). At the ecosystem level, freshwater environments were significantly more diverse in its ARG/MRG composition than both estuaries and marine environments ($p<0.05$, Wilcox-Test) based on Shannon's scoring, yet the Simpson index only agreed that freshwater samples were more diverse compared to estuaries only ($p<0.05$, Wilcox Test). Freshwater environments had the highest Shannon diversity score (3.49), but marine environments had the highest Simpson diversity score with 0.86 on a scale from 0-1 (Figure 24).

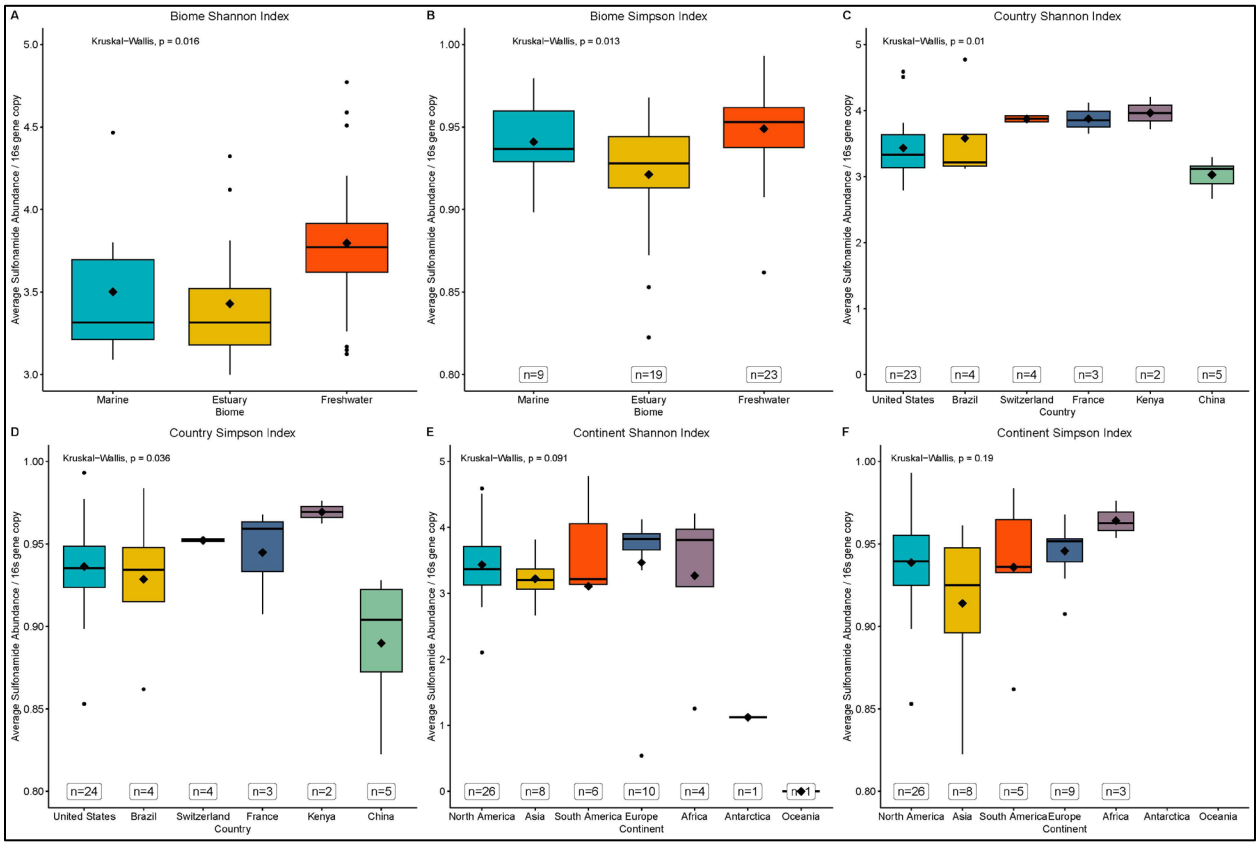

***Figure 23**: Diversity indices for ecosystem, country, and continent level stratification. (A-B) ecosystem, (C-D) country, (E-F) continent. Hemisphere level stratification was left out since the same information was captured by the continent level stratification. The global p-value is reported as a non-parametric Kruska-Wallis test. The mean of each category is represented as a black diamond.*

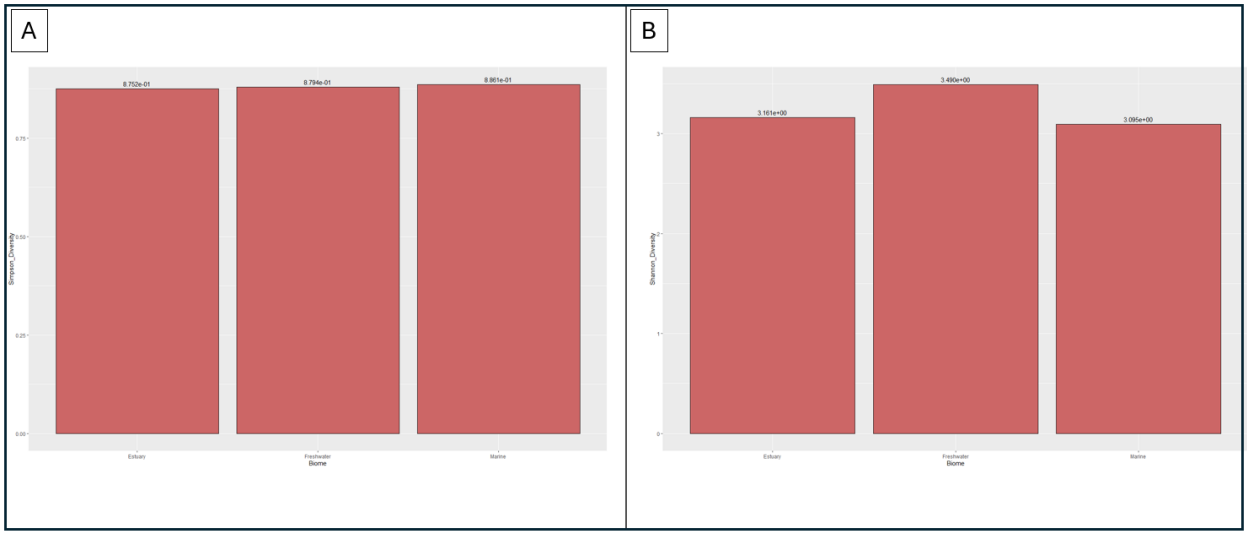

Figure 24: *(A) mean Simpson diversity score and (B) mean Shannon diversity score by aquatic ecosystem*

At the country level (Figure 25), the most diverse resistome existed in samples from Mexico (4.47 Shannon Index; .97 Simpson Index), followed by Kenya (3.96 Shannon Index; .96 Simpson Index) and Rwanda (3.89 Shannon Index; .95 Simpson Index). The least diverse corresponded to New Zealand (0 Shannon & Simpson Index), followed by Denmark (5.39 Shannon Index; .35 Simpson Index). The within-resistome diversity was not significantly different between Kenya and Rwanda ($p>0.05$, Wilcox Test), but was significantly higher in Kenya compared to China ($p<0.05$, Wilcox Test) for both Shannon and Simpson's indices. Kenya was only more diverse ($p<0.05$, Wilcox Test) compared to the United States using Simpson's index, not Shannon's index ($p=0.095$, Wilcox Test). Additionally, the diversity within United States samples was significantly higher than those from Puerto Rico, Denmark, New Zealand, and China ($p<0.05$, Wilcox Test) using both Simpson and Shannon's indices.

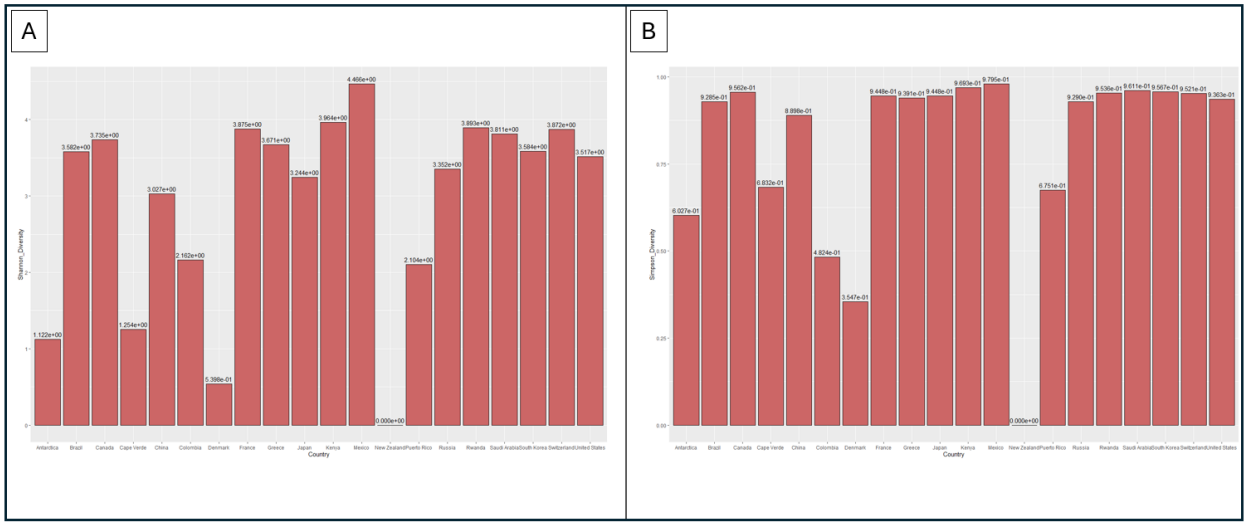

***Figure 25**: (A) mean Shannon diversity score and (B) mean Simpson diversity score by country.*

To assess the compositionality of the resistome and diversity overlap between samples, the Bray-Curtis dissimilarity index was used to construct NMDS ordination plots and additionally, environmental vectors plotted to assess the influence of anthropogenic variables on the composition of the data. Firstly, the compositionality of the resistome based on the total number of resistance genes (defined as the normalized sum of MRGs and ARGs per 16s copy per project) was significantly different across ecosystem, country, continent, and hemisphere stratification ($p<0.05$, PERMANOVA, permutations=999), with most variation captured at the country level ($R^2=0.46$). This was further justified via an ANOSIM, suggesting that most of the dissimilarity is significantly captured at the country level ($p<0.05$, $R= 0.302$). A trend that can be noted from the first NMDS ordination (Figure 26; colored by country while shapes represent the ecosystem) is that there is a tendency for samples of the same ecosystem type to end up closer together in graph space compared to other ecosystem types. For example, most estuary samples (circles) and freshwater (triangles) cluster, indicating they are more similar than those further away. In addition, some marine samples (Figure 27; projects 82106, 100537, and 89308 in right red circle) end up closer together compared to marine samples (Figure 27; projects 82424, 5524 and 5692 in left red circle), yet still end up further away, indicating locality, or site-specific conditions not captured well within the dataset, could be important for the composition of ARGs/MRG. In other cases,

some samples are so dissimilar that they end up distinctly at the extremes of the graphs (projects 80627 and 102713), which come from Antarctica and Oceania, respectively.

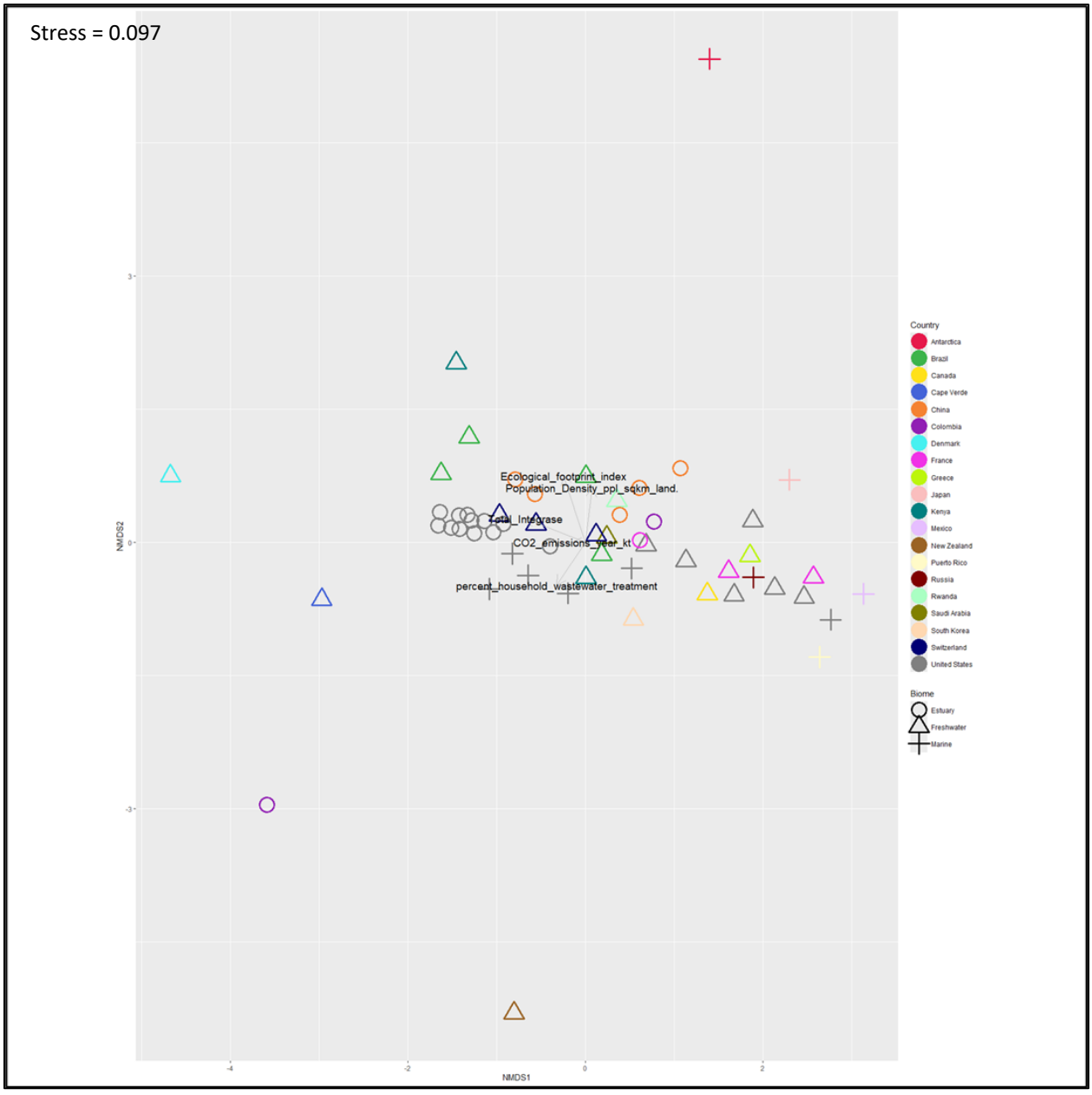

Figure 26: *Non-Metric Dimensional Scaling (NMDS) plot. The shapes are color coded by environment and colored by country. Each project ID is labeled. Environmental vectors were fit using population density, ecological footprint indices, integrase abundance, the percentage of the population with access to wastewater treatment, and CO2 emissions per year at the country level of stratification the year the project was sampled in.*

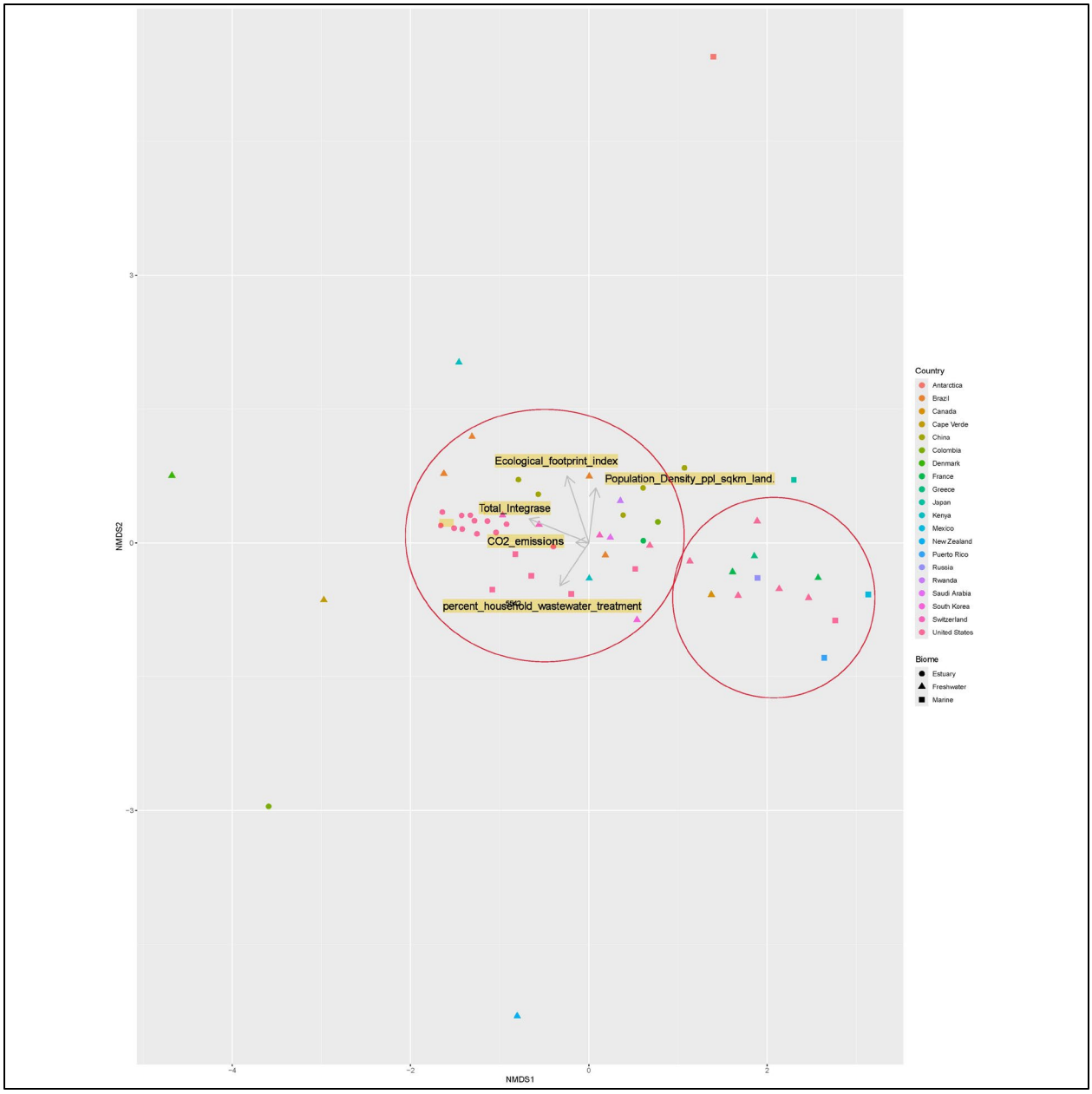

Figure 27: *Non-Metric Dimensional Scaling (NMDS) plot. The shapes are color coded by environment and colored by country. Environmental vectors were fit using population density, ecological footprint indices, integrase abundance, the percentage of the population with access to wastewater treatment, and CO2 emissions per year at the country level of stratification the year the project was sampled. The two red circles indicate observed clusters based on the Bray-Curtis dissimilarity score.*

To discern whether clusters were visible at higher geographic stratifications (i.e continent or hemisphere) based on the Bray-Curtis dissimilarity, the same NMDS plot is presented but colored by country and the shapes now represent the continent (Figure 28). The plot labelled by hemisphere did not provide any additional information not captured by the continent stratification and was therefore left out. In this case, most of the samples from the United States tended to cluster together, but were like some

samples from Asia, South America, and Europe. In general, samples from Asia tended to be closer to other samples from Asia, and samples from Brazil the same. Interestingly, samples from Africa (comprising Kenya, Rwanda, and Cape Verde) were dissimilar from one another (clustering further away from each other).

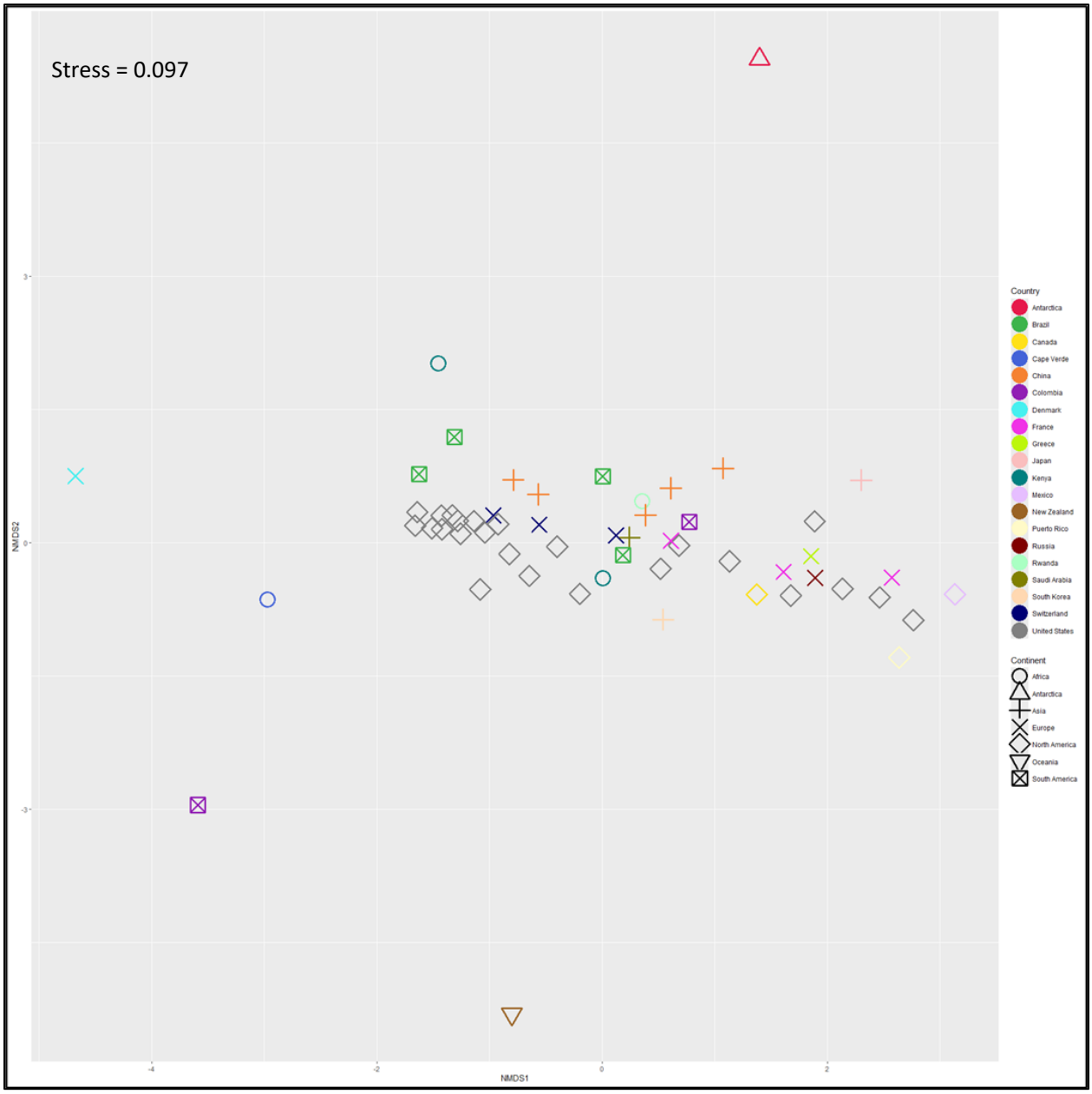

Figure 28: *Non-Metric Dimensional Scaling (NMDS) plot. Each point represents a resistome. The shapes represent the continent and the countries are colored. the sample comes from. The distance metric is the Bray-Curtis Dissimilarity.*

To determine if certain anthropogenic factors could correlate with the ordination axes of the NMDS plots and potentially provide explanation for the differences in compositionality, multiple regression was used to fit environmental vectors onto the NMDS plot (Figure 26 or 27). Within this, no anthropogenic variable was highly and significantly correlated with the ordination axes (Table 2), meaning that these features do not adequately capture or explain the compositionality well ($p>0.05$, $R^2<0.7$). Interestingly, the ecological footprint index is approaching significance ($p=0.082$) and had the lowest p-value of the variables tested, and subsequently explained up to 11% of the variation, followed by the abundance of class I integrase (9.8%) and population density (7.3%).

***Table 2**: Environmental vectors from multiple regression analysis*

Environmental Vector	**NMDS1**	**NMDS2**	**Correlation Coefficient (R^2)**	**P-value**
% of household with access to wastewater treatment	-0.55792	-0.82989	0.0632	0.263
Integrase abundance / 16s gene copy	-0.92759	0.37361	0.0984	0.120
CO_2 emissions / year (kilotons)	-0.99955	0.03015	0.0040	0.962
Population Density (people / sq. km land)	0.12602	0.99203	0.0727	0.173
Ecological Footprint Scoring	-0.30926	0.95086	0.1175	0.082

1.6 Discussion

Metagenomic annotations of these aquatic shotgun metagenomes have revealed interesting differences across ecosystems and geographies in the abundance of ARGs, MRGs, and their potential carrier MGEs. Estuary samples carried several elevated MRGs corresponding to zinc, chromium, arsenic and lead and even elevated ARGs for bacitracin, polymyxin, and tetracycline (comparatively to marine environments). This indicates that estuaries may be more likely to face metal stress from these compounds, likely due to established salinity gradients from freshwater inflow modulating the mobility of free metals in its open waters (De Souza Machado et al. 2016). However, freshwater samples contained a

more diverse resistome composition of ARGs and MRGs, which refutes the initial hypothesis expecting estuaries to be more diverse. This could highlight a need for freshwater microbial communities to adapt and carry more ARG/MRG types because of frequent exposure to metal or antibiotic waste from human activities. It was observed that freshwater environments typically contained higher abundances of copper resistance genes compared to marine environments, which makes sense since copper is limiting in the open ocean (Richon and Tagliabue 2019) but has consistent input into freshwater from terrestrial erosion and the degradation of batteries, pigments or fertilizer compounds (Bashir et al. 2020). Additionally, freshwater environments carried higher amounts of both tetracycline and sulfonamide resistance genes, which have been proposed as indicator genes for contamination alongside the abundance of class I integron-integrase (Bourdonnais et al. 2022). Highly abundant MRGs across any ecosystem or geographic stratification corresponded to copper and arsenic resistance, which coincides with the results of other studies of aquatic environments focusing on coastal waters, lakes, and seas (Yang et al. 2019). However, they found mercury resistance genes to be widely abundant within lakes and seas, but the abundance of mercury resistance genes in this dataset was comparable to that of other resistance genes for metals like copper, and there were no differences noted except for elevation in North America compared to Asia. This is unsuspected, as Asia is responsible for over half of the global atmospheric mercury emissions (Li et al. 2009). One possible explanation is that many of the samples from Asia in this dataset are associated with mangroves, which are known for their ability to sequester or chelate heavy metals, removing them from the surrounding environment and reducing their burden on the surrounding microbial communities (Yadav et al. 2023).

The hypothesis suggesting multidrug resistance genes would be the most abundant across all the annotated ARGs within each project library was not supported since they were not the most abundant ARG surveyed. In contrast, results revealed beta-lactam, bacitracin and polymyxin resistance genes were the highest abundance, which coincides with similar surveys of aquatic environments but not global soils (Yang et al. 2019; Zheng et al. 2022; Delgado-Baquerizo et al. 2022). Within coastal environments, lakes,

and seas, bacitracin resistance was the most abundant ARG present (Bourdonnais et al. 2022), and across mixed studies including wastewater, soil, and lake samples it was within the top five most abundant ARGs (Li et al. 2015). Strictly considering soil metagenomic analyses, multidrug pumps were the most abundant, followed by bacitracin and then polymyxin resistance was the second least abundant ARG in the dataset (Zheng et al. 2022; Delgado-Baquerizo et al. 2022). Further, vancomycin resistance genes were the lowest ARG annotated across these stratifications, where it is typically prescribed as a last-resort antibiotic for infections caused by multidrug-resistant bacteria (Selim 2021), yet Zheng et. al (2022) suggests that it is abundant in soils and was present in nearly 95% of all sediment metagenomes in their study. This could imply that open waters are less likely to harbor vancomycin resistance over time, where its effects may only be observed if it has a chance to accumulate and adsorb to soil (Maghsodian et al. 2022). The beta-lactam resistance genes were highest within one marine sample taken in 2017 originating from Prydz Bay, which is the end of a glacial drainage system off the coast of Antarctica. While Antarctica has traditionally been considered a pristine environment in the past, wastewater drainage from research stations could introduce resistant taxa like *E. coli* to the surrounding waters (Hernández et al. 2012; Stark et al. 2016) and further, interactions between migratory wildlife experiencing higher human contact could facilitate the spread of ARGs from mainland to areas with little to no human contact (Hwengwere et al. 2022).

The hypothesis that geographic differences do exist in resistance gene abundance was supported, yet the compositionality is not easily defined by the stratifications provided here. In many cases, aquatic resistomes clustered according to the environment and those located closer in geographic space tended to cluster closely in graph space, indicating they are more similar in composition. This result is also supported by the findings of Li et. al (2015), where their samples from the same freshwater environment subset (hypolimnion, metalimnion, epilimnion) didn't always cluster together, and the primary conclusion was that local differences played a bigger role than geographic or ecosystem differences in determining resistome composition. This is partially supported by the data here, given that none of the fitted

environmental vectors were significant for any ordination axis and all the metadata was collected at the country level the year the sample was taken, meaning locality isn't captured at all. To further assess this, an increase in the number of aquatic metagenomes would help to make conclusions at much smaller geographic resolutions, allowing for this question to be addressed.

The country of Kenya stood out consistently due to having a high abundance of both tetracycline and sulfonamide resistance compared to samples from the more industrialized and populated United States and China, which refutes the initial hypothesis that countries within Asia would have the highest abundance, since ARG and MRG abundance were often comparable between metagenomes taken from either country. The two sites comprising Kenya include the Winam Gulf of Lake Victoria and Simasi hotspring. While no additional data existed about Simasi hotspring, Winam Gulf is reported to be contaminated by antibiotic waste from nearing pharmaceutical companies, heavy metals, and agrochemicals (Khatiebi et al. 2023). An analysis of metal concentrations at this site in 2006 (Ochieng et al. 2006) revealed that surface water samples had concentrations of both copper, chromium, and zinc around 11.15 ug/L, 11.11 ug/L, and 62.83 ug/L, respectively, and even as of 2016 this has increased to up to 4290 ug/L for copper and 1620 ug/L for zinc in some spots of the lake (Wambu et. al 2016). Copper and zinc are notoriously studied for their ability to co-select and spread tetracycline-resistant bacteria (Vahjen et al. 2015; Li et al. 2021), suggesting that Winam Gulf could harbor resistant-bacteria due to co-existing metal stress. However, up-to-date metal analyses and lab studies are necessary to draw larger conclusions of co-resistance potential.

The abundance of Class I integron-integrase was highest in North American samples followed by Africa, but there were no meaningful differences in their mean ranks except between Asia and Europe, where it appeared to be elevated within Asia. Yet, it has been previously concluded that Class I integron-integrase could be used as proxies for anthropogenic contamination, due to their ability to recombine gene cassettes containing both ARGs and MRGs (Wright et al. 2008; Gaze et al. 2011; Gillings et al. 2015). Additionally, they did not significantly correlate with any ordination axes, implying their effects on the

dataset are less than what was expected or not captured adequately, which refutes the hypotheses that they would be one of the primary explanatory variables on ARG and MRG composition. This finding could be explained by the fact that most of the samples analyzed here are surface-level water samples. Previous work in rivers has suggested that integron-integrase copies were highest in sediments (up to 1.4 x 10^6 copies per gram of sediment) compared to surface water samples (ranging 3.3-6.6 x 10^3 copies per mL of water), due to a compartmentalization effect driven by water chemistry factors like temperature (Koczura et al. 2016). The abundance of Class I integron-integrase therefore may not be well-suited for open-water to accurately gauge contamination present, especially without the aid of site-specific parameters or qPCR measurements, but does highlight other possible roles of transmission, such as through transposase activity. For example, transposase abundance was highest in Antarctic marine samples (although not significantly different), and in previous studies of the Baltic Sea it was found that bacteria from surface water samples contained few transposases (Vigil-Stenman et al. 2017). Yet, the dynamics of transposase activity within large marine ecosystems is complicated, where other work has suggested that viral activity (and therefore transposase activity) increases as depth increases (Zhong et al. 2024), making it difficult to make conclusive observations within the limitations of this dataset. Within large marine environments, transmission of ARGs and MRGs could occur even in the absence of high abundances of integron-integrase typically associated with human activity.

1.7 Conclusions & future directions

It was found that while estuaries may be more likely to harbor MRGs corresponding to arsenic, chromium, or zinc, freshwater environments contained a more diverse resistome comprising important ARGs for bacitracin, polymyxin, tetracycline, sulfonamide resistance, and MRGs for copper. Multidrug resistance was not as abundant as expected, highlighting a potential difference in aquatic and soil-associated environments. The risk of harboring MRGs and ARGs is equally shared by freshwater and estuaries, while marine environments did not have any differences and carried fewer ARGs and MRGs within the dataset. Here, Lake Victoria in Kenya is highlighted as a potential hotspot for ARG/MRG co-selection due to carrying a significantly higher abundance of sulfonamide and tetracycline resistance

genes compared to industrialized countries such as the USA and China, and numerous MRGs like copper and zinc known to co-select for these antibiotics. Future studies at this site should focus on accurately characterizing metal concentrations, culturing environmental samples to detect clinically relevant pathogens of public health interest and assaying their interactions with antibiotics under metal stress within a controlled laboratory setting.

The next steps for this work include expanding the analysis to cover taxonomic identification of the sequences using short-read classifiers like Kraken to assess which taxa harbor these resistance genes. Additional analyses are needed to determine which specific MRGs (like *copA)* are elevated in each environment or if certain clinically important multidrug transporters (like *mexF)* are widely detected. This work would further be supported by the addition of qPCR assays in conjunction with the ARGs-oap annotation tool.

1.8 Data Availability

All code used in this analysis is uploaded to GitHub and can be accessed here: https://github.com/joynerco22/Antibiotics-and-Metal-Biogeography

CHAPTER 2: CO-OCCURRENCE PATTERNS BETWEEN ARGS AND MRGS WITHIN AQUATIC ENVIRONMENTS

2.1 Introduction

The persistence of ARGs in the environment is affected by numerous variables. Its co-occurrence to metals is of growing concern because they are often close together on plasmids or the bacterial chromosome, where it has been shown to cause co-resistance and cross-resistance via shared mechanisms, leading to the persistence of ARGs without direct antibiotic exposure or stress (Perron et al. 2004; Baker-Austin et al. 2006; Murray et al. 2024). Within the environment, metal contamination stems from numerous sources including terrestrial erosion, degradation of items like batteries or car parts, and agricultural use and breakdown of additives within fertilizers and pesticides (Bashir et al. 2020; Zaynab et al. 2022; Singh et al. 2023; Khan and Sklar 2023). Aquatic environments based on previous studies have evidence of harboring co-resistant bacteria due to existing metal stress (Seiler and Berendonk 2012; Berglund 2015; Di Cesare et al. 2016), yet these studies are local, leaving room for additional insights to be gained across the globe.

Frequently implicated metals in co- and cross-resistance include those that are traditionally stressful to microbial communities, such as copper, zinc, chromium, arsenic, cadmium and mercury (Raab and Feldmann 2003). Within this, the presence of copper and arsenic have led to increasing tetracycline resistant bacteria (Zhang et al. 2020; Li et al. 2021), zinc has been shown to increase carbapenem resistance in controlled experiments with *P. aeruginosa* (Perron et al. 2004), yet in other cases the linkage isn't as clear. For instance, the *soxS* gene becomes overexpressed under oxidative stress which may stem from interactions from some metals, but this gene regulates the multidrug *acrABC* pumps in *E. coli* (Seiler and Berendonk 2012), meaning oxidative stress as a byproduct of metal exposure increases resistance to multiple antibiotics.

Here, the potential interactions between MRGs and ARGs are analyzed as a spearman rank pairwise correlation matrix to assess the co-occurrence patterns across aquatic ecosystems combined from

across the globe. If a MRG is strongly associated with an ARG, then it should be positively correlated within the dataset, indicating that evidence exists that the genes tend to increase linearly together, which has been a trusted method for finding evidence of co-resistance in other environmental datasets (Li et al. 2015).

2.2 Research Questions

What does network analysis reveal as frequently co-occurring ARGs and MRGs within aquatic ecosystems?

2.3 Hypotheses

(1) I hypothesize that copper and zinc resistance genes will be the most frequently co-occurring with ARGs, since these metals are abundant by-products of agriculture and industrial activity, and due to their toxicity, could be widely connected to many ARGs.

2.4 Methods

Spearman-rank pairwise correlation analysis

To assess whether certain ARGs and MRGs were correlated across all aquatic environments, a non-parametric spearman-rank pairwise correlation matrix was constructed using the master subtype file (i.e the file containing abundances at the sequence/gene level) with the corrr package (v.0.0.4) using 9130 ARGs from the SARG database and 754 MRGs from the BacMet experimentally verified database. The subsequent matrix was then converted into an "ABC" format table, where column 1 and 2 represented the compared genes, and column 3 and 4 the correlation coefficient and p-value, respectively. The p-values were adjusted using the Benjamini-Hochberg correction for multiple comparisons to control for the false-discovery rate, or the presence of false-positives. The ABC table was filtered to only include significantly correlated comparisons (adj. $p<0.05$, $r^2 \geq 0.70$). Lastly, the table was imported into Python, and a custom script was developed to sift through each of the comparisons using the mapping file given to ARGs-OAP to make its annotations. This ensured that the only comparisons remaining were mostly between MRGs and ARGs.

Network visualization and markov clustering (MCL)

To visualize the connectivity between ARGs and MRGs, the correlation table was imported into Cytoscape (v.3.10.1) as an edge file. A node represents an ARG or MRG (visualized as a labeled circle within the graph), while edges represent the lines connecting them together – the spearman correlation coefficient. The length of the edge does not mean anything, nor does the arrow since the graph is not designed to be directed. To reduce the size of the network for interpretation and to visualize hub genes (genes that connect to many other genes), Markov clustering was performed twice on the network with an inflation parameter of 2.5. The inflation parameter controls the tightness of the clustered network, and 2.5 was chosen compared to higher or lower values because it generated the cleanest network clusters, aiding in overall interpretability and comprehension of potential ARG/MRG pairs.

2.5 Results

The final network was generated using the entire dataset (n=57) combined, meaning all geographies and ecosystem types are considered together. This resulted in 486 total nodes (comprising 67 ARGs and 419 MRGs), with 208 edges (connections) with other genes, with an average of 1.92 neighbors per node, meaning that each node neighbored almost 2 other resistance genes within the same cluster. The low connected components score of 0.1 suggests that each connection represented here (indicated by the spearman correlation coefficient) is strong, whereas a higher value would indicate the opposite (such as something with a score of 1 or 2 would indicate weaker connectivity within the network). Other important parameters are summarized in Table 3. The resulting network figures were included based on visual inspection, meaning they contained genes of interest for further discussion (Figures 29-32).

Table 3: *Summary statistics of the final network after Markov clustering. Values were generated and reported by Cytoscape.*

Network Summary Statistic	**Value**
Number of nodes (genes)	486
Number of edges (connections between genes)	208
Average number of neighbors	1.920
Network diameter	3
Network radius	2

Characteristic path length	2.293
Network density	0.080
Network heterogeneity	1.755
Network centralization	0.683
Connected components	0.103

The first network (Figure 29) consists of two multidrug resistance gene (MDR) hubs (*emrD* and *mdtL,* indicated in green) connected to several multi-metal resistance genes (*mntR*, *modE,dsbA,* and *fecE* indicated in lilac*),* two genes conferring both metal and biocide resistance (*tehB* and *soxS*, indicated in red), and one biocide resistance gene (*cpxA,* indicated in yellow). Within this cluster, the MDR are considered hubs since they have high connectivity to the previously listed genes with 5 and 6 edges linking them, respectively.

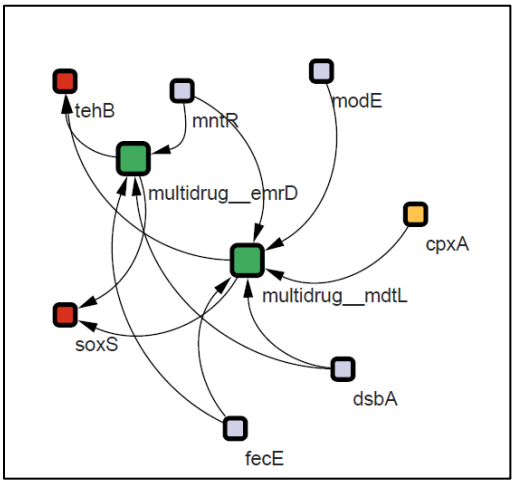

Figure 29*: Network illustrating frequent co-occurrence between two multidrug resistance genes and metal/biocide resistance genes. The hub gene(s) are slightly bigger and have the most connections in this cluster. Multi-metal RGs are in lilac, metal/biocide RGs are in red, and biocide RGs are in yellow.*

The next network is denoted by a high number of copper resistance genes linking to MDR genes (Figure 30). Within this, there are three genes that confer resistance to copper: *cueR, copZ, and yonJ.* These genes frequently connect with the MDR gene *bmr.* It is important to note that this gene does appear twice within this network, but *bmrR* is a regulator of *bmr* and it being significantly correlated makes sense. This regulator also connects with the multidrug *blt* gene, while the only copper resistance genes that connect to this gene are *cueR* and *yonJ.* In addition, *bmrR* and *cueR* are significantly correlated with

the tunicamycin resistance gene *tmrB*. The genes *yonJ* and *bmr* are considered hubs since they had the highest connectivity of all genes in this cluster.

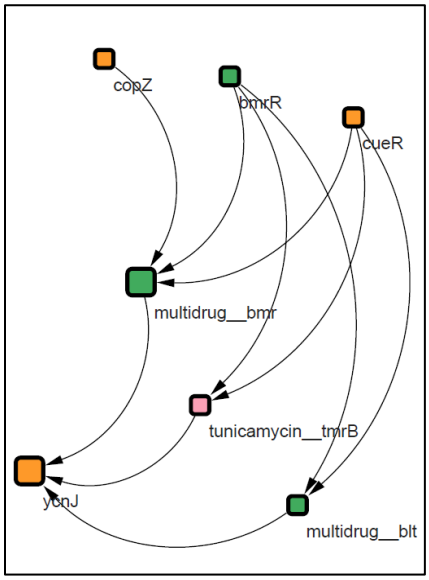

Figure 30: *Network illustrating frequently co-occurring copper resistance genes to multidrug and one tunicamycin resistance gene. The hub gene(s) are slightly bigger and have the most connections in this cluster. Copper resistance genes are in orange, while multidrug are green, and tunicamycin in pink.*

The next network is dominated by resistance genes for vancomycin, a last-resort antibiotic of public health interest, which could be linked to some metal resistance genes not previously studied. This includes *vanXA, vanHF*, and *vanF* (Figure 31). Within this, *vanXA, vanHF, and vanF* are significantly correlated with the cobalt resistance gene *nhlF.* Only one biocidal gene exists in this network, *adeC*, which is connected to *vanHF* only. The cobalt resistance gene *nhlF* is the hub gene in this cluster, and forms three connections with the other vancomycin resistance genes.

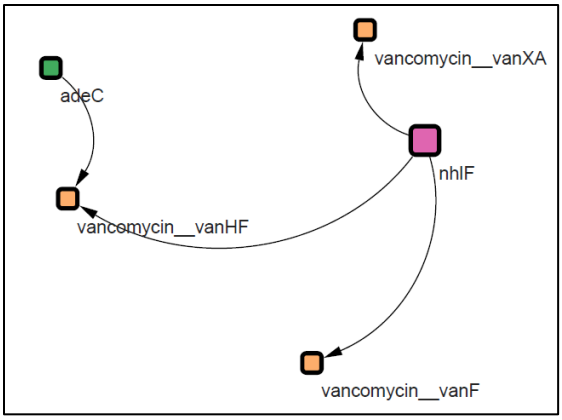

Figure 31: *Network illustrating the connectivity between vancomycin resistance genes, a cobalt resistance gene and a multi-biocide resistance gene. The hub gene(s) are slightly bigger and have the most connections in this cluster. Vancomycin resistance genes are orange, multidrug are green, and cobalt resistance genes are pink.*

The presence of certain resistance genes could provide insight into characteristics of some aquatic ecosystems, and Figure 32 illustrates one with marine environments. Within this network, the chloramphenicol resistance gene *catB11* serves as a hub, making over 17 connections with biocide and metal resistance genes. Most of these genes are multibiocidal (*srpA, vmeC, vmeA, adeT2, bepC, and triC),* while others confer resistance to multi-metal (*nccB, bcrA, mtrR, fbpB, frnE, nccC, and yhcN*). *vmeC and vmeA* according to the BacMet database, are largely present in marine bacteria, namely *Vibrio parahaemolyticus* and members of the genus *Shewanella* (Matsuo et al. 2007).

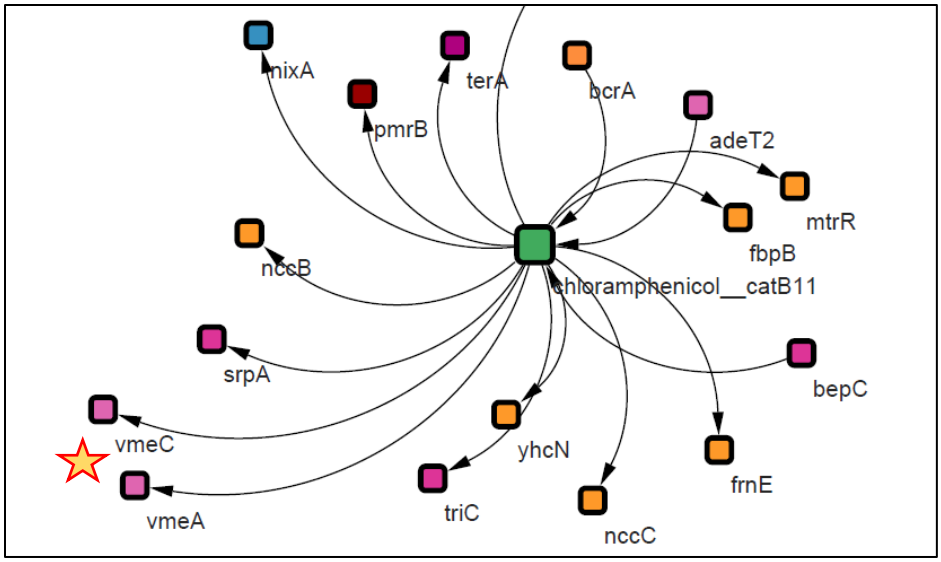

Figure 32: *Network illustrating the connectivity between* the chloramphenicol resistance gene *catB11,* multi-metal, metal, and biocide resistance genes. *vmeA* and *vmeC (starred)* are only characterized in the marine *Vibrio parahaemolyticus* within the Bacterial Metals and Biocides database.

Some antibiotic resistance genes, due to ubiquity in environmental metagenomes, may be implicated more in co-resistance than others. Figure 33 represents comparisons with one of the most abundant ARGs across all aquatic ecosystems, *bacA,* which confers resistance to bacitracin. This gene serves as the hub gene in a cluster and makes connections with 4 other metal resistance genes, including *pstB* and *pstC* which confer resistance to arsenic, *chrA* which confers resistance to chromium, and *ruvB* which confers multi-metal resistance corresponding to chromium, tellurium, and selenium.

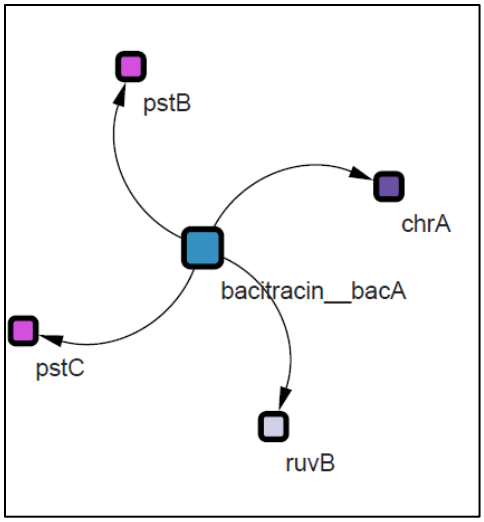

Figure 33: *Network illustrating the connectivity between the bacitracin resistance gene bacA, two arsenic resistance genes, a chromium resistance gene, and a multi-metal resistance gene. The hub gene(s) have bigger nodes and have the most connections in this cluster. The arsenic resistance genes are in light purple, the chromium resistance genes in dark purple, and the multi-metal resistance gene in lilac.*

2.6 Discussion

Network analysis revealed that while copper resistance genes were tied to many ARGs including MDR pumps, other metals may play a larger, unforeseen role in aquatic environments. The initial hypothesis that copper resistance genes would be the most significantly correlated with ARGs was partially supported, since a clear cluster existed connecting copper and multidrug resistance pumps, but zinc resistance was not significantly correlated with any ARG except for trimethoprim resistance in a much smaller network not visualized here. A possible explanation is that zinc resistance genes are present, but do not actually interact with any antibiotic resistance gene, which is an example of co-resistance rather than cross-resistance. One study from isolates taken from pig fecal matter suggested that zinc resistance in isolated bacteria did not correlate at all to increased antibiotic resistance under high zinc supplementation (Vahjen et al. 2015), and the increase in antimicrobial resistance was due to a proliferation of multidrug resistant bacteria co-resistant to zinc, but they were not cross-resistant and thus, there were no reported interactions between the zinc resistance gene and the ARG. This contradicts the results of other studies, which found increased zinc resistance genes did indeed lead to decreased susceptibility of an antibiotic like imipenem through co-regulation (Perron et al. 2004). Networks from Li

et. al (2015) suggest that zinc resistance genes were only significantly correlated with other zinc resistance genes. Since so much variation exists, species specific attributes may be important, since Vahjen et. al (2015) focused on *E. coli,* and Perron et. al (2004) on *P. aeruginosa.* Other metals, like arsenic, were associated with bacitracin resistance in this network, but other studies demonstrate a correlation to tetracycline resistance (Zhang et al. 2020), which was not significantly correlated within this data. Thus, to make further conclusions, also being able to understand the taxa certain resistance genes were linked to would be important for further clarifications and may overall be an example of metabolic plasticity within isolate genomes.

The role of multi-metal resistance genes and those conferring biocide resistance suggest that co-selective processes may be much broader within aquatic ecosystems. While it makes sense that multi-metal resistance genes could confer a similar phenotype under antibiotic stress as genes conferring resistance to one metal, many genes reported here function against metals and biocides or strictly on biocides. Other studies have highlighted that biocides can be tightly associated with ARGs (Murray et al. 2024), and even detergents could select for resistant bacteria in some cases. Within this data, for example, cpxA was significantly correlated with multidrug pumps, yet it confers resistance to chlorohexidine, benzalkonium chloride, and hydrogen peroxide; but also chloramphenicol (Srinivasan et al. 2012). This suggests that aquatic environments carrying multiple contaminants could be at risk, implicating microbial community stress from broad sources as a potential threat to the spread of antibiotic resistance (Khan and Sklar 2023; Khatiebi et al. 2023). This was shown further by the presence of the biocide resistance genes *vmeA* and *vmeC,* which confer resistance to quaternary ammonium compounds (QACs), SDS, and benzalkonium chloride (Matsuo et al. 2007). These genes are largely associated with marine bacteria like *V. parahaemolyticus* and members of the genus *Shewanella,* which suggests that ecosystem differences in co-selection potential exist and should be accounted for in further studies.

Vancomycin-resistant-bacteria pose a serious threat in the treatment of multidrug-resistant infections, and it is often referred to as a “last resort” antibiotic when other treatments fail (Selim 2021).

Within the network, *nhlF* which confers resistance to cobalt, was significantly associated with multiple vancomycin resistance genes including *vanF, vanHF, and vanXA.* One study reports that the vancomycin-resistant enterococci (VMEs) typically hold multi-metal resistance including cobalt, but its combined effects and co-selective potential remain unknown (Sanderson et al. 2019). Further studies suggest that vancomycin resistance may be more associated with biocidal resistance genes, where one study found that the antibiotic diclofenac enhanced resistance to vancomycin (Murray et al. 2024), and within this dataset *vanHF* was significantly correlated to *adeC,* a resistance gene conferring resistance to multiple biocides including quaternary ammonium compounds (detergents), SDS, and chlorohexidine and many other antibiotics (Rajamohan et al. 2010).

One advantage of the generated networks is the creation of new hypotheses to test on both clinical and environmental strains. However, network analysis is limited in its ability to make solid conclusions about the risk of co-selection in aquatic environments, since correlation-based data only provides association and not causation. Another unfortunate setback within this data is that most of the database entries for the metals and antibiotics are characterized from sequencing data mostly on clinical isolates (Murray et al. 2022; Murray et al. 2024), leaving extrapolation to novel antimicrobial genes or unidentified microbial communities difficult.

2.7 Conclusions & future directions

Copper resistance genes (Copper exhibits antimicrobial activity due to its toxicity), were widely associated with numerous MDR pumps and are well-supported for their ability to co-select for antibiotic resistance, where they frequently contaminate aquatic environments from agriculture and human land development. Within aquatic environments, other metal types such as cobalt and arsenic have formed novel connections with clinically relevant ARGs for compounds like bacitracin and vancomycin, yet much more work is needed to assess the influence of these metals on the ARGs within a laboratory setting. Further, the diversity of resistance genes conferring multiple resistance for metals and/or biocides

within aquatic ecosystems is worth exploring, highlighting that microbial community stressors of broad categories may also play a role in the spread of antibiotic resistance.

Future directions for this work would be to explore the interactions between the connected genes present in the network using culturing and transcriptomics. For example, samples from heavy metal contaminated waters could be used to select for highly resistant bacteria by adding the metal in increasing concentrations to agar plates, allowing enrichment. Following this, standard laboratory antibiotic assays could be carried out on agar plates using disk diffusion or preferably in liquid media and growth curves assessed via a plate reader. For those that display enhanced resistance to the antibiotic in conjunction with the metal, transcriptomics could be used to assess whether certain genetic mechanisms are upregulated or downregulated, potentially providing an explanation for the observed differences.

2.8 Data Availability

All code used in this analysis is uploaded to GitHub and can be accessed here: https://github.com/joynerco22/Antibiotics-and-Metal-Biogeography

CHAPTER 3: A LABORATORY CASE STUDY ON THE IMPACT OF CHROMIUM AND SALINITY ON THE ANTIBIOTIC RESISTANCE OF ARTHROBACTER AURESCENS TC1

3.1 Introduction

Arthrobacter aurescens strain TC1 (ATCC BA-1386; also known as *Paenarthrobacter aurescens* TC1) is a gram-positive, aerobic bacterium originally isolated from atrazine-polluted soils, where it was discovered to break down s-triazine ring compounds. Because of this, it is a current target for the bioremediation of herbicides from agricultural and industrial waste, such as atrazine (Strong et al. 2002). Previous genomic-based studies have highlighted the hardiness of the genus *Arthrobacter* using *A. aurescens* TC1 as a case study, where frequently duplicated catabolic genes in its genome were tied to plasmid-borne pathways, allowing it to thrive in a wide variety of environmental conditions ranging toxic chemical exposure and low-nutrient starvation (Mongodin et al. 2006). Aside from atrazine, A. *aurescens* TC1 *has* a notable ability to reduce hexavalent chromium Cr(VI) to its less toxic trivalent form Cr(III), and due to its ubiquity in the environment, could play crucial roles in the bioremediation of chromium-contaminated sites (Horton et al. 2006; Field et al. 2018). The mechanisms for its chromium tolerance include the chromosomally borne chromium efflux pump *chrA* and its regulator ***chrB*****,** and a chromate reductase (E.C 1.6.5.2) (Mongodin et al. 2006).

An interesting study of several members of the class actinomycetes isolated from marine sediments in India has suggested that chromium-resistance through either reduction or efflux increased with the number of antibiotics the bacterium was resistant to, highlighting a possible connection between Cr(VI) stress and antibiotic stress (Ali 2012). Despite this, the synergistic effects of both were not assessed together, and salinity was not a direct variable but was supplemented for halophilic growth, leaving its effects unknown. Therefore, Cr(VI) could provide valuable insights into its co-resistance to antibiotics within *A. aurescens TC1*, which is a member of the actinomycetes. Additionally, new insights

can be gained into this specifically under saline conditions comparable to those commonly seen in estuaries and ocean environments.

If chromium or salinity does improve the antibiotic resistance of *A. aurescens* TC1, then the minimum inhibitory concentration (MIC) should also increase for that corresponding antibiotic, indicating that there is some coupling of the chromate reductase or chromate efflux pump to the ARG responsible, which is demonstrated as a decrease in the zone of inhibition (ZOI) on a standard Kirby-Bauer disk diffusion assay. Using this information, new insights into the chromium-reduction of an environmental *Arthrobacter* isolate can be gained to understand how it impacts the antibiotic resistance under estuarine conditions.

3.2 Research Question

Does the addition of low-concentration chromium or increased salinity decrease the zone of inhibition for the plated antibiotics, and what are the effects of combining the two?

3.3 Hypotheses

(1) I hypothesize that the addition of chromium or marine salts will decrease the ZOI for some antibiotics, but not others, showing that the mechanism of action for the antibiotic could be important; if a decrease is seen, it is likely due to coupling of the regulation of the chromium reductase gene to the ARG or enhanced activity of an efflux pump.

(2) I hypothesize that the addition of chromium plus the added effects of increased salinity will decrease the zone of inhibition for some antibiotics due to the coupling of the regulation of the chromium reductase gene to the ARG, but there will also be an increase in the ZOI for some, indicating the added salt stress worsens its ability to tolerate the antibiotic.

3.4 Methods

Preparation of cultures, plates, and stock solutions

To prepare the bacterial cultures, 500 µL of *A. aurescens* TC1 cryostock was pipetted into 50 mL of sterilized nutrient broth (Remel) and grown at 20°C for 24 hours before use.

Solid nutrient agar plates (Difco) were prepared per the 1-liter recipe with modified adjustments to include Cr(VI), Cr(VI) and Instant Ocean ®(marine salts), and control plates containing neither. A concentrated potassium dichromate salt was filter sterilized (Millex-GS 0.22 µm filter) and used as a stock for the subsequent experiments. The volume was adjusted accordingly to make a final concentration per experimental condition of: 0.05mM Cr(VI) – 500 mM Cr(VI) and 1%, 5%, and 10% marine salts. The concentration of Cr(VI) was assessed with 10-fold increases to gain a general idea of the max concentration the bacterium could tolerate while also visualizing potential changes in the ZOI. The final concentration of marine salts was assessed at 1%, 5% and 10% to assess low, mid, and high salinity ranges. To assess the impacts of both Cr(VI) and salinity, 0.8 uM Cr(VI) was chosen since it is comparable to concentrations typically found to contaminate some aquatic environments (Bonnand et al. 2013), and 2% salinity was chosen as it is a good representative of estuarine salinity conditions, where the dissolved salt content can reach 20 parts per thousand (PPT) or 2% dissolved salt per kg of water (National Ocean Services). Nine filter-sterilized antibiotics (Table *4*) were obtained from the ECU microbiology teaching labs.

***Table 4**: Antibiotics included in assay & their concentration.*

Antibiotic	**Concentration (mg/mL)**
Kanamycin (K)	45
Streptomycin (SM)	5
Carbenicillin (C)	250

Ampicillin (AP)	100
Penicillin G (PG)	100
Tetracycline (T)	15
Gentamicin (GM)	50
Bacitracin (BC)	30
Chloramphenicol (CHL)	15

Kirby-Bauer disc-diffusion protocol

Bacterial lawns were created by pipetting 700 µl of freshly grown *A. aurescens* TC1 culture and then aseptically spreading it back and forth in an overlapping motion using a sterile cotton swab. Once the lawns dried, a sterile 6 mm diameter sterile cellulose disk was aseptically transferred with frequent flaming of the metal tweezers until 9 discs were evenly spread across the agar. The discs were lightly

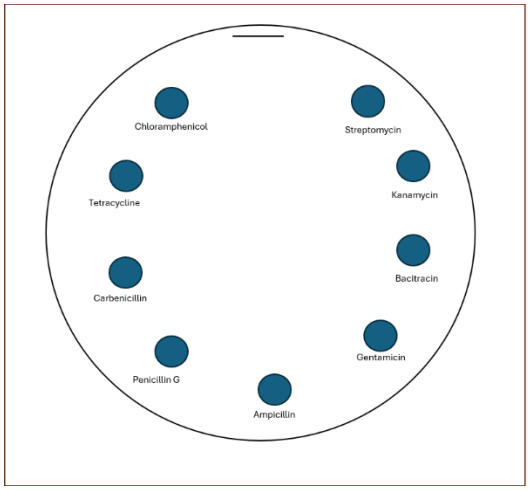

***Figure 34**: Arrangement of antibiotic discs on all disk diffusion assays.*

tapped down to ensure they adhered to the media if inverted during incubation. Lastly, 10 µl of each antibiotic was pipetted onto the cellulose discs. The plates were incubated for an additional 24 hours at 20°C and any inhibition zones were measured the next day. The arrangement of each antibiotic on every plate prepared is presented in Figure 32.

3.5 Results

Assessing the general antibiotic resistance of *A. aurescens* TC1.

The bacterium was susceptible to 7 of the 9 antibiotics used, while being intermediately resistant to ampicillin and bacitracin (Table 5). Based on this, there were no antibiotics that *A. aurescens* TC1 was completely resistant to, according to the CLSI criteria for gram-positive bacteria (Humphries et al. 2018). The average ZOI (n=5) suggests that the most effective antibiotics against *A. aurescens* TC1, in descending order, were penicillin G, carbenicillin, chloramphenicol and tetracycline. These results were used to establish standard reference values to determine if ZOI measurements significantly differed with treatment. Penicillin G exhibited the largest ZOI size (37.5mm ± 0.06 mm SE), while the smallest corresponded to bacitracin at 12 mm ± 0.13 mm SE). The ZOI for kanamycin and streptomycin were comparable, at 24 mm ± 0mm SE and 25 mm ± 0.03 mm SE, respectively.

Table 5: *Antibiotic resistance of A. aurescens TC1* by averaging ZOI measurements on the control nutrient agar plates. R/I/S represents the ZOI size criteria to classify the bacterium as resistant, intermediate, or susceptible to the antibiotic, respectively.

Antibiotic	Average ZOI (mm)	CLSI classification (G+ bacterium)	Standard error (mm)	R (mm)	I (mm)	S (mm)
Chloramphenicol	37.5	Susceptible	0.158114	<12	13-17	>18
Tetracycline	35	Susceptible	0.063246	14	15-18	>19
Carbenicillin	39	Susceptible	0.063246	<18	19-22	>23
Pencillin G	50	Susceptible	0.063246	<14	NA	>15
Ampicillin	28	Intermediate	0.063246	<28	NA	>29
Gentamycin	19	Susceptible	0.031623	<12	13-15	>16
Bacitracin	12	Intermediate	0.126491	<8	9-12	>13
Kanamycin	24	Susceptible	0	<13	14-17	>18
Streptomycin	25	Susceptible	0.031623	<13	14-17	>18

Assessing the concentration of Cr(VI) on zone of inhibition size.

Arthrobacter aurescens TC1 was able to grow on nutrient agar supplemented with 0.5 mM and 0.05 mM Cr(VI), but did not grow in higher concentrations (Figure 33), indicating that the added chromium inhibited growth of the bacterium.

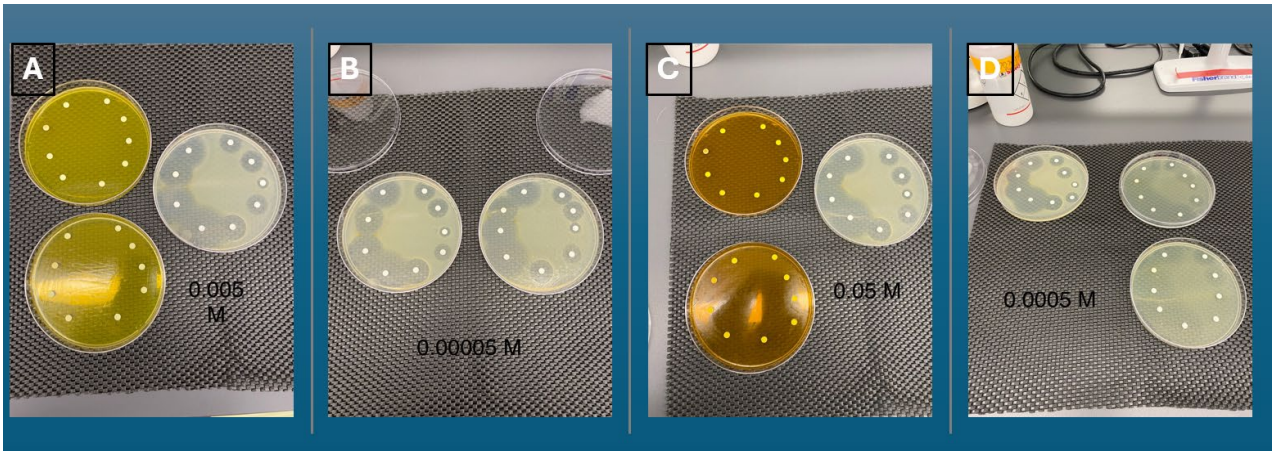

***Figure 35**: Nutrient agar with Cr(VI) supplementation. Cr(VI) concentrations were assessed with 10-fold increases in molar concentration. (A) 5mM, (B) 0.05 mM, (C) 50 mM, and (D) 0.5mM Here, each chromium plate is shown next to a control nutrient agar plate with no Cr(VI) added (Right-most plate, A-C). In Image D, the control nutrient agar plate is to the left. Image B is missing a replicate because it was growing mold, potentially skewing the results, and was discarded.*

Subsequently, the 0.5 mM plates were chosen for further analysis because the bacterium grew and had replication for statistical testing and comparison (Figures 33 and 34).

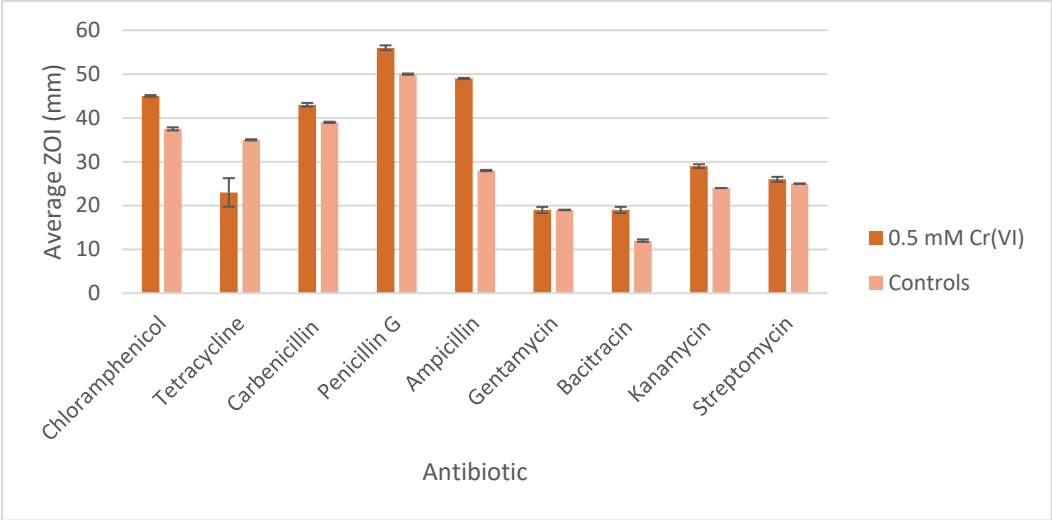

***Figure 36:** Nutrient agar plus 0.5 mM Cr(VI) ZOI results. The error bars represent the standard error of the mean of the Cr(VI) enriched plates (n=2) and the control plates (n=5). A star indicates that the bacterium became more tolerant to the antibiotic with the addition of Cr(VI) before significance was assessed.*

***Table 6**: Welch's t-test for zone of inhibition sizes with 0.5 mM Cr(VI) addition compared to the control after 24 hours at 20°C. Significant p-values are bolded.*

0.5 mM Cr(VI) enrichment	Average ZOI (mm)	Standard deviation (mm)	Standard error (mm)	t-statistic	p-value
Chloramphenicol	45	0.212132	0.15	50	**0.006365**
Tetracycline	23	3.252691	2.3	-5.21739	**0.060278**
Carbenicillin	43	0.424264	0.3	13.33333	**0.023829**
Penicillin G	56	0.565685	0.4	15	**0.021189**
Ampicillin	49	0.141421	0.1	210	**0.001516**
Gentamycin	19	0.707107	0.5	0	0.5
Bacitracin	19	0.707107	0.5	14	**0.022698**
Kanamycin	29	0.424264	0.3	16.66667	**0.019076**
Streptomycin	26	0.565685	0.4	2.5	0.121119

The bacterium's tolerance to the antibiotic was noted to improve if the ZOI significantly decreased with the addition of Cr(VI), compared to the reference standard (Table 6). The bacterium in most cases became significantly less tolerant to chloramphenicol, carbenicillin, penicillin, ampicillin, bacitracin, and kanamycin ($df=2$, $p<0.05$, $t>0$) with the addition of 0.5 mM Cr(VI) (Table 6). However, the average ZOI was smaller for tetracycline ($df=2$, $t=-5.2$), but it was not significant compared to the reference ($p=0.06$). There were no significant differences between the reference and chromium supplemented ZOIs for gentamycin and streptomycin ($p>0.05$).

Since the replicate was compromised in the 0.05 mM plates, no significant differences were able to be assessed between the treatment and reference ZOI using Welch's t-test for that concentration. One insight still noted here is that low dosages of Cr(VI) at 0.5 mM or smaller tended to be more conducive for growth of the bacterium. 0.5 mM Cr(VI) alone did not appear to make a difference in the antibiotic resistance of *Arthrobacter aurescens* TC1.

Assessing the effect of marine salts on zone of inhibition size

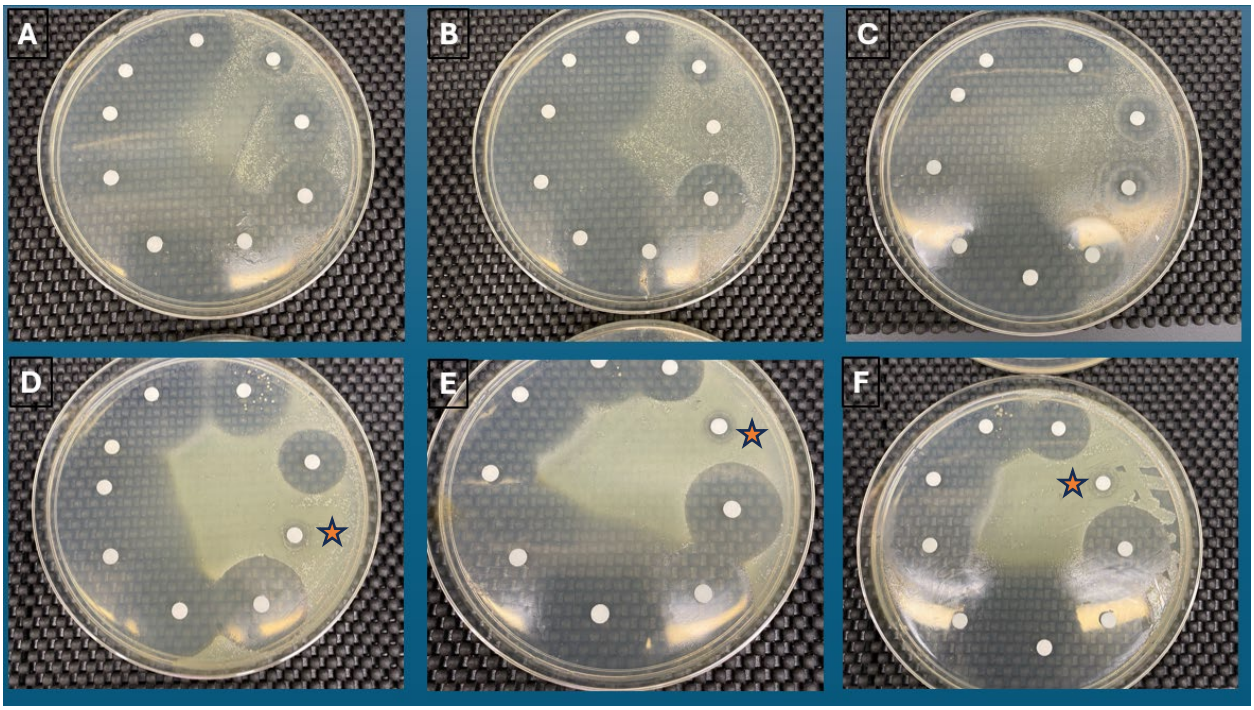

Figure 37: *1% and 5% marine salt enriched nutrient agar plates. (A-C) represent the replicate 5% salt enriched nutrient agar plates and (D-F) the replicate 1% salt enriched plates after 24 hours at 20°C.*

Growth of the bacterium was visible at 1% marine salts and decreased at 5% marine salts (Figure 35), indicated by patchy and spotted lawns characteristic of bacteria under stress. The bacterium did not grow at all on plates with 10% marine salts.

With the addition of 1% marine salts, the lowest average ZOI measurement (Figure 36) corresponded with bacitracin at 11.33 mm ± 0.16 mm (SE) and penicillin at 54.67 mm ± 5.70 mm (SE). The effects of 1% marine salt addition did not significantly change the size of the ZOI for ampicillin, carbenicillin, chloramphenicol, penicillin, and tetracycline ($p>0.05$, $df=2$). The ZOI was significantly smaller for Bacitracin ($p<0.05$, $df=2$, $t<0$), but significantly larger for gentamycin, streptomycin, and kanamycin ($p<0.05$, $df=2$, $t>0$).

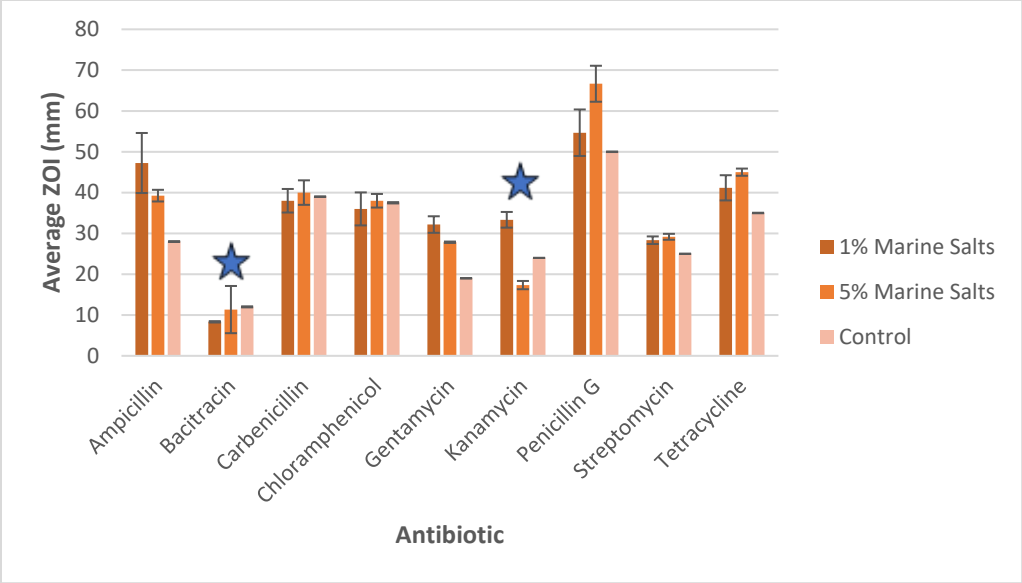

Figure 38: *1% and 5% marine salt addition. The error bars represent the standard error of the mean for the 1% marine salt plates (n=3) and 5% marine salt plates (n=3) to the control plates with no salt (n=9). A star indicates the bacterium became better at tolerating the antibiotic with the addition of either 1% or 5% marine salts.*

With the addition of 5% marine salts, the lowest average ZOI measurement (Figure 36) corresponded with bacitracin at 11.33 ± 5.78 mm (SE) and the highest with penicillin G at 66.67 mm ± 4.41 mm (SE). There was a significantly larger ZOI for ampicillin, carbenicillin, chloramphenicol, gentamicin, penicillin G, streptomycin, and tetracycline ($p<0.05$, $df=2$, $t>0$). The ZOI was significantly smaller for kanamycin ($p<0.05$, $df=2$, $t<0$). The ZOI for bacitracin was not significantly different from the reference control value taken from plain nutrient agar without salt supplementation. The averages, standard deviations, standard errors, t-statistics, and corresponding p-values for the one-tail t-tests for both 1% and 5% marine salt addition are summarized in Table 7 and Table 8, respectively.

Table 7*: One-tail t-test results for growth in the presence of 1% marine salts. Significant p-values are in bold.*

1% marine salt	Average ZOI (mm)	Standard deviation (mm)	Standard error (mm)	t-statistic	p-value
Ampicillin-10	47.25	12.73	7.35	2.617574243	0.060098144
Bacitracin-	8.33	0.28	0.16	-22	**0.001029867**
Carbenicillin-	38	5	2.89	-0.34641016	0.381042262
Chloramphenicol	37	7	4.04	-0.37115374	0.373075671
Gentamicin-30	32.17	3.51	2.03	6.493759999	**0.01145131**
Kanamycin-	33.33	3.33	1.92	4.855815829	**0.019945133**

Penicillin G-	54.67	9.87	5.70	0.81928803	0.249359794
Streptomycin-	28.33	1.61	0.93	3.592106041	**0.034757895**
Tetracycline-30	41.17	5.35	3.09	1.997812214	0.091900732

***Table 8**: One-tail t-test results for growth in the presence of 5% marine salts. Significant p-values are in bold.*

5% marine salt	Average ZOI (mm)	Standard deviation (mm)	Standard error (mm)	t-statistic	p-value
Ampicillin-10	39.25	2.47	1.42	7.873359888	**0.007875774**
Bacitracin-	11.33	10	5.78	-0.11527808	0.459377777
Carbenicillin-	61	5.19	3	7.333333333	**0.009045973**
Chloramphenicol	58.33	2.89	1.67	12.5	**0.003169604**
Gentamicin-30	27.83	0.28	0.17	53	**0.000177904**
Kanamycin-	17.33	1.75	1.01	-6.57595949	**0.011176283**
Penicillin G-	66.67	7.63	4.41	3.77964473	**0.031707094**
Streptomycin-	29.17	1.26	0.73	5.735393347	**0.014540227**
Tetracycline-30	56.33	1.53	0.88	24.18972627	**0.000852308**

Assessing the compound effect of Cr(VI) and marine salts on zone of inhibition size.

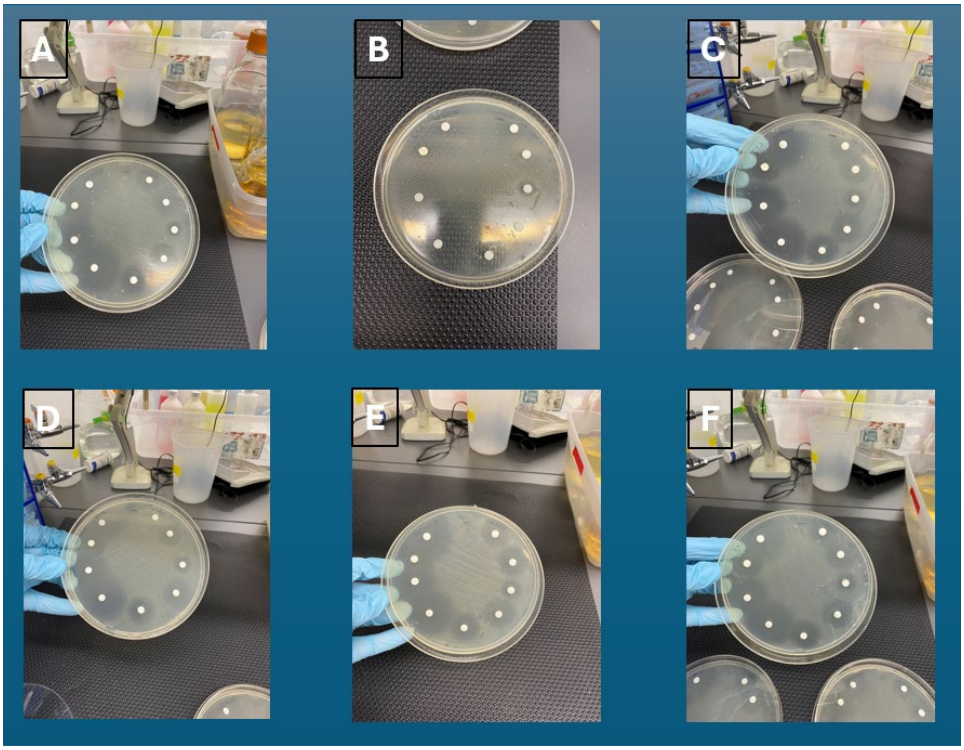

***Figure 39**: (A-F) Nutrient agar supplemented with 2% salinity and 0.8 uM Cr(VI) after 24 hours of incubation time at 20°C.*

The bacterium grew under 2% salinity and 0.8 µM Cr(VI) (0.0008 mM Cr(VI), for comparison) supplementation (Figure 37), although the lawns looked sickly compared to growth on normal nutrient agar. The effect of increasing the media's salinity to 2% plus 0.8 µM Cr(VI) enrichment resulted in an improvement in the ZOI for many of the reported antibiotics (Figure 38). Within this, the bacterium tolerated tetracycline, carbenicillin, penicillin G, ampicillin, bacitracin, kanamycin, and streptomycin better compared to the ZOIs measured on regular nutrient agar, by Welch's t-test ($df=4$, $p<0.05$). All t-statistics for these antibiotics were negative, indicating the sample mean was less than the reference value (Table 8). The bacterium was significantly worse at tolerating chloramphenicol ($df=4$, $t=5.10$, $p<0.05$) and gentamicin ($df=4$, $t=7.09$, $p<0.05$).

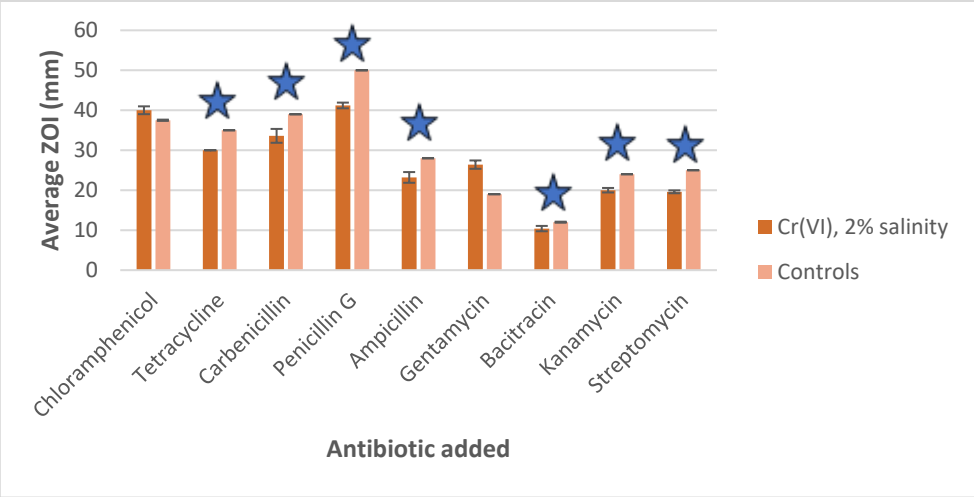

***Figure 40**. Cr(VI) and 2% salinity factorial experiment. The error bars represent the standard error of the mean for Cr(VI), 2% marine salt plates (n=5) and their control (n=5). The antibiotic is starred if the bacterium tolerated it better under Cr(VI) + 2% salinity.*

Table 9: *Welch's t-test for growth 2% salinity and Cr(VI) enrichment. Significant p-values are bolded.*

Antibiotic	**Average ZOI (mm)**	**Standard deviation (mm)**	**Standard error (mm)**	**t-stat**	**P-value**
Chloramphenicol	40	2.19089	0.979796	5.103104	**0.00348376**
Tetracycline	30	0.5	1E-07	-4E+07	**1.1719E-30**
Carbenicillin	33.6	3.878144	1.734359	-2.53696	**0.03209392**
Penicillin G	41.2	1.6	0.715542	-12.2984	**0.00012555**
Ampicillin	23.2	2.993326	1.338656	-3.58569	**0.01152518**
Gentamycin	26.4	2.332381	1.043072	7.094426	**0.00104234**
Bacitracin	10.4	1.496663	0.669328	-2.39046	**0.03756523**
Kanamycin	20	1.264911	0.565685	-7.07107	**0.00105532**
Streptomycin	19.6	0.8	0.357771	-15.0935	**5.6152E-05**

3.6 Discussion

The hypothesis that the addition of Cr(VI) or marine salts alone could decrease the ZOI was partially supported, as the addition of Cr(VI) alone did not significantly decrease the ZOI of *A. aurescens* TC1, while the addition of 1% salinity alone improved its tolerance to bacitracin and at 5%, kanamycin. The hypothesis that the effect of combining the two would decrease the ZOI was supported. When Cr(VI) was added in combination with marine salts significant improvements were observed, highlighting that salinity may be an important factor in the co-resistance of Cr(VI) and antibiotics. The bacterium became more tolerant of all beta-lactam class antibiotics (ampicillin, penicillin and carbenicillin), which function by inhibition of peptidoglycan synthesis (Denyer et al. 2007), and all aminoglycosides except for gentamycin. Interestingly, the bacterium became worse at tolerating chloramphenicol but not tetracycline;

both of which inhibit protein synthesis but target different structures within the bacterial cell (Singhal et al. 2023)

Bacitracin, which is an antimicrobial peptide, works by inhibition of cell wall synthesis and its resistance is conferred by the *bcrC* transport permease and *bceAB* cellular efflux pumps in gram-positive bacteria (Cao and Helmann 2002). An increase in resistance was seen when exposed to 1% salinity, where previous studies have shown that induction of the *bcrC* transport permease is mediated by the sigma factor σ^M, which becomes highly expressed under stressors such as high salinity, heat, and antibiotic treatment (Cao and Helmann 2002; Thackray and Moir 2003). Therefore, one plausible mechanism of action suggests that the salt stress combined with the antibiotic stress over-expressed the *bcrC* transport permease, leading to a decrease in ZOI size due to enhanced efflux, which was supported since the control nutrient agar plates containing trace amounts of salt were larger than those treated with 1% marine salts. However, the fact that this result was not visualized at 5% marine salts suggests that this may only occur within a low range of salinities, whereas higher salt concentrations could result in alterations to membrane permeability and a subsequent increase in uptake of bacitracin and cell death (Falghoush et al. 2017). However, this is inconclusive given that the ZOI for bacitracin at 5% marine salt was not significantly different from the control. Higher salt concentrations could play a role in aminoglycoside resistance since the bacterium became more tolerant of kanamycin at 5% salinity but not at 1%. Other work has contradicting results, where it was found that increased aminoglycoside resistance in *P. aeruginosa* and *E. coli* was attributed to ionic strength and its subsequent inhibition of the antibiotic (Beggs and Andrews 1976), showing that abiotic influence could also impact the ZOI. In other cases, aminoglycoside resistance was found to increase due to the over-production of aminoglycoside phosphotransferases in a marine *Halomonas sp.* at salinities up to 10% but not at 1%, where environmental conditions, adaption to salinity stress, and species-specific interactions may play significant roles in the interplay between aminoglycosides, salts, and bacterial resistance (Park et al. 2021).

Given the interaction with salinity, the mechanism for the combined effect of low-dose Cr(VI) remains unclear. The *chrA* efflux pump, part of the *chrBACF* operon, is specific only for Cr(VI) efflux and is only induced under chromate stress or oxidative stress (Branco et al. 2008), but it is not understood if this pump has dual-activity for any antibiotics. It has been previously reported that metal exposure could facilitate decreased uptake of antibiotics through decreased expression of the associated membrane porin (Perron et al. 2004). In *S. aureus*¸ it was shown that chromate exposure increased the expression of many multidrug efflux pumps, and RT-PCR analyses implicated the *acrAB* pump as the primary candidate conferring resistance under these conditions. *Arthrobacter aurescens* TC1 is capable of this and within its genome are annotations for several TetR/AcrR family type proteins (WP_014921249.1, WP_0438060371.1) located on either the PTC1 or PTC2 plasmids, which regulate its *acrAB* pumps (Subhadra et al. 2018). However, additional culture-based studies combined with transcriptomics would be necessary to understand if these systems are upregulated with Cr(VI) addition, thereby increasing resistance to the antibiotic either through increased efflux or inactivation.

3.7 Conclusions and future directions

It was found that salinity alone could cause an increase in resistance to bacitracin and kanamycin at 1% salinity and 5% salinity, respectively, but no significant differences were seen with Cr(VI) alone. However, 2% salinity and 0.8 μM Cr(VI) are comparable to concentrations traditionally found in some estuaries, which displayed an increase in resistance for most antibiotics except chloramphenicol and gentamicin. The most adverse effects on resistance are seen when both are combined, meaning a risk exists of this occurring in contaminated estuaries frequently exposed to salinity fluctuation and combined chromium-waste from neighboring industry or waste sites. Future directions should focus on studying this with isolates taken from chromium-contaminated estuaries to pinpoint which taxa this process could be associated with, in combination with Cr(VI) and salinity measurements. Additionally, transcriptomic-based studies would be necessary to answer larger questions about the up-regulation or down-regulation of systems linking the MRGs and ARGs under estuarine conditions.

LITERATURE CITED

Ali. 2012. ANTIBIOTIC RESISTANCE AND CHROMIUM REDUCTION PATTERN AMONG ACTINOMYCETES. American Journal of Biochemistry and Biotechnology. 8(2):111–117. https://doi.org/10.3844/ajbbsp.2012.111.117

Baker-Austin C, Wright MS, Stepanauskas R, McArthur JV. 2006. Co-selection of antibiotic and metal resistance. Trends in Microbiology. 14(4):176–182. https://doi.org/10.1016/j.tim.2006.02.006

Baquero F, Martínez J-L, Cantón R. 2008. Antibiotics and antibiotic resistance in water environments. Current Opinion in Biotechnology. 19(3):260–265. https://doi.org/10.1016/j.copbio.2008.05.006

Bashir I, Lone FA, Bhat RA, Mir SA, Dar ZA, Dar SA. 2020. Concerns and Threats of Contamination on Aquatic Ecosystems. In: Hakeem KR, Bhat RA, Qadri H, editors. Bioremediation and Biotechnology [Internet]. Cham: Springer International Publishing; [accessed 2024 Mar 14]; p. 1–26. https://doi.org/10.1007/978-3-030-35691-0_1

Beggs WH, Andrews FA. 1976. Role of Ionic Strength in Salt Antagonism of Aminoglycoside Action on Escherichia coli and Pseudomonas aeruginosa. Journal of Infectious Diseases. 134(5):500–504. https://doi.org/10.1093/infdis/134.5.500

Berglund B. 2015. Environmental dissemination of antibiotic resistance genes and correlation to anthropogenic contamination with antibiotics. Infection Ecology & Epidemiology. 5(1):28564. https://doi.org/10.3402/iee.v5.28564

Bombaywala S, Purohit HJ, Dafale NA. 2021. Mobility of antibiotic resistance and its co-occurrence with metal resistance in pathogens under oxidative stress. Journal of Environmental Management. 297:113315. https://doi.org/10.1016/j.jenvman.2021.113315

Bonnand P, James RH, Parkinson IJ, Connelly DP, Fairchild IJ. 2013. The chromium isotopic composition of seawater and marine carbonates. Earth and Planetary Science Letters. 382:10–20. https://doi.org/10.1016/j.epsl.2013.09.001

Bourdonnais E, Colcanap D, Le Bris C, Brauge T, Midelet G. 2022. Occurrence of Indicator Genes of Antimicrobial Resistance Contamination in the English Channel and North Sea Sectors and Interactions With Environmental Variables. Front Microbiol. 13:883081. https://doi.org/10.3389/fmicb.2022.883081

Branco R, Chung AP, Johnston T, Gurel V, Morais P, Zhitkovich A. 2008. The Chromate-Inducible *chrBACF* Operon from the Transposable Element Tn *OtChr* Confers Resistance to Chromium(VI) and Superoxide. J Bacteriol. 190(21):6996–7003. https://doi.org/10.1128/JB.00289-08

Cao M, Helmann JD. 2002. Regulation of the Bacillus subtilis bcrC Bacitracin Resistance Gene by Two Extracytoplasmic Function Factors. J BACTERIOL. 184.

Chakraborty P, Ramteke D, Chakraborty S, Nagender Nath B. 2014. Changes in metal contamination levels in estuarine sediments around India – An assessment. Marine Pollution Bulletin. 78(1–2):15–25. https://doi.org/10.1016/j.marpolbul.2013.09.044

Chen S, Zhou Y, Chen Y, Gu J. 2018. fastp: an ultra-fast all-in-one FASTQ preprocessor. Bioinformatics. 34(17):i884–i890. https://doi.org/10.1093/bioinformatics/bty560

De Souza Machado AA, Spencer K, Kloas W, Toffolon M, Zarfl C. 2016. Metal fate and effects in estuaries: A review and conceptual model for better understanding of toxicity. Science of The Total Environment. 541:268–281. https://doi.org/10.1016/j.scitotenv.2015.09.045

Delgado-Baquerizo M, Hu H-W, Maestre FT, Guerra CA, Eisenhauer N, Eldridge DJ, Zhu Y-G, Chen Q-L, Trivedi P, Du S, et al. 2022. The global distribution and environmental drivers of the soil antibiotic resistome. Microbiome. 10(1):219. https://doi.org/10.1186/s40168-022-01405-w

Denyer SP, Hodges NA, Gorman SP. Pharmaceutical Microbiology.

Di Cesare A, Eckert E, Corno G. 2016. Co-selection of antibiotic and heavy metal resistance in freshwater bacteria. J Limnol [Internet]. [accessed 2023 Apr 5] 75(s2). https://doi.org/10.4081/jlimnol.2016.1198

Du D, Wang-Kan X, Neuberger A, Van Veen HW, Pos KM, Piddock LJV, Luisi BF. 2018. Multidrug efflux pumps: structure, function and regulation. Nat Rev Microbiol. 16(9):523–539. https://doi.org/10.1038/s41579-018-0048-6

Dubbels BL, DiSpirito AA, Morton JD, Semrau JD, Neto JNE, Bazylinski DA. 2004. Evidence for a copper-dependent iron transport system in the marine, magnetotactic bacterium strain MV-1. Microbiology. 150(9):2931–2945. https://doi.org/10.1099/mic.0.27233-0

Emerson D, Fleming EJ, McBeth JM. 2010. Iron-Oxidizing Bacteria: An Environmental and Genomic Perspective. Annu Rev Microbiol. 64(1):561–583. https://doi.org/10.1146/annurev.micro.112408.134208

Emerson D, Weiss JV. 2004. Bacterial Iron Oxidation in Circumneutral Freshwater Habitats: Findings from the Field and the Laboratory. Geomicrobiology Journal. 21(6):405–414. https://doi.org/10.1080/01490450490485881

Falghoush A, Beyenal H, Besser TE, Omsland A, Call DR. 2017. Osmotic Compounds Enhance Antibiotic Efficacy against Acinetobacter baumannii Biofilm Communities.Dozois CM, editor. Appl Environ Microbiol. 83(19):e01297-17. https://doi.org/10.1128/AEM.01297-17

Fergus CE, Lapierre J-F, Oliver SK, Skaff NK, Cheruvelil KS, Webster K, Scott C, Soranno P. 2017. The freshwater landscape: lake, wetland, and stream abundance and connectivity at macroscales. Ecosphere. 8(8):e01911. https://doi.org/10.1002/ecs2.1911

Field EK, Blaskovich JP, Peyton BM, Gerlach R. 2018. Carbon-dependent chromate toxicity mechanism in an environmental Arthrobacter isolate. Journal of Hazardous Materials. 355:162–169. https://doi.org/10.1016/j.jhazmat.2018.05.020

Gaze WH, Zhang L, Abdouslam NA, Hawkey PM, Calvo-Bado L, Royle J, Brown H, Davis S, Kay P, Boxall ABA, Wellington EMH. 2011. Impacts of anthropogenic activity on the ecology of class 1 integrons and integron-associated genes in the environment. ISME J. 5(8):1253–1261. https://doi.org/10.1038/ismej.2011.15

Gillings MR, Gaze WH, Pruden A, Smalla K, Tiedje JM, Zhu Y-G. 2015. Using the class 1 integron-integrase gene as a proxy for anthropogenic pollution. ISME J. 9(6):1269–1279. https://doi.org/10.1038/ismej.2014.226

Hernández J, Stedt J, Bonnedahl J, Molin Y, Drobni M, Calisto-Ulloa N, Gomez-Fuentes C, Astorga-España MS, González-Acuña D, Waldenström J, et al. 2012. Human-Associated Extended-Spectrum β-Lactamase in the Antarctic. Appl Environ Microbiol. 78(6):2056–2058. https://doi.org/10.1128/AEM.07320-11

Hicks LA, Bartoces MG, Roberts RM, Suda KJ, Hunkler RJ, Taylor TH, Schrag SJ. 2015. US Outpatient Antibiotic Prescribing Variation According to Geography, Patient Population, and Provider Specialty in 2011. Clinical Infectious Diseases.:civ076. https://doi.org/10.1093/cid/civ076

Horton RN, Apel WA, Thompson VS, Sheridan PP. 2006. Low temperature reduction of hexavalent chromium by a microbial enrichment consortium and a novel strain of Arthrobacter aurescens. BMC Microbiol. 6(1):5. https://doi.org/10.1186/1471-2180-6-5

Hossain MB, Shanta TB, Ahmed ASS, Hossain MdK, Semme SA. 2019. Baseline study of heavy metal contamination in the Sangu River estuary, Chattogram, Bangladesh. Marine Pollution Bulletin. 140:255–261. https://doi.org/10.1016/j.marpolbul.2019.01.058

Humphries RM, Ambler J, Mitchell SL, Castanheira M, Dingle T, Hindler JA, Koeth L, Sei K, Hardy D, Zimmer B, et al. 2018. CLSI Methods Development and Standardization Working Group Best Practices for Evaluation of Antimicrobial Susceptibility Tests.Kraft CS, editor. J Clin Microbiol. 56(4):e01934-17. https://doi.org/10.1128/JCM.01934-17

Hwengwere K, Paramel Nair H, Hughes KA, Peck LS, Clark MS, Walker CA. 2022. Antimicrobial resistance in Antarctica: is it still a pristine environment? Microbiome. 10(1):71. https://doi.org/10.1186/s40168-022-01250-x

Kappler A, Bryce C, Mansor M, Lueder U, Byrne JM, Swanner ED. 2021. An evolving view on biogeochemical cycling of iron. Nat Rev Microbiol. 19(6):360–374. https://doi.org/10.1038/s41579-020-00502-7

Keely SP, Brinkman NE, Wheaton EA, Jahne MA, Siefring SD, Varma M, Hill RA, Leibowitz SG, Martin RW, Garland JL, Haugland RA. 2022. Geospatial Patterns of Antimicrobial Resistance Genes in the US EPA National Rivers and Streams Assessment Survey. Environ Sci Technol. 56(21):14960–14971. https://doi.org/10.1021/acs.est.2c00813

Khan MMdT, Sklar L. 2023. Editorial: Environmental contaminants in aquatic systems and chemical safety for environmental and human health, volume II. Front Public Health. 11:1157834. https://doi.org/10.3389/fpubh.2023.1157834

Khatiebi S, Kiprotich K, Onyando Z, Wekesa C, Chi CN, Mulambalah C, Okoth P. 2023. Shotgun Metagenomic Analyses of Microbial Assemblages in the Aquatic Ecosystem of Winam Gulf of

Lake Victoria, Kenya Reveals Multiclass Pollution.Sánchez García F, editor. BioMed Research International. 2023:1–18. https://doi.org/10.1155/2023/3724531

Koczura R, Mokracka J, Taraszewska A, Łopacinska N. 2016. Abundance of Class 1 Integron-Integrase and Sulfonamide Resistance Genes in River Water and Sediment Is Affected by Anthropogenic Pressure and Environmental Factors. Microb Ecol. 72(4):909–916. https://doi.org/10.1007/s00248-016-0843-4

Kong L. 2022. Copper Requirement and Acquisition by Marine Microalgae. Microorganisms. 10(9):1853. https://doi.org/10.3390/microorganisms10091853

Li B, Yang Y, Ma L, Ju F, Guo F, Tiedje JM, Zhang T. 2015. Metagenomic and network analysis reveal wide distribution and co-occurrence of environmental antibiotic resistance genes. The ISME Journal. 9(11):2490–2502. https://doi.org/10.1038/ismej.2015.59

Li J, Phulpoto IA, Zhang G, Yu Z. 2021. Acceleration of emergence of E. coli antibiotic resistance in a simulated sublethal concentration of copper and tetracycline co-contaminated environment. AMB Expr. 11(1):14. https://doi.org/10.1186/s13568-020-01173-6

Li P, Feng XB, Qiu GL, Shang LH, Li ZG. 2009. Mercury pollution in Asia: A review of the contaminated sites. Journal of Hazardous Materials. 168(2–3):591–601. https://doi.org/10.1016/j.jhazmat.2009.03.031

Lu X-M, Liu X-P. 2021. Distribution of Metal Resistance Genes in Estuarine Sediments and Associated Key Impact Factors. Microb Ecol. 82(3):581–590. https://doi.org/10.1007/s00248-021-01699-7

Maghsodian Z, Sanati AM, Mashifana T, Sillanpää M, Feng S, Nhat T, Ramavandi B. 2022. Occurrence and Distribution of Antibiotics in the Water, Sediment, and Biota of Freshwater and Marine Environments: A Review. Antibiotics. 11(11):1461. https://doi.org/10.3390/antibiotics11111461

Matsuo T, Hayashi K, Morita Y, Koterasawa M, Ogawa W, Mizushima T, Tsuchiya T, Kuroda T. 2007. VmeAB, an RND-type multidrug efflux transporter in Vibrio parahaemolyticus. Microbiology. 153(12):4129–4137. https://doi.org/10.1099/mic.0.2007/009597-0

McAllister SM, Polson SW, Butterfield DA, Glazer BT, Sylvan JB, Chan CS. 2020. Validating the Cyc2 Neutrophilic Iron Oxidation Pathway Using Meta-omics of *Zetaproteobacteria* Iron Mats at Marine Hydrothermal Vents.Lloyd KG, editor. mSystems. 5(1):e00553-19. https://doi.org/10.1128/mSystems.00553-19

Merchant SS, Helmann JD. 2012. Elemental Economy. In: Advances in Microbial Physiology [Internet]. Vol. 60. [place unknown]: Elsevier; [accessed 2023 Jun 27]; p. 91–210. https://doi.org/10.1016/B978-0-12-398264-3.00002-4

MOiler G. Heavy metals in sediments of the rhine and elbe estuaries: Mobilization or mixing effect?

Mongodin EF, Shapir N, Daugherty SC, DeBoy RT, Emerson JB, Shvartzbeyn A, Radune D, Vamathevan J, Riggs F, Grinberg V, et al. 2006. Secrets of Soil Survival Revealed by the Genome Sequence of Arthrobacter aurescens TC1. PLoS Genet. 2(12):e214. https://doi.org/10.1371/journal.pgen.0020214

Mori JF, Scott JJ, Hager KW, Moyer CL, Küsel K, Emerson D. 2017. Physiological and ecological implications of an iron- or hydrogen-oxidizing member of the Zetaproteobacteria, Ghiorsea bivora, gen. nov., sp. nov. ISME J. 11(11):2624–2636. https://doi.org/10.1038/ismej.2017.132

Murray CJL, Ikuta KS, Sharara F, Swetschinski L, Robles Aguilar G, Gray A, Han C, Bisignano C, Rao P, Wool E, et al. 2022. Global burden of bacterial antimicrobial resistance in 2019: a systematic analysis. The Lancet. 399(10325):629–655. https://doi.org/10.1016/S0140-6736(21)02724-0

Murray LM, Hayes A, Snape J, Kasprzyk-Hordern B, Gaze WH, Murray AK. 2024. Co-selection for antibiotic resistance by environmental contaminants. npj Antimicrob Resist. 2(1):9. https://doi.org/10.1038/s44259-024-00026-7

Ochieng EZ, Lalah JO, Wandiga SO. 2006. Heavy Metals in Water and Surface Sediments in Winam Gulf of Lake Victoria, Kenya. Bull Environ Contam Toxicol. 77(3):459–468. https://doi.org/10.1007/s00128-006-1087-7

Paczian T, Trimble WL, Gerlach W, Harrison T, Wilke A, Meyer F. 2019. The MG-RAST API explorer: an on-ramp for RESTful query composition. BMC Bioinformatics. 20(1):561. https://doi.org/10.1186/s12859-019-2993-0

Pan K, Wang W-X. 2012. Trace metal contamination in estuarine and coastal environments in China. Science of The Total Environment. 421–422:3–16. https://doi.org/10.1016/j.scitotenv.2011.03.013

Park Y-L, Choi T-R, Kim HJ, Song H-S, Lee HS, Park SL, Lee SM, Kim SH, Park S, Bhatia SK, et al. 2021. NaCl Concentration-Dependent Aminoglycoside Resistance of *Halomonas socia* CKY01 and Identification of Related Genes. J Microbiol Biotechnol. 31(2):250–258. https://doi.org/10.4014/jmb.2009.09017

Pärnänen K, Karkman A, Hultman J, Lyra C, Bengtsson-Palme J, Larsson DGJ, Rautava S, Isolauri E, Salminen S, Kumar H, et al. 2018. Maternal gut and breast milk microbiota affect infant gut antibiotic resistome and mobile genetic elements. Nat Commun. 9(1):3891. https://doi.org/10.1038/s41467-018-06393-w

Pei R, Kim S-C, Carlson KH, Pruden A. 2006. Effect of River Landscape on the sediment concentrations of antibiotics and corresponding antibiotic resistance genes (ARG). Water Research. 40(12):2427–2435. https://doi.org/10.1016/j.watres.2006.04.017

Perron K, Caille O, Rossier C, Van Delden C, Dumas J-L, Köhler T. 2004. CzcR-CzcS, a Two-component System Involved in Heavy Metal and Carbapenem Resistance in Pseudomonas aeruginosa. Journal of Biological Chemistry. 279(10):8761–8768. https://doi.org/10.1074/jbc.M312080200

Raab A, Feldmann J. 2003. Microbial Transformation of Metals and Metalloids. Science Progress. 86(3):179–202. https://doi.org/10.3184/003685003783238671

Rajamohan G, Srinivasan VB, Gebreyes WA. 2010. Novel role of Acinetobacter baumannii RND efflux transporters in mediating decreased susceptibility to biocides. Journal of Antimicrobial Chemotherapy. 65(2):228–232. https://doi.org/10.1093/jac/dkp427

Rensing C, Grass G. 2003. *Escherichia coli* mechanisms of copper homeostasis in a changing environment. FEMS Microbiol Rev. 27(2–3):197–213. https://doi.org/10.1016/S0168-6445(03)00049-4

Richon C, Tagliabue A. 2019. Insights Into the Major Processes Driving the Global Distribution of Copper in the Ocean From a Global Model. Global Biogeochem Cycles. 33(12):1594–1610. https://doi.org/10.1029/2019GB006280

Sanders CJ, Santos IR, Barcellos R, Silva Filho EV. 2012. Elevated concentrations of dissolved Ba, Fe and Mn in a mangrove subterranean estuary: Consequence of sea level rise? Continental Shelf Research. 43:86–94. https://doi.org/10.1016/j.csr.2012.04.015

Sanderson H, Ortega-Polo R, McDermott K, Hall G, Zaheer R, Brown RS, Majury A, McAllister TA, Liss SN. 2019. Quantification and Multidrug Resistance Profiles of Vancomycin-Resistant Enterococci Isolated from Two Wastewater Treatment Plants in the Same Municipality. Microorganisms. 7(12):626. https://doi.org/10.3390/microorganisms7120626

Seiler C, Berendonk T. 2012. Heavy metal driven co-selection of antibiotic resistance in soil and water bodies impacted by agriculture and aquaculture. Frontiers in Microbiology [Internet]. [accessed 2023 Apr 5] 3. https://www.frontiersin.org/articles/10.3389/fmicb.2012.00399

Selim S. 2021. Mechanisms of gram-positive vancomycin resistance (Review). Biomed Rep. 16(1):7. https://doi.org/10.3892/br.2021.1490

Shen W, Le S, Li Y, Hu F. 2016. SeqKit: A Cross-Platform and Ultrafast Toolkit for FASTA/Q File Manipulation.Zou Q, editor. PLoS ONE. 11(10):e0163962. https://doi.org/10.1371/journal.pone.0163962

Singh V, Singh N, Rai SN, Kumar A, Singh AK, Singh MP, Sahoo A, Shekhar S, Vamanu E, Mishra V. 2023. Heavy Metal Contamination in the Aquatic Ecosystem: Toxicity and Its Remediation Using Eco-Friendly Approaches. Toxics. 11(2):147. https://doi.org/10.3390/toxics11020147

Singhal M, Agrawal M, Bhavna K, Sethiya NK, Bhargava S, Gondkar KS, Joshi K, Rana VS, Sahoo J, Arora MK. 2023. Chloramphenicol and tetracycline (broad spectrum antibiotics). In: Antibiotics - Therapeutic Spectrum and Limitations [Internet]. [place unknown]: Elsevier; [accessed 2024 Apr 12]; p. 155–165. https://doi.org/10.1016/B978-0-323-95388-7.00019-X

Srinivasan VB, Vaidyanathan V, Mondal A, Rajamohan G. 2012. Role of the Two Component Signal Transduction System CpxAR in Conferring Cefepime and Chloramphenicol Resistance in Klebsiella pneumoniae NTUH-K2044.Forestier C, editor. PLoS ONE. 7(4):e33777. https://doi.org/10.1371/journal.pone.0033777

Stark JS, Corbett PA, Dunshea G, Johnstone G, King C, Mondon JA, Power ML, Samuel A, Snape I, Riddle M. 2016. The environmental impact of sewage and wastewater outfalls in Antarctica: An example from Davis station, East Antarctica. Water Research. 105:602–614. https://doi.org/10.1016/j.watres.2016.09.026

Strong LC, Rosendahl C, Johnson G, Sadowsky MJ, Wackett LP. 2002. *Arthrobacter aurescens* TC1 Metabolizes Diverse *s* -Triazine Ring Compounds. Appl Environ Microbiol. 68(12):5973–5980. https://doi.org/10.1128/AEM.68.12.5973-5980.2002

Subhadra B, Kim J, Kim DH, Woo K, Oh MH, Choi CH. 2018. Local Repressor AcrR Regulates AcrAB Efflux Pump Required for Biofilm Formation and Virulence in Acinetobacter nosocomialis. Front Cell Infect Microbiol. 8:270. https://doi.org/10.3389/fcimb.2018.00270

Thackray PD, Moir A. 2003. SigM, an Extracytoplasmic Function Sigma Factor of *Bacillus subtilis* , Is Activated in Response to Cell Wall Antibiotics, Ethanol, Heat, Acid, and Superoxide Stress. J Bacteriol. 185(12):3491–3498. https://doi.org/10.1128/JB.185.12.3491-3498.2003

Thevenon F, Graham ND, Herbez A, Wildi W, Poté J. 2011. Spatio-temporal distribution of organic and inorganic pollutants from Lake Geneva (Switzerland) reveals strong interacting effects of sewage treatment plant and eutrophication on microbial abundance. Chemosphere. 84(5):609–617. https://doi.org/10.1016/j.chemosphere.2011.03.051

Vahjen W, Pietruszyńska D, Starke IC, Zentek J. 2015. High dietary zinc supplementation increases the occurrence of tetracycline and sulfonamide resistance genes in the intestine of weaned pigs. Gut Pathog. 7(1):23. https://doi.org/10.1186/s13099-015-0071-3

Vigil-Stenman T, Ininbergs K, Bergman B, Ekman M. 2017. High abundance and expression of transposases in bacteria from the Baltic Sea. The ISME Journal. 11(11):2611–2623. https://doi.org/10.1038/ismej.2017.114

Wright MS, Baker-Austin C, Lindell AH, Stepanauskas R, Stokes HW, McArthur JV. 2008. Influence of industrial contamination on mobile genetic elements: class 1 integron abundance and gene cassette structure in aquatic bacterial communities. ISME J. 2(4):417–428. https://doi.org/10.1038/ismej.2008.8

Yadav KK, Gupta N, Prasad S, Malav LC, Bhutto JK, Ahmad A, Gacem A, Jeon B-H, Fallatah AM, Asghar BH, et al. 2023. An eco-sustainable approach towards heavy metals remediation by mangroves from the coastal environment: A critical review. Marine Pollution Bulletin. 188:114569. https://doi.org/10.1016/j.marpolbul.2022.114569

Yang Y, Jiang X, Chai B, Ma L, Li B, Zhang A, Cole JR, Tiedje JM, Zhang T. 2016. ARGs-OAP: online analysis pipeline for antibiotic resistance genes detection from metagenomic data using an integrated structured ARG-database. Bioinformatics. 32(15):2346–2351. https://doi.org/10.1093/bioinformatics/btw136

Yang Y, Li Z, Song W, Du L, Ye C, Zhao B, Liu W, Deng D, Pan Y, Lin H, Cao X. 2019. Metagenomic insights into the abundance and composition of resistance genes in aquatic environments: Influence of stratification and geography. Environment International. 127:371–380. https://doi.org/10.1016/j.envint.2019.03.062

Yi J, Lo LSH, Liu H, Qian P-Y, Cheng J. 2021. Study of Heavy Metals and Microbial Communities in Contaminated Sediments Along an Urban Estuary. Front Mar Sci. 8:741912. https://doi.org/10.3389/fmars.2021.741912

Zaynab M, Al-Yahyai R, Ameen A, Sharif Y, Ali L, Fatima M, Khan KA, Li S. 2022. Health and environmental effects of heavy metals. Journal of King Saud University - Science. 34(1):101653. https://doi.org/10.1016/j.jksus.2021.101653

Zhang M, Wan K, Zeng J, Lin W, Ye C, Yu X. 2020. Co-selection and stability of bacterial antibiotic resistance by arsenic pollution accidents in source water. Environment International. 135:105351. https://doi.org/10.1016/j.envint.2019.105351

Zhang Y-J, Hu H-W, Yan H, Wang J-T, Lam SK, Chen Q-L, Chen D, He J-Z. 2019. Salinity as a predominant factor modulating the distribution patterns of antibiotic resistance genes in ocean

and river beach soils. Science of The Total Environment. 668:193–203. https://doi.org/10.1016/j.scitotenv.2019.02.454

Zheng D, Yin G, Liu M, Hou L, Yang Y, Van Boeckel TP, Zheng Y, Li Y. 2022. Global biogeography and projection of soil antibiotic resistance genes. Sci Adv. 8(46):eabq8015. https://doi.org/10.1126/sciadv.abq8015

Zhong J, Osborn T, Del Rosario Hernández T, Kyrysyuk O, Tully BJ, Anderson RE. 2024. Increasing transposase abundance with ocean depth correlates with a particle-associated lifestyle.Chaffron S, editor. mSystems. 9(3):e00067-24. https://doi.org/10.1128/msystems.00067-24